

**PRODUCTION OF ACTIVATED CARBON NANOFIBERS  
USING NATURAL CATALYSTS AND THEIR USE IN  
miRNA BIOSENSORS**

**Karima SAHTANI**



T.C.  
BURSA ULUDAĞ UNIVERSITY  
GRADUATE SCHOOL OF NATURAL AND APPLIED SCIENCES

**PRODUCTION OF ACTIVATED CARBON NANOFIBERS USING NATURAL  
CATALYSTS AND THEIR USE IN miRNA BIOSENSORS.**

Karima SAHTANI  
0000-0002-4424-8855

Prof. Dr. Yakup AYKUT  
(Supervisor)

PhD THESIS  
DEPARTMENT OF TEXTILE ENGINEERING

BURSA – 2022  
**All Rights Reserved**

## THESIS APPROVAL

This thesis titled “PRODUCTION OF ACTIVATED CARBON NANOFIBERS USING NATURAL CATALYSTS AND THEIR USE IN MIRNA BIOSENSORS.” and prepared by Karima SAHTANI has been accepted as a **PhD THESIS** in Bursa Uludağ University Graduate School of Natural and Applied Sciences, Department of TEXTILE ENGINEERING following a unanimous vote of the jury below.

**Supervisor** : Prof Dr. Yakup AYKUT

<b>Head :</b>	Prof. Dr. Yakup AYKUT 0000-0002-5263-1985 Uludağ University, Faculty of Engineering, Department of Textile Engineering	Signature
<b>Member:</b>	Prof. Dr. Recep EREN 0000-0001-9389-0281 Bursa Uludağ University, Faculty of Engineering, Department of Textile Engineering	Signature
<b>Member:</b>	Asst. Prof. Gökçe TANER 0000-0002-0290-1166 Bursa Technical University, Faculty of Engineering and Natural Sciences Department of Bioengineering	Signature
<b>Member:</b>	Prof. Dr. Hasan BASRI KOÇER 0000-0003-2612-6712 Bursa Technical University, Faculty of Engineering and Natural Sciences, Department of Fiber and Polymer Engineering	Signature
<b>Member:</b>	Assoc. Prof. Dilek PIRIM 0000-0002-0522-9432 Bursa Uludağ University, Faculty of Science, Department of Molecular Biology and Genetics	Signature

**I approve the above result**

**Prof. Dr. Hüseyin Aksel EREN**  
**Institute Director**

.././.....

**I declare that this thesis has been written in accordance with the following thesis writing rules of the U.U Graduate School of Natural and Applied Sciences;**

- All the information and documents in the thesis are based on academic rules,
- audio, visual and written information and results are in accordance with scientific code of ethics,
- in the case that the works of others are used, I have provided attribution in accordance with the scientific norms,
- I have included all attributed sources as references,
- I have not tampered with the data used,
- and that I do not present any part of this thesis as another thesis work at this university or any other university.

**.../.../2022**

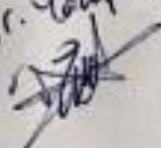
**Karima SAHTANI**

**TEZ YAYINLANMA  
FİKRİ MÜLKİYET HAKLARI BEYANI**

Enstitü tarafından onaylanan lisansüstü tezin/raporun tamamını veya herhangi bir kısmını, basılı (kâğıt) ve elektronik formatta arşivleme ve aşağıda verilen koşullarla kullanıma açma izni Bursa Uludağ Üniversitesi'ne aittir. Bu izinle Üniversiteye verilen kullanım hakları dışındaki tüm fikri mülkiyet hakları ile tezin tamamının ya da bir bölümünün gelecekteki çalışmalarda (makale, kitap, lisans ve patent vb.) kullanım hakları tarafımıza ait olacaktır. Tezde yer alan telif hakkı bulunan ve sahiplerinden yazılı izin alınarak kullanılması zorunlu metinlerin yazılı izin alınarak kullandığını ve istenildiğinde suretlerini Üniversiteye teslim etmeyi taahhüt ederiz.


Yükseköğretim Kurulu tarafından yayınlanan "Lisansüstü Tezlerin Elektronik Ortamda Toplanması, Düzenlenmesi ve Erişime Açılmasına İlişkin Yönerge" kapsamında, yönerge tarafından belirtilen kısıtlamalar olmadığı takdirde tezin YÖK Ulusal Tez Merkezi / B.U.Ü. Kütüphanesi Açık Erişim Sistemi ve üye olunan diğer veri tabanlarının (Proquest veri tabanı gibi) erişimine açılması uygundur.

Danışman Adı-Soyadı  
Tarih

Prof. Dr. Yahya Aykır  


07/07/2022

Öğrencinin Adı-Soyadı  
Tarih

Karime Sahtani  


07/07/2022

İmza

Bu bölüme kişinin kendi el yazısı ile okudum anlamında yazmalı ve imzalanmalıdır.

İmza

Bu bölüme kişinin kendi el yazısı ile okudum anlamında yazmalı ve imzalanmalıdır.

## ÖZET

Doktora Tezi

### DOĞAL KATALİZÖR KULLANARAK AKTİF KARBON NANOLİF ÜRETİMİ VE miRNA BİYOSENSÖRLERDE KULLANIMI

**Karima SAHTANI**

Bursa Uludağ Üniversitesi  
Fen Bilimleri Enstitüsü  
Tekstil Mühendisliği Anabilim Dalı

**Danışman:** Prof. Dr. Yakup AYKUT

Bilimsel, teknolojik ve tıbbi araştırmalar, önceden makro-boyutlu malzemelerin üzerinde çalışmalar yapıldı. Günümüzde makroskobik boyuttan nano boyuttaki malzemeler tercih edilir. Nanoteknoloji, malzemeleri nano boyuta indirerek yeni özelliklerin keşfedilmesidir ve kazandırılmıştır. Nano-boyut sayesinde malzemenin fiziksel, kimyasal ve biyolojik mekanizmalarında farklı özellikler ortaya çıkar. Nanoteknolojinin biyomedikal testlerle birlikte kullanılması çok sayıda hastalığın teşhis kalitesinin iyileştirilmesine yönelik avantajlıdır. Günümüzde nano biyosensör araştırmaları üzerine hızlı bir gelişim gözlenmektedir. Literatürde, birçok çalışmalar biyosensör yüzeyinden alınan sinyali arttırmaya yönelik sunulmuştur.

Bu tez, doğal katalizör kullanarak (lawsone ve Hemoglobin) aktif karbon nanolif farklı oranlarla elektroçekim yöntemiyle üretilmiştir ve bu nanoliflerin MiRna Biyosensörler kullanımını test edilmiştir. Elde edilen takviyeli karbon nanoliflerin morfolojik, termal ve mekanik karakterizasyonları yapılmıştır ve bu analizlerin sonuçlarına göre elektrokimyasal biyosensöründe kullanım potansiyeli incelenmiştir. miRNA biyosensörlerinde tanıma yüzeyi olarak miRNA kullanılmış. DNA Biyosensörler üzerine literatürde birçok çalışma bulunurken miRNA Biyosensörler üzerine yapılan çalışmalar son yıllarda yoğunluk kazanmıştır. Bu çalışma literatüre katkı sağlayan bir araştırma olacaktır ve biyomedikal alanında bazı hastalık tayininde ve teşhisinde kolaylaştırılmasını sağlayacaktır. Bu çalışmada beklenen hedef, nanoliflerin gözenekli yapıda üretilmiştir ve böylece yüzey alanını arttırılmıştır. Daha fazla miRNA molekülünün elektrotla teması ve immobilizasyonu sağlayacaktır, böylece küçük hacimde daha yüksek sinyaller alımı gerçekleştirilmesini test edilmiştir ve elektrokimyasal testlerin optimizasyonu yapılmıştır.

**Anahtar Kelimeler:** Nanolifler, Elektroçekim, Elektrokimyasal Biyosensörler, Lawsone, Hemoglobin, Karbon nanolifler, miRNA.

**2022, vii + 171 sayfa.**

## ABSTRACT

PhD Thesis

### **PRODUCTION OF ACTIVATED CARBON NANOFIBERS USING NATURAL CATALYSTS AND THEIR USE IN miRNA BIOSENSORS.**

**Karima SAHTANI**

Bursa Uludağ University  
Graduate School of Natural and Applied Sciences  
Department of Textile Engineering

**Supervisor:** Prof. Dr. Yakup AYKUT

In recent years of researches, sciences and technologies have been focused on the nanoscale for enhancing the properties and efficiency of materials. Nanotechnology investigates the production, manipulation and analysis of materials in the molecular scale. The nanomaterials are known for their large surface area that promote a wider active zone for modification, control and improvement of the conceived surface structures. Electrochemical biosensors are one of the widely used detection technique for the investigation of biomolecules. The efficiency of these biosensors and their selectivity depends mostly on the surface characteristics of working electrodes. Enhancing the quality of the electrode's surface led to a better immobilization and enhance the hybridization process, for this reason many materials were used and carbon nanofibers shows high performances and flexibility with ease of use which made researchers focused on its development. PAN is the most common polymer used as electrospun carbon nanofiber precursor

In the light of the plethora of researches converged on the nanomaterial's applications, the present study focused on combining the properties of natural catalyst as Lawsone and Hemoglobin in different amounts for the production of an activated carbon nanofibers by electrospinning methods. The obtained carbonized nanofibers and their graphitic properties were electrochemically investigated to enhance the sensitivity of the biosensory system, and the amelioration of the selectivity detection of miRNA molecules. A study of the optimization of the electrochemical measurements was also investigated to determine the efficient temperature, storage time and concentrations in the electrochemical measurements. The electrochemical measurements result for both Lawsone and Hemoglobin enriched CNFs investigations validates the efficiency of the miRNA molecules employing CNFs for a biosensing apparatus using SPEs with a low content of catalyst added (Leading to improve the level of catalysation observed in the carbonisation step). The conceived biosensory configuration can be safely used for a detection of specific RNA molecules.

**Key words:** Electrospinning, Electrochemistry, miRNA Biosensor carbon nanofibers, catalyst, Hemoglobin, Lawsone, Polyacrylonitrile.

**2022, vii + 171 pages.**

## PREFACE AND/OR ACKNOWLEDGEMENT

First and foremost, I would like to like to express my gratitude and respect to my supervisor, Prof. Dr. Yakup AYKUT for his support and guidance and for giving me the chance to accomplish this project in the best conditions. This thesis would not have been without his efforts and experience. He has given me the confidence to shape my Ph.D. with providing directions and resources. I am very thankful for his continuous encouragements, advices and support along this journey. I would like to thank you for introducing me the field of research on DNA biosensors and nanomaterials science and for your contribution to my academic studies since 2018. During my Ph.D. journey, I realized that it's not only the results are important but also the process of experimenting and finding solutions for every obstacle to discuss the research-related study and I feel like there is a lot to learn from you and from your persistency and methodology of research. It has been an important and rich journey and experience that I will stay grateful for.

I would like to express my special thanks to Prof. Dr. Recep EREN for the motivation, support and advices you provided me from the beginning of my researches. It was an honor and a privilege to work under your support. I would like to express my respect and my gratitude to all my professors during this scientific journey.

I would like to thank Nefise YAVUZ, Ayşe BOSTANCI for helping me in the phase of nanofiber's electrospinning. Also, I would like to thank Nilay ALADAĞ for the directives and helps in the preliminary steps of the electrochemical analysis, and thank Mehmet TIRITOĞLU for the help he provided in the laboratory experiments that will be remembered.

Finally, a deep gratitude and thank to the most important people, my family, whom I have to present this work and thank for their unconditional support, patience and love during my Ph.D. thesis. I can't express enough my gratitude and respect to my father for carefully following me with support and advices in every step and in the hard moments. The unconditional love and prayers of my mother and moral support of my sister. Without them, this journey was impossible to accomplish and to be in the place I am.

Sincere thanks to my friends, colleagues and every person who trust on my potential and helped me. I will remember your contributions.

Karima SAHTANI  
07/07/2022



## CONTENTS

	<b>Page</b>
ÖZET.....	i
ABSTRACT.....	ii
PREFACE AND/OR ACKNOWLEDGEMENT .....	iii
SYMBOLS and ABBREVIATIONS .....	viii
FIGURES .....	x
TABLES.....	xv
1. INTRODUCTION .....	1
2. LITERATURE REVIEW AND THEORETICAL BASICS .....	6
2.1. General View .....	6
2.2. Outline of Thesis .....	14
2.3. Biosensors .....	15
2.3.1. Brief history of biosensors: .....	15
2.3.2. Definitions and limitations:.....	18
2.3.3. Characteristics of biosensors:.....	23
2.3.4. Classification of biosensors.....	24
2.4. Nucleic Acids .....	25
2.4.1. General basics .....	25
2.4.2. The structure of DNA.....	26
2.4.3. The structure of RNA.....	28
2.4.4. The structure of miRNA.....	29
2.4.5. miRNA transcription.....	31
2.4.6. miRNA nuclear processing .....	32
2.5. Electrochemistry .....	34
2.5.1. General view .....	34
2.5.2. Voltammetry .....	36
2.5.3. Types of voltammetric techniques .....	40
2.6. Electrochemical DNA biosensors .....	45
2.6.1. General aspect .....	45
2.6.2. Methods of DNA immobilization onto sensor surfaces.....	46
2.6.3. Molecular binding interaction to DNA .....	50
2.6.4. The electrochemical DNA biosensors investigation in detection for compounds DNA binding reactions: label-free and label-based electrochemical DNA detection. ...	53
2.7. Electrochemical miRNA biosensors .....	56
2.7.1. General view .....	56
2.7.2. Electrochemical label-based biosensing for miRNA analysis .....	57
2.7.3. Electrochemical miRNA biosensors based on catalysts .....	58
2.7.4. Electrochemical Biosensor Based on RedOx Intercalating Agent.....	60
2.7.5. Oxidation of guanine method for electrochemical miRNA biosensors .....	60

2.8. Carbon nanofibers in biosensors .....	61
2.8.1. General view .....	61
2.8.2. Carbon nanofibers .....	62
2.9. Production of carbon nanofibers from electrospun PAN .....	64
2.9.1. Electrospinning of nanofibers .....	64
2.9.2. Solution based electrospinning .....	66
2.9.3. Carbon nanofibers derived from electrospun PAN .....	67
3. MATERIALS and METHODS .....	70
3.1. Materials.....	70
3.1.1. Raw and chemical materials .....	70
3.1.2. Sequences of oligonucleotides .....	70
3.1.3. miRNA and anti-miRNA solutions .....	71
3.1.4. Buffer solutions for electrochemical measurements .....	72
3.1.5. Testing station for the electrochemical miRNA biosensor system .....	73
3.2. Preparation of precursor nanofibers .....	74
3.2.1. Preparation of precursor Law/PAN nanofibers .....	74
3.2.2. Preparation of precursor Hemoglobin/PAN nanofibers .....	76
3.3. Heat treatment of the precursor nanofibers .....	77
3.3.1. Heat treatment of the precursor Law/PAN nanofibers .....	77
3.3.2. Heat treatment of the precursor Hb/PAN nanofibers .....	80
3.4. Characterizations of the prepared nanofibers.....	81
3.4.1. Characterizations of the prepared Law/PAN nanofibers. ....	81
3.4.2. Characterizations of the prepared Hb/PAN nanofibers.....	82
3.5. Experimental procedure for the electrochemical miRNA biosensor measurements	85
3.5.1. Electrochemical activation of the SPEs surfaces .....	85
3.5.2. Immobilization of CNFs on the SPEs surfaces .....	85
3.5.3. Immobilization of anti-miRNA and miRNA molecules on the SPEs.....	86
3.5.4. Electrochemical measurements .....	87
4. RESULTS and DISCUSSION .....	88
4.1. Morphological investigation of PAN, PAN/Law and PAN/Hb nanofibers .....	88
4.1.1. Morphological analysis of PAN and PAN/Law nanofibers .....	88
4.1.2. Morphological analysis of PAN and PAN/Hb nanofibers .....	91
4.2. Chemical investigation of PAN, PAN/Law and PAN/Hb nanofibers.....	95
4.2.1. Chemical analysis of precursor PAN and PAN/Law nanofibers .....	95
4.2.2. Chemical analysis of precursor PAN and PAN/Hb nanofibers .....	97
4.3. Thermal investigation of PAN, PAN/Law and PAN/Hb nanofibers .....	98
4.3.1. DSC analysis of PAN and PAN/Law nanofibers.....	98
4.3.2. DSC analysis of PAN and PAN/Hb nanofibers .....	99
4.3.3. TGA investigations of PAN and PAN/Law nanofibers .....	100

4.3.4. TGA investigation of PAN and PAN/Hb nanofibers.....	102
4.4. Carbonaceous investigations of PAN, PAN/Law and PAN/Hb derived carbon nanofibers.....	103
4.4.1. Raman spectra analysis of Law enriched CNFs.....	103
4.4.2. X-ray diffraction analysis of Law enriched CNFs.....	104
4.4.3. Raman spectra analysis of Hb enriched CNFs.....	105
4.4.4. X-ray diffraction analysis of Hb enriched CNFs.....	106
4.5. Study of the Anti-miRNA immobilization optimization on the screen-printed electrodes without NFs for electrochemical miRNA biosensors.....	107
4.5.1. Preparation of samples and chemicals.....	107
4.5.2. Immobilization of anti-miRNA molecules on SPEs surfaces.....	107
4.5.3. Electrochemical measurements of the biosensory system.....	108
4.5.4. Results of the DPV measurements by using PBS and ABS buffer solution.....	109
4.5.5. Results of the DPV measurements with different rate of anti-miRNA immobilized SPEs.....	111
4.5.6. Storage time and temperature study of anti-miRNA immobilized SPEs.....	112
4.6. Electrochemical analysis for miRNA detection by using law enriched CNFs immobilized on screen printed electrodes.....	114
4.6.1. Preliminary guanine oxidation measurements.....	114
4.6.2. Selectivity of the miRNA biosensory system.....	115
4.7. Electrochemical investigation for a selective miRNA detection by using Hb enriched CNFs immobilized on screen printed electrodes.....	118
4.7.1. Preliminary electrochemical measurements.....	118
4.7.2. Selectivity and investigation of the biosensory system.....	119
5. CONCLUSION.....	123
5.1. Effect of Lawsone enhancement on the miRNA biosensor performance.....	123
5.2. Effect of Hemoglobin enhancement on the miRNA biosensor performance.....	124
REFERENCES.....	125
APPENDIX.....	144
APPX 1 Differential calorimetry analysis results for PAN and Law/PAN samples. Maximum peak points were considered for T <sub>m</sub> determination.....	144
APPX 2 Thermogravimetric (TGA) analysis of PAN and PAN/Law nanofibers.....	144
APPX 3 Representation of A: DTA and B: DTG plots of PAN/Law nanofibers.....	145
APPX 4 Data point obtained from DTA and DTG plots.....	145
APPX 5 Maximum peak positions of D and G bands at Raman spectra for PAN and Law/PAN samples.....	146
APPX 6 Thermogravimetric (TGA) analysis results of PAN and PAN/Hb nanofibers.....	146
APPX 7 Representation of C: DTA and D: DTG plots of PAN/Hb nanofibers (a) pure PAN, (b) H <sub>0.5</sub> , (c) H <sub>1</sub> , (d) H <sub>3</sub> , (e) H <sub>5</sub> , (f) H <sub>15</sub> and (g) H <sub>30</sub> .....	147
APPX 8 Data point obtained from DTA and DTG plots.....	147
APPX 9 Maximum peak positions of D and G bands at Raman spectra for PAN and PAN/Hb samples.....	148
APPX 10 The contact angle for pure carbon nanofibers using PBS buffer.....	148

APPX 11 The contact angle of Lawsons enriched carbon nanofibers with PBS buffer	149
APPX 12 the contact angle of Hemoglobin enriched carbon nanofibers with PBS buffer	149
RESUME.....	150

## SYMBOLS and ABBREVIATIONS

<b>Symbols</b>	<b>Definition</b>
°C	Celsius
μA	Microampere
μl	Microliter
cm	Centimetre
kV	Kilovolts
ml	Millilitre
mm	Millimetre
mV	Millivolts
Nm	Nanometers
Sec	Seconds
V	Volt
wt. %	Weight percent
<b>Abbreviation</b>	<b>Definition</b>
ABS	Acetate Buffer Solution
Anti-miRNA	PolyT(G) And PolyT(I)
CNF	Carbon Nanofibers
DMF	N,N-Dimethylformamide
DPV	Differential Pulse Voltammetry
DSC	Differential Scanning Chromatography
DTA	Differential Thermal Analysis
DHPLC	Denaturing High Performance Liquid Chromatography
dsDNA	Double stand DNA
EDC	1-Ethyl-3-(3-Dimethylaminopropyl)-Carbodiimide
FTIR	Fourier Transformation Infrared Spectroscopy
G	Guanine
H	Enthalpy
Hb	Hemoglobin
HLC	Hydrochloric acid
I	Inosine
IUPAC	International Union of Pure and Applied Chemistry
K <sub>2</sub> HPO <sub>4</sub>	Potassium phosphate dibasic
KH <sub>2</sub> PO <sub>4</sub>	Potassium phosphate monobasic
Law	Lawsone
miRNA	Micro Ribonucleic Acid
NaCl	Sodium chloride
NaOH	Sodium hydroxide
NC.miRNA	Non-Complementary Micro Ribonucleic Acid
NF	Nanofiber
NHS	N-Hydroxysuccinimide
NP	Nanoparticle

PAN	Polyacrylonitrile
PBS	Phosphate Buffer Solution
PolyA	Oligonucleotide Has Only Adenine Bases On Its Chain Structure
PolyT(G)	Oligonucleotides With Guanine Base On Its Chain Structure
PolyT(I)	Oligonucleotides Without Guanine Base On Its Chain Structure
RT-PCR	Real Time-Polymerase Chain Reaction
SEM	Scanning Electron Microscopy
SM.miRNA	Single-Base Mismatched Micro Ribonucleic Acid
SPE	Screen Printed Electrode
ssDNA	Single strand DNA
Sw-CNT	Single walled carbon nanotubes
TGA	Thermo Gravimetric Analysis

## FIGURES

	<b>Page</b>
Figure 2.1. Outlines and chronology of the study research .....	14
Figure 2.2. Schematic illustration of basic biosensor assembly including three components: detector, transducer and output system (Mohd Said, 2014) .....	20
Figure 2.3. General classification of biosensors (Najeeb et al., 2017).....	24
Figure 2.4. Structure and components of nucleotides (Nakatsu, 2021).....	25
Figure 2.5. Schematic illustration of the DNA double helix model (Bano et al., 2016) .....	27
Figure 2.6. Biochemical structure of nucleotides and nucleoside's structure (Giuliani et al., 2019) .....	27
Figure 2.7. Basic structure of RNA (Thies, 2015) .....	29
Figure 2.8. miRNAs biogenesis and functions (Magri et al., 2018).....	31
Figure 2.9. Schematic illustration of translocation occurring in microRNA from nucleus to cytoplasm (Durası, 2018).....	33
Figure 2.10. Schematic illustration of pre-miRNA exported by EXP5-RAN•GTP transport complex (Durası, 2018) .....	34
Figure 2.11. The schematic representation of electrochemical biosensors types with three main electrodes: working (WE), reference (RE) and counter (CE) connected to a potentiostat.(Damıati and Schuster, 2020) .....	37
Figure 2.12. A typical cyclic voltammogram showing oxidation and reduction current peaks (Kumar and Bankoti, 2009) .....	41
Figure 2.13. IUPAC and US convention for Cyclic voltammogram (Elgrishi et al., 2018b) .....	43
Figure 2.14. The important parameters in pulse voltammetry (Amin et al., 2016) .....	44
Figure 2.15. General design of DNA biosensor (Liu et al., 2012b) .....	46
Figure 2.16. DNA probe immobilization via electrostatic adsorption (Rashid and Yusof, 2017).....	48
Figure 2.17. Covalent binding to the electrode surfaces (Ligaj et al., 2006) .....	48

Figure 2.18.	Schematic representation of the immobilization strategies of biotinylated DNA probe; a) avidin/streptavidin-functionalized electrode activated with carboxyl groups; b) biotin/avidin (streptavidin)/biotin as sandwiches technique representation (Rashid and Yusof, 2017) .....	50
Figure 2.19.	Schematic representation of binding mode of redox indicator to DNA (Rashid and Yusof, 2017).....	51
Figure 2.20.	Electrochemical detection schemes for compound-DNA interactions (Ozkan-Ariksoysal et al., 2012).....	55
Figure 2.21.	Schematic illustration of an electrochemical biosensors based on labelled probe with RedOx molecules before and after hybridization. (A) Basic design; (B) elimination of labelled probe sequence; (C) the use of secondary probe labelled with RedOx molecule; (D) the use of two-probe labelled sequence, (a) before and (b) after hybridization (El Aamri, Yammouri, Mohammadi, Amine, & Korri-Youssoufi, 2020) .....	57
Figure 2.22.	Schematic illustration of electrochemical biosensor based on a RedOx molecule labelled probe via a linker molecule (a) before and (b) after hybridization (El Aamri et al., 2020) .....	58
Figure 2.23.	Electrochemical biosensor based on different types of catalysts before (a) and after hybridization (b) with micro-RNA, (A) enzyme, (B) chemical catalyst, (C) DNAzyme (El Aamri et al., 2020).....	59
Figure 2.24.	Electrochemical biosensor based on RedOx intercalating agent before (a) and after hybridization (b) with micro-RNA, (A) direct intercalation, and (B) intercalation via the template (El Aamri et al., 2020) .....	60
Figure 2.25.	Schematic representation of electrospinning process (Aykut, 2011)	67
Figure 2.26.	a) Aligned PAN nanofibers produced with rotating collector b) PAN nanofibers produced with fixed collector (Gergin et al., 2017) .....	68
Figure 2.27.	Representation of carbonization process starting from polyacrylonitrile (Gergin et al., 2017) .....	69
Figure 3.1.	The purchased oligonucleotides PolyA, miRNA and anti-miRNA ..	72
Figure 3.2.	Testing station for electrochemical measurements .....	73
Figure 3.3.	Screen printed electrodes used in the study. ....	74
Figure 3.4.	The prepared PAN/DMF/Law solutions .....	75



Figure 3.5.	solution preparation and electrospinning process of PAN/Law nanofibers.....	75
Figure 3.6.	Prepared precursor PAN/Law nanofibers .....	76
Figure 3.7.	The prepared PAN/DMF/Hb solutions .....	77
Figure 3.8.	A: prepared as-spun PAN/Law precursor nanofibers. B: stabilized PAN/Law precursor nanofibers .....	78
Figure 3.9.	Carbonized PAN/Law samples .....	79
Figure 3.10.	Schematic illustration of electrospun precursor nanofiber preparation (Stage 1) and stabilization and carbonization of as-spun precursor nanofibers (Stage 2), and transformation of Law/PAN NFs into Law enriched CNFs .....	79
Figure 3.11.	Stabilized and carbonized PAN/Hb nanofibers samples.....	80
Figure 3.12.	Schematic illustration of the electrospinning of PAN/Hb hybrid nanofibers, and their carbonization into Hb-CNFs via heat treatment processes. ....	81
Figure 4.1.	SEM images (subscript 1 and 2) and diameter distribution (subscript 3) of electrospun PAN/Law precursor nanofibers with different wt.% of Lawsone respect to PAN content: (A1-3) 0, (B1-3) 1, (C1-3) 3, (D1-3) 5, (E1-3) 30, (F1-3) 50, (G1-3) 70, and (H1-3) 100 .....	88
Figure 4.2.	SEM images (subscript 1 and 2) and diameter distribution (subscript 3) of stabilized PAN/Law precursor nanofibers. The contents are in the precursor PAN/Law nanofibers before the stabilization process as wt.% of Lawsone respect to PAN content: (A1-3) 0, (B1-3) 1, (C1-3) 3, (D1-3) 5, (E1-3) 30, (F1-3) 50, (G1-3) 70, and (H1-3) 100 .....	90
Figure 4.3.	SEM images (subscript 1 and 2) and diameter distribution (subscript 3) of the carbonized nanofibers. The contents are in the precursor PAN/Law nanofibers before the stabilization process as wt.% of Lawsone respect to PAN content: (A1-3) 0, (B1-3) 1, (C1-3) 3, (D1-3) 5, (E1-3) 30, (F1-3) 50, (G1-3) 70, and (H1-3) 100 .....	91
Figure 4.4.	SEM images of as-spun PAN/Hb nanofibers and their diameter distribution charts: (A1-3) pure PAN, (B1-3) PAN/H0.5, (C1-3) PAN/H1, (D1-3) PAN/H3, (E1-3) PAN/H5, (F1-3) PAN/H15, and (G1-3) PAN/H30. ....	93
Figure 4.5.	SEM images of stabilized PAN/Hb nanofibers and their diameter distribution charts: (A1-3) pure stb-PAN, (B1-3) stb-PAN/H0.5, (C1-3) stb-PAN/H1, (D1-3) stb-PAN/H3, (E1-3) stb-PAN/H5, (F1-3) stb-PAN/H15, and (G1-3) stb-PAN/H30 .....	94

Figure 4.6.	SEM images of carbonized PAN/Hb nanofibers and their diameter distribution charts: (A1–3) pure CNF, (B1–3) CNF/H0.5, (C1–3) CNF/H1, (D1–3) CNF/H3, (E1–3) CNF/H5, (F1–3) CNF/ H15, and (G1–3) CNF/H30 .....	95
Figure 4.7.	FTIR spectra of (A) pure PAN nanofibers, (B) pure Lawsone powder, and (C) precursor PAN/Law nanofibers with different wt.% of Lawsone respect to PAN content: (a) 1, (b) 3, (c) 5, (d) 15, (e) 30, (f) 50, (g) 70, and (h) 100 (T, Transmittance).....	96
Figure 4.8.	ATR-FTIR spectra of pure Hb powder and PAN/Hb nanofibers: (a) pure PAN, (b) PAN/H0.5, (c) PAN/H1, (d) PAN/H3, (e) PAN/H5, (f) PAN/H15, and (g) PAN/H30 .....	97
Figure 4.9.	DSC thermograms of precursor Law/PAN nanofibers with different wt.% of Lawsone respect to PAN content: (a) 0, (b) 1, (c) 3, (d) 15, (e) 30, (f) 50, (g) 70, and (h) 100 .....	99
Figure 4.10.	DSC analysis of PAN/Hb nanofibers with different ratio: (a) pure PAN, (b) PAN/H0.5, (c) PAN/H1, (d) PAN/H3, (e) PAN/H5, (f) PAN/H15, and (g) PAN/H30 .....	100
Figure 4.11.	Thermogravimetric (TGA) analysis results of PAN/Law nanofibers with different wt.% of Lawsone respect to PAN content: (a) 0, (b) 1, (c) 3, (d) 15, (e) 30, (f) 50, (g) 70, and (h) 100 .....	101
Figure 4.12.	Thermogravimetric analysis of PAN/Hb nanofibers (A and B) TGA: (a) pure PAN, (b) PAN/H0.5, (c) PAN/H1, (d) PAN/H3, (e) PAN/H5, (f) PAN/H15 and (g) PAN/H30 .....	102
Figure 4.13.	(A) Raman spectra and (B) X-ray diffraction patterns of carbonized nanofibers. The contents are in the precursor PAN/Law nanofibers before the stabilization process as wt.% of Lawsone respect to PAN content: (a) 0, (b) 3, (c) 15, (d) 30, (e) 50, (f) 70 and (g) 100.....	104
Figure 4.14.	Raman Spectra of carbonized nanofiber: (a) CNF, (b) CNF/H0.5, (c) CNF/H1, (d) CNF/ H3, (e) CNF/H5, (f) CNF/H15, and (g) CNF/H30 .....	105
Figure 4.15.	X-Ray diffraction plots of carbonized nanofibers (a) CNF, (b) CNF/H1, (c) CNF/H3, (d) CNF/H5, (e) CNF/H15, and (f) CNF/H30 .....	106
Figure 4.16.	Surface cleaning and activation, anti-miRNA attachment and measurement process .....	108
Figure 4.17.	DPV measurement with PBS: (a) anti-miRNA/PBS (with PAE), (b) anti-miRNA/PBS wait 60 min-wash –measure (with PAE), (c) anti-miRNA/PBS (with CAE) and (d) anti-miRNA/PBS wait 60 min-wash – measure (with CAE) .....	110

Figure 4.18.	DPV measurement with ABS buffer solution.....	111
Figure 4.19.	DPV measurement with different rate of anti-miRNA attached SPEs: anti-miRNA measurement solution/PBS (v/v) rates are (a) 1/50, (b) 2/50, (c) 5/50, (d) 10/50 and (e) 20/50 .....	112
Figure 4.20.	DPV measurements of anti-miRNA attached SPEs at different storage times at -18, +5 and +25 oC stored samples: (A) 1 day, (B) 3 days, (C) 14 days and (D) 21 days .....	113
Figure 4.21.	Guanine and adenine oxidation peaks of (a) miRNA, (b) PolyT(G), (c) PolyT(I), and (d) PolyA, anti-miRNA via DPV measurement by using bare SPEs.....	115
Figure 4.22.	Electrochemical biosensor measurements plots after attachment of miRNA, anti-miRNA molecules and their hybridized forms by using NHS/EDC modified and CNFs immobilized SPEs: (A) PolyT(G), (B) PolyT(G)-miRNA, (C) PolyT(G)-SM.miRNA, (D) PolyT(G)-NC.miRNA, (E) PolyT(I), (F) PolyT(I)-miRNA, (G) PolyT(I)-SM.miRNA, and (H) PolyT(I)-NC.miRNA.....	116
Figure 4.23.	Electrochemical biosensor measurements plots of guanine containing anti-miRNA and its hybridized form with miRNA by using just CNFs immobilized SPEs without NHS/EDC modification: (A) PolyT(G) and (B) PolyT(G)-miRNA. the image is the illustration of SPE with immobilized CNFs on its carbon electrode part.....	117
Figure 4.24.	Electrochemical miRNA biosensor measurements plots by using NHS/EDC modified and Hb-CNFs immobilized SPEs: (A) PolyT(G), (B) PolyT(G)-miRNA, (C) PolyT(G)-SM.miRNA, (D) PolyT(G)-NC.miRNA, (E) PolyT(I), (F) PolyT(I)-miRNA, (G) PolyT(I)-SM.miRNA, and (H) PolyT(I)-NC.miRNA.....	120
Figure 4.25.	Electrochemical miRNA biosensor measurements plots by using just Hb-CNFs immobilized SPEs without NHS/EDC modification: A) PolyT (G), (B) PolyT (G)-miRNA, and (C) PolyT(G)-NC.miRNA .....	121

## TABLES

	<b>Pages</b>
Table 2.2. Categories of the electrochemical transducer classification types of measurement, with corresponding analytes to be measured (Bergveld & Thevenot, 1993) .....	22
Table 2.3. Morphology of fiber affected by electrospinning parameters.....	65
Table 3.1. Sequences of the miRNA and anti-miRNA molecules used in this study .....	71
Table 4.1. Characteristics of Measured Electrospinning Solution Parameters and Diameters of Electrospun PAN and PAN/Lawa Nanofibers.....	89
Table 4.2. Characteristics of Measured Electrospinning Solution Parameters and Diameters of Electrospun PAN and PAN/Hba Nanofibers.....	92

## 1. INTRODUCTION

The fast change in the world climate, production and consumption strategies, impact the human lifestyle, the unhealthy living conditions which are opposing the natural life cycle of the humans, solicited by the environmental pollutions and stress leads automatically to the apparition of several diseases which are sometimes uncontrollable, this makes the researchers in a very entangled deal of detecting as earlier as possible the source of the diseases before its propagation in order to minimize risks of mortality or several deteriorations. The purpose is to converge the efforts to design and develop of diagnostic and analysis methods which have efficiency, high precisions and easily accessibility and repeatability properties.

Immobilization and hybridization degree are the main fundamental aspects impacting the performance and quality of a biosensor. Working on the improvement of the surface of the transducer lead to a better immobilization and enhance the hybridization process, for this reason many materials was used and carbon nanofibers shows better performances and flexibility with ease of use which made researchers more focused on its development. PAN is the most common polymer used as electrospun carbon nanofiber precursor (Inagaki et al., 2012), the obtained electrospun polymer nanofibers to carbon nanofibers, a proper stabilization and carbonization process have to be applied (Gergin et al., 2017; Zhang et al., 2014a). Aiming to improve the properties of the obtained surface and to catalyze the carbonization for an activated carbon nanofiber structures, inorganic materials were studied as zinc (J. Liu et al., 2014), cobalt (Aykut, 2012), iron (Park et al., 2005) and nickel (Li et al., 2009) have been incorporated into precursor PAN nanofibers. All the result of these researches showed that the loading of an optimized amounts of materials enhanced the electrochemical stability and the efficiency of the composite electrodes. Despite their many advantages, the inorganic materials stay with higher risks for an in-vivo test or for biological disease analyses.

The incorporation of organic elements as catalysts in the prepared PAN solution for an electrospinning process can be studied to ameliorate the graphitic and morphological performances of the obtained nanofibers after being carbonized for an efficient use in electrochemical genetic sensory applications. Also, the researches converged on the

organic catalysts must take consideration of the suitability to preserve the carbonaceous criteria during the whole process of carbon nanofibers preparation, production and heat treatments to assure all the expected properties. Recently, herbal extracts have been the center of interest of a wide range of scientific researches due to their fewer spinoff reactions and biodegradability in contrast with the chemical materials especially for a biological's applications. The incorporation of *Tecomella Undulata* into polycaprolactone-polyvinyl pyrrolidone nanofiber was studied by (Suganya et al., 2011) to investigate the antibacterial activities of the electrospun nanofibers and showed an bactericidal reaction to the tested microorganisms therefore an efficient wound dressing abilities and great potential for biomedical applications and a basic material for treating surfaces containing pathogenic microorganisms. The herbal loaded nanofibers were also cited in a large number of scientific studies, (Ahmadi et al., 2021) incorporated cinnamon into chitosan/gelatin nanofibers with using glutaraldehyde vapor as crosslinker to enhance the activity and performance of antibacterial nanofiber membrane, the biocompatibility and antibacterial activity were highly inflated in the sample containing 4% of cinnamon extract with a superior cell immobilization which promotes the application as drug delivery nanofibers membrane and a large scale of biomedical applications as wound healing patches and orthopedic healing construct. In addition to these herbal extract catalysts Lawsone (2-Hydroxy-1,4-naphthoquinone) is defined as organic molecule derived from plant and exhibits different properties including anticarcinogenic, antioxidant and hepatoprotective properties (Endrini et al., 2002), historically was used for the treatment of burn, wound, ulcer and skin infections due to its anti-inflammatory and antibacterial properties. (Muhammad and Muhammad, 2011) reported the performance of water and chloroform extracted from the Lawsonia's inermis leaves and resulted a promising ability of inhibiting the growth of microorganisms in the case of burn wound infections, therefore this plant extract contributes in the amelioration of the management of burns and the improvement of the traditional used wound dressing due to their side effects as imparting stains and time consuming (case of silver nitrate). This herbal extract was also used by (Hadisi et al., 2018) for a development of an nano-fibrous dressing in burn wound due to the it antibacterial and anti-inflammatory properties, the study used an amalgam of Lawsonia inermis and gelatin-oxidized starch electrospun mat for a burn wound treatment approach and reveal the efficiency of the Lawsonia of an fully

incorporation into the nanofibers during the electrospinning process and its amorphous state was positively revealed and also fibroblast proliferation, antibacterial activities and collagen secretion was proportionally enhanced with the increase of the Lawsonia content, therefore the healing process was dramatically ameliorated and gives an opportunity for future researches.

The integration of Lawsonia inermis extract in the electrospun nanofibers has been frequently reported in the literature due to the multiple biological characteristics of this natural compound for medicinal purposes, (Avci et al., 2013) studied the antibacterial activity of the loaded Lawsonia inermis (henna) into the poly(ethylene oxide) (PEO) and poly(vinyl alcohol) (PVA) electrospun nanofibers, they have reported that 2.793 wt.% of Lawsonia inermis in the PEO and PVA based solutions have successfully showed a bactericidal effect against *Staphylococcus aureus* and a bacteriostatic action to *Escherichia coli*, also it has been reported that the control of the concentration of this compound due to its several relationship with the antibacterial activities. Lawsonia inermis is therefore present in the scientific literature base as a strong eco-friendly antimicrobial agent. This informational platform makes the focus on this agent to be studied for its interaction with human cells as well as pathology and development of new approaches of diagnostic and treatments.

Lawsonone (2-hydroxy-1,4-naphthoquinone) is the principal dye molecule contained at 1.0–1.4% in the leaves of Henna (*Lawsonia inermis*) (Kirkland and Marzin, 2003), not only recognized as dye material but was also studied for its genotoxicity in a wide range of projects. Lawsonone's applications tend from cosmetics to biomedicine for the treatment of some diseases as microbial infections, hypertension and hypoglycemia and as cited below for a treatment as immunostimulant, hepatic protector and analgesic (Badoni Semwal, Semwal et al., 2014; Xavier et al., 2020). Chemically, this herbal extract molecule is a family of naphthoquinones and its structure rich in quinones allows the interference in biochemical processes especially the inhibition of electron transport and redox homeostasis (Kurtyka et al., 2016; Xavier et al., 2020) but also the inhibition of DNA topoisomerase (Ramos-Pérez et al., 2014; Xavier et al., 2020). The lawsonone is therefore considered as a bioactive compound with several cytotoxic and antitumoral activities

(Badoni Semwal et al., 2014). In the literature the focus in the study of lawsone was converged in this sense and give prominent results.

In the research section of electrochemical genosensors field, the implementation of carbon nanofibers has been reported in many researches, due to the high suitability for the electrochemical miRNA analysis, the sensitivity of such biosensors could be dramatically enhanced by adding catalysts to the electrospinning PAN solution in order to improve the morphological and carbonaceous performances of the prepared nanofibers. In the literature different organic and inorganic catalyst were loaded in the precursor nanofibers to obtain an enhanced properties of the activated carbon nanofibers which can be used in the surface of the biosensors. However, all the cited properties and suitability of Lawsone to get involve the carbonaceous structure are possible and need to be investigated. The investigation of enriching CNFs with Lawsone as a natural catalyst for an electrochemical biosensory miRNA detection apparatus has not yet been sufficiently reported. Different mechanisms and alternatives approaches are possible and will be investigated in this present research.

In the same convergence aiming to enhance the sensitivity of the biosensory system, and the amelioration of the selectivity detection of miRNA molecules, the research of an efficient catalyst leads to focalize on its ability to be homogeneously dispersed and chemically suitable for electrospinning and thermal processes, for this purpose hemoglobin loaded carbon nanofibers CNFs was investigated to analyze to catalytic effect on adding it proportionally in the precursor PAN nanofibers and observe it during all the stages of production and electrochemical analyses.

In the literature, Hemoglobin is studied as a natural compound that have been a part of different scientific projects. Due to the presence of iron atoms and its ability to catalyze the carbonization of the nanofibers, different concentrations of the globular protein hemoglobin were studied by (Barnes et al., 2006) with its effects on the electrospinning process by dissolution of the Hemoglobin's particles in 2,2,2-Trifluoroethanol and reported that the increase of the solution's concentration positively correlate with the porosity and also the capacity of the electrospun hemoglobin structure to maintain the mechanical properties required for use in wound dressings and present a high potential



for an biological use due to the oxygen-caring ability of the hemoglobin. The catalytic properties of the hemoglobin was also investigated in the electrochemical biosensor field and was reported in the literature by (Baghayeri and Veisi, 2015) in which the conception and fabrication of an electrochemical biosensors, the research reveal that the addition of the hemoglobin on the surface of the nanocomposite dramatically enhanced the reduction of hydrogen peroxide and improved the obtained electrochemical signal with a significant improvement of the sensitivity, the investigations also shows the higher capacity of the nanocomposite to enhance the electron conductivity. The researches present in the literature demonstrate that the integration of the hemoglobin in the electrochemical and nanocomposites fields can efficiently provide good results in term of catalysation and amelioration of the surface quality of the biosensors for biological and clinical applications.

In this direction of research, the sensitive detection of miRNA via hemoglobin enriched carbon nanofibers CNFs immobilized SPE systems have been studied.

## **2. LITERATURE REVIEW AND THEORETICAL BASICS**

### **2.1. General View**

In the recent years a wide range of researches were focused on the genetic diagnostic as a very strong tool for the earlier detection and prediction of some diseases in order to prepare the convenient treatment methods, the principle of the genetic diagnostic is the recognition of specific nucleic acids and microorganisms, depending on the working strategies that makes the light on the genomes or the genomes of the microorganisms responsible of the diseases, the convenient approaches and genetic methods are decided and investigated. In this term a proper extraction of the genetic molecules from the virus extricated from human from nasopharyngeal or throat swab (Hung et al., 2020) then an amplification with RT-PCR (Real time polymerase chain reaction) method was applied for the molecules (Park et al., 2020), the detection of the infiltration of viruses in a living organism via the molecular methods still a subjects of multi-disciplinary researches present in the literature such the influenza detection (Van et al., 2012) and also the new pandemic Covid-19 diagnostic which penetrate the human body and proliferate with incarnating its genetic code into the living cells (Chan et al., 2020). The purpose of analyzing the molecular behavior by a genetic diagnostic open the opportunity for an medical need in the case of some fateful diseases like breast cancer, Haemophilia A (Wooster and Weber, 2003), cystic fibrosis (Dequeker et al., 2009) and Prenatal genetic diagnosis of retinoblastoma (Shah et al., 2016).

The scientific researches in the field of the detections of nucleic acid sequences are exponentially increasing due to the efficiency of the obtained results, the process of detection and analyses require the use of DNA, RNA or miRNA as strong biomarkers especially for early cancer prognostic, great scientific progresses have been made in cancer fields over the past decades and had confirmed that noncoding RNA (ncRNA) have an efficient role in both pathological and physiological cell processes as proliferation, apoptosis and differentiation (Bai and Wu, 2019).

MicroRNAs (miRNAs) a subordinate type of non-coding RNAs, are defined highly conserved and single stranded RNAs with approximately a length of 20-22 nucleotides and obtained via biogenesis (Peng and Croce, 2016), owing a primordial function in the

RNAs silencing and expression of genes, this class of RNA have been reported to be also acting both oncogenes and in the same time as tumor suppressors, depending of a varieties of factor like cancer type and physiological environments (Keshavarzi et al., 2017; Salarinia et al., 2016), this fact have been demonstrated by a dysregulation of miRNAs expression in human cancer by an amplification or deleting of miRNA genes (Peng and Croce, 2016). The miRNA can also regulate gene expression in the transcriptional and posttranscriptional levels (Tavakolizadeh et al., 2018). The miRNAs database recorded approximately 2500 miRNAs located in the human genome, in which 1000 and more plays the role of regulation of 50% of protein-coding human genes (Bai & Wu, 2019). Therefore, miRNAs can be used as an efficient tool for biomedical applications, early diagnostic and cancers biomarker (Mashreghi et al., 2018; Mirzaei et al., 2017; Saeedi Borujeni et al., 2018; Zhu et al., 2018).

The literature present a wide type of methods for detecting miRNA such TR-PCR and considered as a highly efficient due to higher degree of selectivity and sensitivity for MiRNA detection (Zhou et al., 2019), the northern blotting technique was also cited in many articles and was studied as one of the conventional MiRNA analyzing methods (Shabaninejad et al., 2019), the use of serum MiRNA microarray analysis for the detection of mi-4429 and miR-4689 as the most important diagnostic biomarkers in the case of biliary atresia (BA) (Dong et al., 2016).

Even if these conventional techniques are considered efficient and gives prominent results and a strong literature base for future research, the cost, long process consuming have been an important reason for developing a new alternative technique with a high specificity and sensitivity, fast, low cost and easy processing abilities. All these properties and more were combined in an electrochemical genetic biosensor's technology as a promising candidate for genetic molecules analyses due to its high performances, requiring less consumables, optimized energy used and the most important is the suitability for kit development which is a new platform for the future pathogenic diseases diagnostics as well as the control of environmental and food safety, also these biosensors are known for their ability and selectivity for detecting a particular oligonucleotides sequences due to the immobilization of the surfaces of the electrode with a specific oligonucleotides which is another advantage with a wide types of electrodes surfaces that

could be modified and enhanced for a better performances. The level of precision in the capture probe immobilization process is extremely important and impact the probe orientation, therefore the interaction of the probe target and the charge transfer reactions is an interpretable and analyzable electrical signal (Huey et al., 2005).

The nucleic acid-based (NABs) cited in the literature are aptamers, ribonucleic acids (RNA), peptide nucleic acids (PNA) and deoxyribonucleic acids (DNA) (Sobiepanek and Kobiela, 2018). During the investigation the nucleic acids must be immobilized optimally on the sensor's surface and this step has a crucial role in the performance of the biosensor. The commons used methods for immobilization of DNA onto electrode surface are nowadays useless due to their low hybridization efficiency (Levicky et al., 1998; Pividori et al., 2000; Sobiepanek and Kobiela, 2018), techniques including adsorption, self-assembly, biotin-avidin interaction have been widely used for surface immobilization of ss-DNA probes on electrodes but were limited by the constraint of cost and level of sensitivity which is an important parameter (Abu-Salah et al., 2015). (Ozkan et al., 2002a) have investigated the hybridization electrochemically by deploying methylene blue (MB) and peptides nucleic acids (PNA) on self-assembled alkanethiol monolayer (SAM) modified gold electrodes (AuE), in which a hybridization of the (covalently) immobilized probe with a target DNA can be occurred and resulted that the self-assembled alkanethiol monolayer was strongly adsorbed on a AuE surface forming an efficacy film on which amino linked peptides nucleic acids segments could be attached and this methods enhanced the efficiency of the biosensors for the detection of hybridization. However after some months (Gooding et al., 2003) published a review about the self-assembled monolayers for modifying electrodes as a field of developing the sensing interfaces, the gold-thiol coupling have been proved to be resistive for a mild potentials range and the alkanethiols have been studied to be totally tempted to damages resulted from oxidation and thermal desorption. Also, even if the monolayer produced by self-assembly present a higher flexibility with different applications, a long list of limitations is intolerable like the sensitivity of the immobilized enzyme to the change in pH, ionic strength and temperature that a minimal change can lead to a loose of biological activities, also the precursors of SAMs shows the chemical instability and fast oxidation in air (Chaki and Vijayamohan, 2002), these disadvantages leads to a decrease in DNA immobilization

and impact the efficiency of the biosensors. The reaction between the bioreceptor and targets is synthesized on external part in the electrode's surface, the modification of this part aim to enhance the performance of the biosensors, (Li et al., 2011) developed a highly sensitive DNA biosensor with an electrochemical technique by exploiting a dendritic gold (DenAu) modified electrode, the developed electrode highly enhanced the performance of the electrode surface area. The efficiency of this results increased the performances of probe DNA immobilization amount and automatically enhanced the hybridization occurred with target DNA, but the use of gold electrodes is limited by different factors as the size of the gold nanoparticles used, charge on surface, nature of the protective layer on the gold nanoparticles (AuNP) (Rasheed and Sandhyarani, 2017). All these limitations can be skipped by the use of carbon electrodes that present a wide range of advantages and flexibility that will be discussed in the following part.

After the process of DNA probe's immobilization on the adequate electrode surface, the following step of detection the MiRNA molecules is assured by visualizing the hybridization of the probes on the surfaces, many researches are converged on the enhancement of electrochemical detection of MiRNA. Magnetic bead-based bioassay were used for electrochemically detection of MiRNA-222, using paramagnetic bead and enzyme amplification (Bettazzi et al., 2013). Nanoparticles have also been used in electrochemical genetic sensor technologies to enhance sensitivity. An electrochemically detection of miRNA-21 was investigated by using  $\text{CoFe}_2\text{O}_4$  magnetic nanoparticles and padlock exponential rolling circle amplification circle taking advantage from their high sensitivity (Yu et al., 2017). Trans et al. conceived a carbon nanotube system characterized by its interpenetrative ability and electroactive polymer in order to detect miRNA-141 known as a widely used prostate biomarker by analyzing the DNA probe's hybridization occurred on the surface (Tran et al., 2013). (Zhang et al., 2018) studied the performance of the  $\text{Fe}_3\text{O}_4$  nanoparticles with DNA molecules in order to detect miRNA by using electrochemical sensing approach, this research used for cathode's material the indium tin oxide and the graphene oxide/gold nanoparticle/glucose oxidase was chosen as the anode material.

It is widely known that carbon materials present a good flexibility and efficiency in the electrode's conception and their covalent modification for their electrochemical

application because of their flexible surface features (Downard, 2000), and also for their diversified morphological structures. Carbon materials are also used as a surface base in electrochemical transducer for DNA hybridization biosensors. Glassy carbon (Millan and Mikkelsen, 1993; Millan et al., 1992), carbon pastes (Mahmoudi-Moghaddam et al., 2019) and pencil lead (Mirmoghtadaie et al., 2013) are cited in the literature as an used item for the conception and fabrication of DNA biosensors but for a better precision and a more molecular-scale control, these electrodes are considered unsuitable.

The changement of scale of materials development from microscopic to nanoscopic improved the molecular size structures understanding and obviously gives the opportunity for an enhancement of functionalities and characteristics of the sensor taking advantage from the highly large surface area of the nanoscale materials and the large active zone in it which allow a possibility for modification, control and improvement of the final conceived surface structures. Various nanostructured materials have been deployed in order to enhance the detection performance of the electrochemical nucleic acid biosensors, such as graphene quantum dots studied to detect gene mutations in pancreatic cancer (Joshi and Waghmode, 2016), metal nanoparticles (Han et al., 2020) and polymeric nanofibers (Bostanci et al., 2019).

The literature present various studies of using the polymeric nanofibers in electrochemical genetic sensors applications and proved a prominent result for a future in vivo test. The application of conducting polymer in the fabrication of an electrochemical biosensors was studied, conjugates the polyaniline, polypyrrole and polythiophenes that shown an higher stability and electrical conductivity, the combination of two or more polymers with a catalytic nanomaterial enhanced the sensitivity of the signal (Naveen et al., 2017). In zeptomolar scale, the use of electrospun manganese (III) oxide nanofibers for a label-free electrochemical detection of the primers from the dengue virus have been reported by (Tripathy et al., 2017). (Guler et al., 2018) studied the performance of using Polyurethane/poly (m-anthranilic acid) electrospun nanofibers for a impedimetric DNA biosensor application in order to detect *Salmonella* spp, a proper covalent immobilization of the DNA molecules on the nanofiber's surfaces after a process of activation, the study results shown a highly sensitive performance for the electrochemically analysis of *Salmonella* spp based on DNA biosensor with a stability of the electrode. In another

research paper published by Tripathy et al. a chemiresistive nanobiosensor was developed for an electrochemically detection of the DNA hybridization, for this purpose, a Polyaniline electrospun nanofibers was prepared and analyzed, Polyaniline/polyethylene oxide nanofibers were properly inserted in an aligner form between the conductive electrodes and interacted with DNA for electrochemical measurements and analysis (Tripathy et al., 2017). Also, in the field of DNA biosensing a wide use of neat polyacrylonitrile and polymers in their electrospun nanofibers forms as efficient working electrodes was reported in the last decades of researches and have been widely used for the panoply of advantages and flexibility they propose (Aladag Tanik et al., 2018; Cam et al., 2018). A similar papers were reported in the literature as the study elaborated by Bostanci et al. in which a hybrid nanofibers of cellulose monoacetate/nafion were electrospun for a use as working electrode to analyze electrochemically the oxidation of guanine occurred on the single strand DNA molecules (Bostanci et al., 2019).

The amalgam of the graphitic and nanofibers properties of carbon with high recognition properties of the biomolecules enhanced the quality of the transducer and the electrochemical techniques development. Carbon nanostructured materials are nowadays the most used in electrochemical genetic biosensors and have been a subjects of many researches, the use of nanostructured carbon black was studied for a proper insertion of antibodies, immobilization of enzymes and also for an efficient incorporation and analyses of specific DNA sequences in the diagnostic and prognostic of some cancer cases (Silva et al., 2017). The use of carbon nanotubes defined as a highly potential nanomaterial for their conductivity, biocompatibility and large surface to volume ration in electrochemical biosensors was studied, non-covalent property and function of carbon nanotubes favorize the fact of retention in pristine mechanical and electronics properties of CNT with preserving the intrinsic properties, it also provides a good strategy for biomolecules immobilization with an important biocompatibility (Zhou et al., 2019). In another study a covalent modification with L-lysine of single-walled carbon nanotubes aiming to investigate and enhance the sensing performance of the electrochemical measurement of guanine, adenine and 8-hydroxy-20-deoxyguanosine was reported by (Gutiérrez et al., 2016). A research paper made by (Jun Li et al., 2003) in which a DNA sensor tested highly sensitive integrating carbon nanotube made electrode was studied,

electrode conception incorporated the multi-walled carbon nanotubes produced perpendicularly to the surface of the electrode, this study revealed a dramatical enhance of the sensitivity degree in the sensor which was proportional to the decrease of the density in the nanotube. The use of multi-walled carbon nanotubes was also a research subject of a wide range of fields as its combination with chemical functional groups deployed on the surface proved efficient for the measurement of the DNA of *Escherichia coli* (*E.coli*) microorganism and was investigated by inserting single-strand DNA (ssDNA) molecules onto the nanomaterial then immobilizing it on the surface of a pencil graphite electrode (PGE) for the detection of the DNA hybridization, the designed sensor has the performance to detect *E.coli* DNA in 20 min (Ozkan-Ariksoysal et al., 2017). In the same convergent subject the chitosan and carbon nanofiber modified pencil graphite electrode (PGE) was studied for the enhancement monitoring of DNA hybridization due to Hepatitis B virus, the chitosan-carbon modified pencil graphite electrode (PGE) was prepared and electrochemically investigated (Eksin and Erdem, 2016). Graphene was also used as based material modifying pencil graphite electrode for the enhancement of the electrochemical bio interaction, in the study a reduced graphene oxide (rGO) modified pencil graphite electrode (PGE) were synthesized for the detection of anticancer drug, daunorubicin (DNR) and DNA, also for the analyses of the bio-interaction occurred between DNR and DNA with an electrochemical characterization of the electrodes and conclude that the rGO-PGE allowed more electron transfer at  $[\text{Fe}(\text{CN})_6]^{3-/4-}$  redox system than the unmodified PGE with an augmentation of the surface area by 55%, the DNA detection was in just 15 min (Eksin et al., 2017).

As reported from the researches, the use of pencil graphite electrode attracts a several number of research due to its advantages and have been widely used as a flexible and efficient working electrode in electrochemical genosensors systems.

Screen printed electrodes showed a higher performances combined with the use of carbon nanofibers for enhancing their surfaces and used in wide range of application for an indicator free electrochemical biosensors for detecting RNA with miRNA-34a target (Erdem et al., 2015).



The development and conception of a biosensing system imply a focus on the choice of the right materials and its suitable application environment as the surface of the working electrode and the measurement techniques. Carbon nanofibers has received high attentions taking advantages from its panoply of performances, chemical, thermal, electrical and physical properties in the biorecognition area.

The nanofibers are proved very efficient materials for the electrochemical MiRNA detection, due to the high conductivity of the carbon nanofibers, an enhanced guanine signal with a high producibility was obtained using a CNF-SPEs for the detection of MiRNA-34a compared to the conventional electrodes, the CNF-SPEs are proved highly stable and sensitive base for analyses of indicator free nucleic acids hybridization (Erdem et al., 2015).

In another study, the carbon nanofibers were classed to be the better matrix in the conception and development of biosensors better than graphite powder or even carbon nanotubes in a research project made by (Vamvakaki et al., 2006), in which they used carbon nanofibers for the conception of a catalytic electrochemical glucose biosensors.

The successful integration of carbon nanofibers in the conception and production of the electrochemical biosensors is referred to the multi-advantages of this nanostructures as the high surface area and active zone in it that allow efficiently the immobilization process and electrons mediations, and also the availability of these materials due to the ease of production.

The manufacture of carbon nanofibers have been a subject of a wide researches aiming in the same time to improve the properties of this materials, due to the special morphological and chemical properties of the carbon nanofibers, it become a strong candidate for electrode materials as immobilization substates of biological molecules (Huang et al, 2010).

Also produced from various precursor polymers as polyacrylonitrile (K. J. Lee et al., 2010), polyvinyl alcohol (Gupta and Dhakate, 2017), polyimide (Chung et al., 2005), cellulosic (Naboka et al., 2013), etc.

## 2.2. Outline of Thesis

The objective of this research project is to combine the properties of the natural catalysts with the biosensing fields improvement to produce an activated carbon nanofibers reinforced natural catalysts and their use in miRNA biosensors.

In order to meet the aims mentioned above, the research have been treated in four parts as structured as follows:

After a proper literature research in the same similar field presented in the chapter 2, the chapter 3 presents the materials and chemical used during the preparation of the nanofibers precursors solutions, the nanofibers production with the following morphological, mechanical and thermal analyses for a proper characterization of the prepared nanofibers. The next parts are the preparation of the necessary steps for the electrochemical analyses including the preparation of oligonucleotides, buffers and electrodes surfaces. The chapter 4 presents the analyses of the different obtained results with the interpretations of the obtained results from characterizations and electrochemical measurements for an efficient analysis.

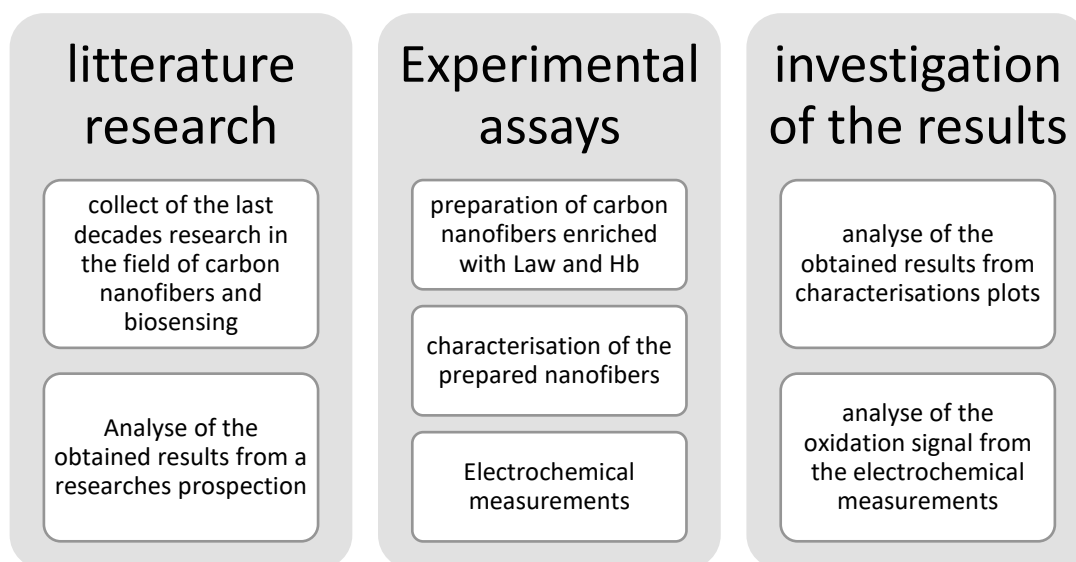


**Figure 2.1.** Outlines and chronology of the study research

## **2.3. Biosensors**

### **2.3.1. Brief history of biosensors:**

The last decades of researches related to the biosensors is described as an exponentially growing field due to the high interest of the researcher by this attractive revolutionary technology aiming to shorten the process of different traditional techniques especially in biology and pathology specialties. Several researchers with different backgrounds converged the efforts in this branch and their multidiscipline tends from chemistry to microbiology without skipping the electrical engineering deeply concentrated in the improvement of the tool 'biosensors'.

The history of the biosensors presented in the literature started 70 years ago, the beginning of this research activities was presented through a publication of the Prof. Leland C. Clark in 1956 about the development of an oxygen probe, the obtained results from this research initiated to expand the range of analytes for the measurements and was presented during a conference in 1962 at the New York academy of science, where he presented the mechanism developed for enhancing the performance and intelligence of an electrochemical sensor by inducing enzymes transducers in a form of membrane-enclosed sandwich (Clark, 1956). Historically, the first model was investigated by entangling in the dialysis membrane the glucose oxidase enzyme over the oxygen probe, the fact of adding perpetually and proportionally the glucose demonstrate the decline of concentration occurred in oxygen. The first biosensor was presented as an "enzyme electrode" (Leland et al., 1962). The researches exponentially increase to form a wide base of projects, in 1967 the term "enzyme electrode" appear in a publication of Updike and Hicks in which they define a similar device in which the use of polyacrylamide gel was studied onto the surface of the electrode for enhancing the immobilization of the enzyme glucose oxidase (Updike and Hicks, 1967). In addition to the amperometry, Guilbault and Montalvo used glass electrodes combined with urease using potentiometric measurement to quantify urea concentration (Guilbault and Montalvo, 1969).

Since from 1970, a noticeable increase of research in this field was presented to sculpt the concept of biosensors, the combination of the electrochemical biosensors an enzyme

was signed by different authors, to form a clear informational base of a new concept and research where the biological components were coupled with electrochemical sensors.

In the electrochemical side of researches at the period, the analysis on Ion selective electrodes (ISE) was the nucleus point of active researches and many ideas was accepted in this sense like to enlarge the range of sensors to the non-ionic and non-electrochemical active compounds, the research area was widely extended and the researches on ISE have been reported to be initiating to the development and research in the electroanalytical biosensory field (Palchetti and Mascini, 2010). In this side Professor G. Rechnitz published an article in 1971 in which he developed an “amygdaline” sensor, the obtained results showed a superior performances to earlier design with promoting the analyses of samples as smaller as 0.2 ml (Llenado and Rechnitz, 1971).

All the cited results were just a launch points for a large scientific activity in which different research areas were unified and the obtained coupling have been multiplied by the changement of the biological elements and the type of the transducers. Organelles, bacteria, enzymes, biological tissues possessing particular enzymes were combined and investigated with amperometric or potentiometric devices, then piezoelectric, thermometric, optical, etc. the researches continue to enlarge the panoply of the usable and safely investigated physical sensors (Palchetti and Mascini, 2010).

The results of the research have led to a commercial exploitation of the conceived apparatus. The first biosensor presented in the market was the glucose biosensor used for diabetes diagnostics. The integration of ferrocene and its derivatives for amperometric biosensors application was presented in the literature by (Cass et al., 1984). The commercialization of the biosensors marks a positive and fast evolution for the clinical practices with the Medisense Exatech Glucose Meter and became the biosensor's world's best-selling ranked. The pen-shaped meter was the first electrochemical blood glucose monitor for diabetics patients with a self-controlling property and was presented in 1987 using GDH-PQQ and ferrocene derivative, and marks a revolutionary success in the health control process of diabetic patients (Matthews et al., 1987), it's also important to note that the enhance of the quality of the electrons transfer occurring between the glucose oxidase Gox redox center and the electrode surface was studied by integrating ferrocene

of ferricyanide in the conception of the glucose biosensors self-monitored, various strategies have been employed in this aim like enzyme wiring of GOx by electrons-conducting redox hydrogels (Yoo and Lee, 2010).

In 1960 the article published by Emil Palecek studied the electroactivity of the nucleic acids deploying the oscillographic polarography methods for an polymerized deoxyribonucleic acids (Paleček, 1960), few years later in 1996, Joseph Wang and it research group studied the sequence DNA biosensors using the peptides nucleic acid as probes and was one of highly performing projects in the DNA hybridization biosensors fields (Wang et al., 1996).

Chronologically, the development of the biosensors during the period 1970-1992 was marked by the article published by (Suzuki et al., 1975) about the First microbe-based immunosensor in which electrochemical and enzymatic reactions were studied in the aim of designing a sensor of ethanol and lactic acid, the investigation of the activity and stability of the enzyme immobilized in the collagen membrane showed a good results and gives the opportunities for future researches. Also in 1983, a research article published by (Liedberg et al., 1983) who investigate theoretically and experimentally the plausibility in a new flow of chemical biosensing area by studying the gas detection and biosensing with deploying surface plasmon resonance in which this optical technique under specific conditions was studied. An outstanding development and progress has been accomplished in the biosensory research field combining a multidisciplinary area of researches and bridged the conventional basic sciences as chemistry, physics and biology with the micro/nanotechnology, applicatory medicines and electronics (Bhalla et al., 2016).

The last thirty years, the annual publication's number in the biosensory field was few and numerable and the total World market was worth less than US\$ 5 million. The literature counted an annual international investment in biosensory research and development estimated around \$300 US million from 1999 (Alocilja and Radke, 2003; Spichiger-Keller, 1998; Weetall, 1999). The commercialization of biosensors technology had lagged behind the researches output as demonstrated by a plethora of research articles and patents. The period 1984-1990, more than 3000 articles and around 200 patents on

biosensors were presented in the literature (Collings and Caruso, 1997; Fuji-Keizai USA Inc, 2004). the considerable advancement in nanobiotechnology in the period 1998-2004 opened the gate for a plethora of 6000 publications and more than 1100 patents issued (Fuji-Keizai USA Inc, 2004) and gives the opportunity to the biosensors technology for a better efficiencies and performances especially in the selectivity and sensitivity improvements of the biosensors for a large exploitations. A continuous and impressive R&D activities were noticed in the literature for the role of biosensors in health, drug discovery and pharmaceutical and environmental sectors as main beneficiary sectors of this fields (Andreescu and Sadik, 2004; Hall, 1990). The combination of the laboratory diagnostics techniques with the automation and system integrations technology poses a high challenge in biosensor field to amalgam single of multiple target analytes and proved its effectiveness with a validation by an established test procedures due to its flexibilities. As the technological branch get developed as its serve better the biosensors improvements better and it's proved in the last decades, today, USD 22.4 billion is the biosensory market size value invested in 2020 and tends to increase to USD 41.8 billion in 2026 expected according to the Grand View Research, Inc report An exponential increase of both publications and commercially products is noted and calculated at a CAGR (compound annual growth rate) of 7.9% in the period 2021-2028, due to the rapid technological advancements as a main factor for the market growth and the rising prevalence of chronic diseases as diabetes and obesity.

### **2.3.2. Definitions and limitations:**

The concept of the biosensors has been tremendously progressed during the years, molding it concept and applications with enhancing the efficiency of every component to serve the science increase in all the touched fields, in the early years of apparition of this research area, the biosensor was defined as a self-sufficient analytical device interacting with chemical species in a biological environment. Annoying the important role of the active biological material in the device. This definition stayed absurd and causing misunderstanding, since any type of sensors investigated and used in biological samples can be named a biosensor (Luong et al., 2008). The biomolecular sensing was defined as the capacity to detect analytes in the biological molecules, environmental interests and other technological fields in which the concentration of a compound is able to

quantification in a sample, the selectivity of the biological element is considered the main important factor of the quality of the biosensor (Palchetti and Mascini, 2010).

The concretization of a definition of the biosensor started in 2000 with the International Unions of Pure and Applied Chemistry (IUPAC) have elaborated the definitions, nomenclature and classifications about electrochemical biosensors and the suggestions have been admitted and generalized to other types of biosensors (Thévenot et al., 2001). The IUPAC suggestions are given below:

“a biosensor is defined as a self-contained integrated device, which is capable of providing specific quantitative or semi-quantitative analytical information using a biological recognition element which is retained in direct spatial contact with an electrochemical transduction element. Because of their ability to be repeatedly calibrated, a biosensor should be clearly distinguished from a bioanalytical system, which requires additional processing steps, such as reagent addition. A device that is both disposable after one measurement, i.e., single use, and unable to monitor the analyte concentration continuously or after rapid and reproducible regeneration should be designated a single use biosensor.”

Few years later another concept was introduced, defining the biosensor as "a compact analytical device incorporating a biological or biologically-derived sensing element either integrated within or intimately associated with a physicochemical transducer", therefore including chemical compounds that imitate the biological materials during the conception of the biosensors (Newman et al., 2004).

A chemical sensor are a measurement devices used to convert a chemical or physical information of a specific analyte to a measurable signal, in which the magnitude is proportionally correlating with the analyte's concentration (Ohashi and Dai, 2006), chemical sensors include two basics parts serially interconnected: a chemical recognition part (receptor) that interact with the target molecules or ions in the sample and the consequence of the binding reveals a change in the material property (electrical conductivity and mass), and a physicochemical transduction part that convert the chemical interaction into a measurable and readable signal, generally an electronic signal (Gil et al., 2019; Mandoj et al., 2018). Biosensors are defined to be a chemical sensors,

the receptor part is a biochemical system (Cammann, 1977; Turner et al., 1987). The figure below presents the main component of a biosensor as detector, transducer and output system.

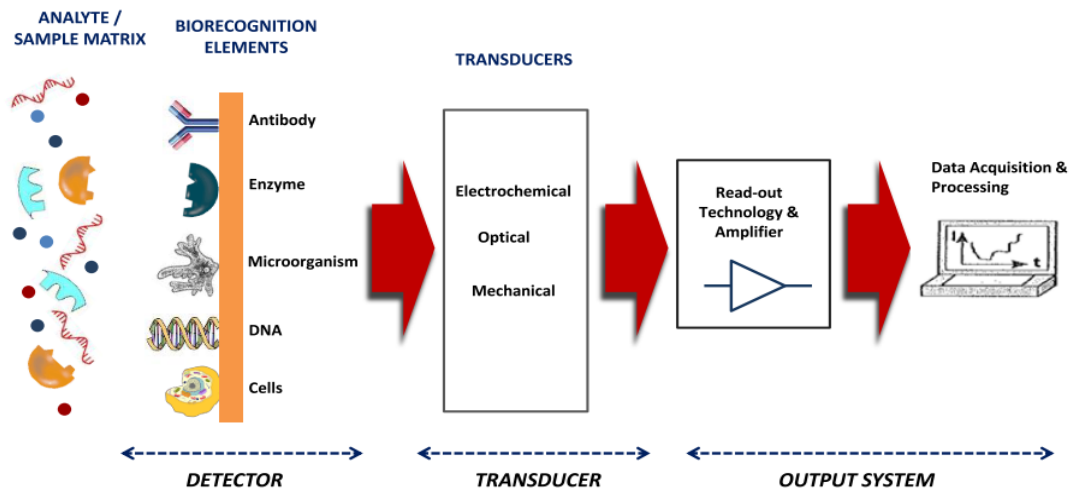


**Figure 2.2.** Schematic illustration of basic biosensor assembly including three components: detector, transducer and output system (Mohd Said, 2014)

The bioreceptor is a biological element (Enzyme, antibody, cell or DNA probe), is acting as a sensitive recognition element of the analyte that can be a complementary DNA, antigen or an enzyme substrate, etc. this part plays an important role for a biosensor due to its level of sensitivity that affect the quality of the obtained result and the analyse of the final data. It is crucial for a biosensor to be highly sensitive and selective in order to prevent interference caused by other substances or signal sources from the sample matrix (Liu et al., 2019). Examples of receptors used in biosensors are presented in table 2.2 and are restricted to the widely used biosensors.

The transducer part is a converter element responsible in the switch operation of a biorecognition event into a calculable and interpretable signal. This step is called signalization. This part of biosensor assure the transfer of the electrical or optical signal reflecting the amount of the interaction occurring between the analyte and the bioreceptor (Bhalla et al., 2016), example of electrochemical transducers, generally used for the precedent cited types of measurements in Table 2.1 are cited in Table 2.2 with examples



of analytes. The classification of the transducers depending on the recognition element is presented in the (Table 2.1) or by electrochemical transducer model (Table 2.2).

An electrochemical biosensor is defined as including an electrochemical converter as noted in Table 2.1 and reported to be chemically modified electrodes (CME), as semi-conducting, ionic conducting or electronic conducting material is covered with a biochemical film (Durst et al., 1997; Kutner et al., 1998).

**Table 2.1.** Types of receptors used in biosensors and the electrochemical measurement techniques, linked to them, which recognize specific species (Halilovic et al, 2019)

Transducers	Examples	Biological materials
Electrochemical		
1.Amperometric	1.Clark oxygen electrode, mediated electrode systems	Enzymes, immunological systems; Gases, enzyme, organelle, cell or tissue; Enzyme electrodes;
2.Potentiometric	2.Redox electrodes, ion selective electrodes, field effect transistors, light addressable potentiometric sensors	
3.Conductometric	3.Platinum or gold electrodes for the measurement of change in conductivity of the solution due to the generation of ions	
Optical	Photodiode, waveguide systems, integrate optical sensors	pH; enzymes; immunological analytes
Piezoelectric/ Acoustic	Piezoelectric crystals, surface acoustic devices	Volatile gases and vapors, antibodies
Calorimetric	Thermistor or thermopile	Enzyme, organelle, gases, pollutants, antibiotics

It's important to note that beside quantification of all the mentioned analytes, the biosensors are also used to detect and quantify microorganisms: the receptors in this case are yeast, bacteria or oligonucleotides probes coupled to piezoelectric, calorimetric, optical or electrochemical transducers. The chemical sensors, are considered self-sufficient and industrially conceived in one packed small unit. In which the receptor is directly connected with the transducing element to facilitate and flexibly the detection and measurement of the analyte.

The bioanalytical systems are mainly integrating four main components: presentation of the samples to be analyzed, bio-transduction, instrumentation and data quantification, as cited above, the activity of a biosensor can be extended to follow up biological or non-biological matrices, the biosensors containing arrays of nucleic acids hybridization sites are called genosensors and are used for genomic analysis (Beattie et al., 1995).

**Table 2.2.** Categories of the electrochemical transducer classification types of measurement, with corresponding analytes to be measured (Bergveld & Thevenot, 1993)

Measurement type	Transducer	Transducer analyte
1. Potentiometric	Ion-selective electrode (ISE); glass electrode; gas electrode; metal electrode.	K <sup>+</sup> , Cl <sup>-</sup> , Ca <sup>2+</sup> , F <sup>-</sup> H <sup>+</sup> , Na <sup>+</sup> ... CO <sub>2</sub> , NH <sub>3</sub> redox species
2. Amperometric	Metal or carbon electrode; chemically modified electrodes (CME)	O <sub>2</sub> , sugars, alcohols... sugars, alcohols, phenols, oligonucleotides. . .
3. Conductometric, impedimetric	Interdigitated electrodes; metal electrode	Urea, charged species, oligonucleotides . . .
4. Ion charge or field effect	Ion-sensitive field-effect transistor (ISFET); enzyme FET (ENFET)	H <sup>+</sup> , K <sup>+</sup> . . .

An electrochemical genosensors can be defined as a device containing biological receptors (oligonucleotides, aptamers, DNA) immobilized in the surface of the biosensors

for the identification of the analytes (nucleic acids) due to their affinity by complementary duplexes (Goumi, 2017). Such applications will be investigated in this thesis.

As seen from the classification of the biosensors above, several types of transducers can be investigated, as electrochemical, optical, thermal and piezoelectric types and shows common features, this thesis is restricted to the investigation in electrochemical biosensors.

The panoply of tested molecular recognition apparatus and also the used electrochemical transducers in the biosensors gives a higher flexibility of applications and facilitate the use in a wide range of fields.

### **2.3.3. Characteristics of biosensors:**

During the conception of a biosensors, as cited above, all biosensors possess some static and dynamic attributes and the performance of the biosensor is related to the optimization of these properties, it is primordial to control the important characteristics of a biosensor for an efficient performance.

**Stability** is one of the important properties of a biosensor, its defined as the level of susceptibility to environmental disturbances occurring around the system, and can affect the output signal of a biosensor during measurement and directly cause a change in the precision and accuracy level, this crucial characteristic is generally an axis of control in applications requiring continuous monitoring or long incubation process. Many factors impacting the stability is affinity of a biosensor and is related to the degree of the analyte binding to the bioreceptor, the degradation of a biosensor over a period of use is also an important factor impacting the stability level (Bhalla et al., 2016).

**Reproducibility** is the defined as the performance of a biosensor to be able to prompt the same signal in multiple experimental setups, these properties indicate the degree of accuracy and precision of both transducer and electronics, producing alike results respectively is an indicator of a high degree of precision and is a sign of the performance of the biosensor. A reproducible signal provide good reliability made on the response of a biosensor (Bhalla et al., 2016).

**Sensitivity** is the performance related to the ability of detection the minimum amount of analyte by a biosensor and it defines its limit of detection (LOD) (Bhalla et al., 2016).

**Selectivity** is a very important property that must be present in all the biosensors, it includes the ability of a biosensory system for detecting a specific analyte in a sample of different mixtures and contaminants, the widely cited example of selectivity in the literature is the case of the interaction of an antigen with an antibody, in this case antibodies interact as bioreceptors and are directly immobilized on the surface of the transducer. The solution containing antigens (generally buffer containing salts) is in direct contact with the transducer where the antibodies and antigens are in interaction only. In the conception and fabrication of a biosensor it's very important to take into consideration the degree of the selectivity due to its higher impact on the performance and efficiency expected (Bhalla et al., 2016).

### 2.3.4. Classification of biosensors

The literature presents a plethora of references detailing the classification of biosensors, but generally it is reported to be classified in accordance with the type of transducer or with the biological specificity mechanism as presented in this part of research.

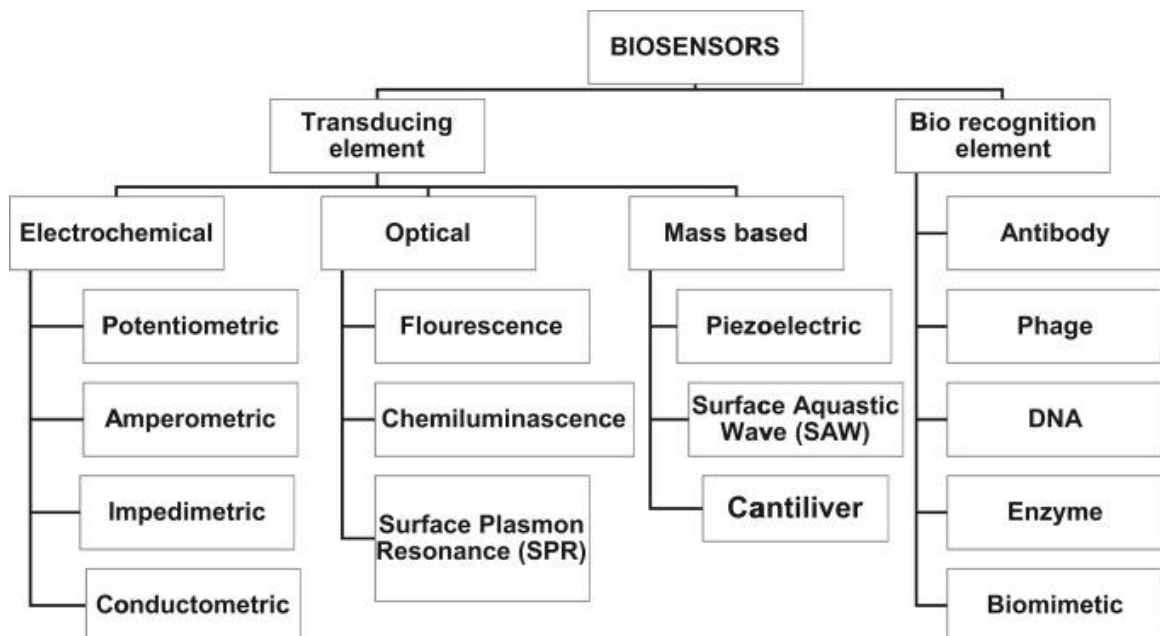


**Figure 2.3.** General classification of biosensors (Najeeb et al., 2017)

## 2.4. Nucleic Acids

### 2.4.1. General basics

Nucleic acids are defined as the vital constituents of living (with a range from the single-celled bacteria until multicellular mammals), is a long chain polymer composed of nucleotides, the two main types of nucleic acids are ribonucleic acids (RNA) and deoxyribonucleic acids (DNA), it is found in the nucleus of the eucaryotes and in the chloroplasts and mitochondria (Boundless.com, n.d.).

Both of DNA and RNA are composed of monomers known as nucleotides, combined each other to form polynucleotides. There are five basic types of nucleotides: Adenine (A), Cytosine (C), Thymine (T), Uracil (U) and Guanine (G).

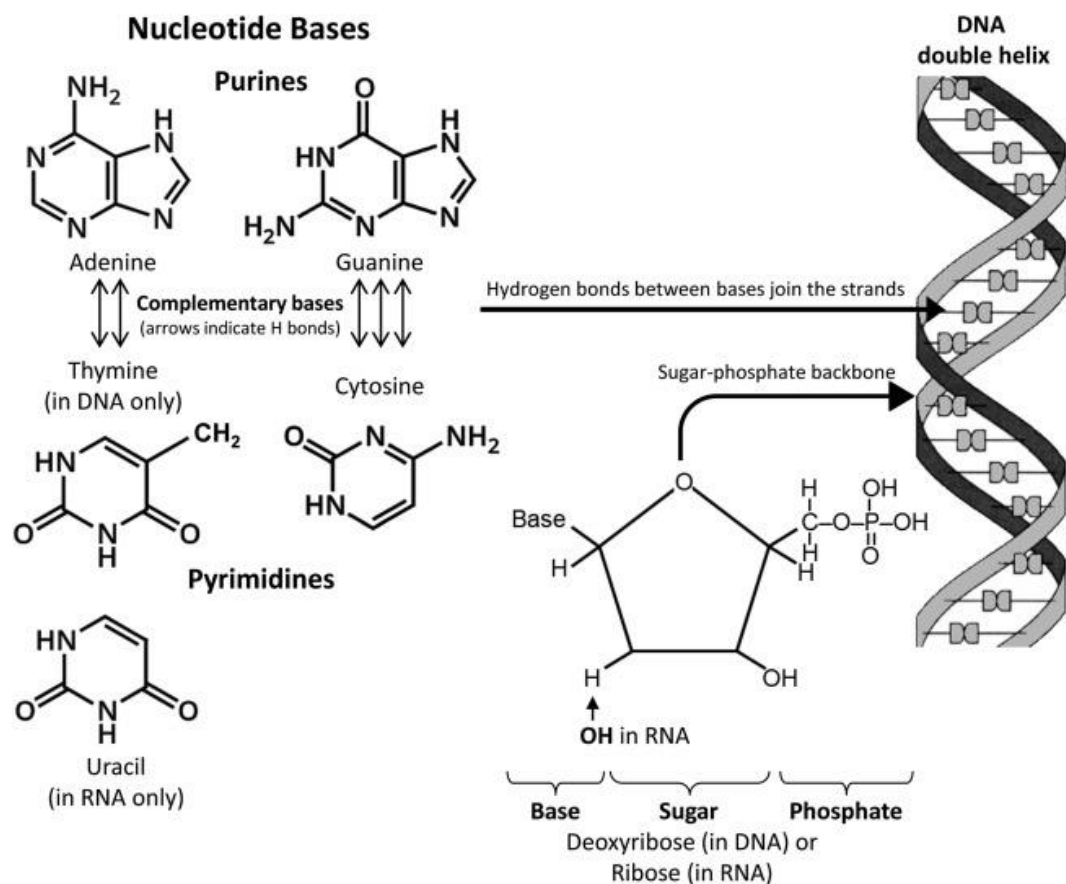


**Figure 2.4.** Structure and components of nucleotides (Nakatsu, 2021)

In the case of DNA or RNA, the nucleotide is skeletally composed of three main parts:

**A nitrogenous base** is an organic molecule, containing amino group that can bind an extra hydrogen, each nucleotide in DNA or RNA contains a nitrogenous bases as cited above. Adenine and Guanine are defined as purines and their structure is defined of two carbon nitrogen rings. Cytosine, Thymine and Uracil are defined and classed as pyrimidine which have one carbon-nitrogen ring being their main primary structure. DNA contains A, T, C and G, whereas RNA contains A, U, C and G.

**Five carbon sugar** in DNA is defined as deoxyribose and in RNA as ribose. The two forms are the most important part of the nucleic acid's structures and the difference between this pentose sugar is the hydroxyl group present on the second carbon of the ribose (which makes the RNA more hydrolysable) and hydrogen on the second carbon of the deoxyribose (the properties make the DNA more stable to be a genetic material).

**Phosphate groups** is defined from the structure to be attached to the hydroxyl group of the 5' carbon of the sugar base and the hydroxyl group of the 3' carbon of the sugar of the next nucleotide, and lead to the formation of the 5'3' phosphodiester linkage.

#### **2.4.2. The structure of DNA**

DNA structure is characterized by an arrangement of the nucleotides in a spiral as double helix form and looks like a twisted staircase with phosphate and sugar molecules placed outside of the helix surrounding complementary nitrogen bases. The nitrogenous bases are organized in pairs and are bounded via hydrogen bounds.

The movement in strands of the helix is in oppositely directions and this characteristic of a parallelism plays a major role in the DNA replication and an important factor for multiple nucleic acid's interactions.

The base pairs in the case of DNA are limited in 2 pairs allowed, Adenine pairs with Thymine and Guanine with Cytosine and this pairing is defined in the literature as the base complementary rule.

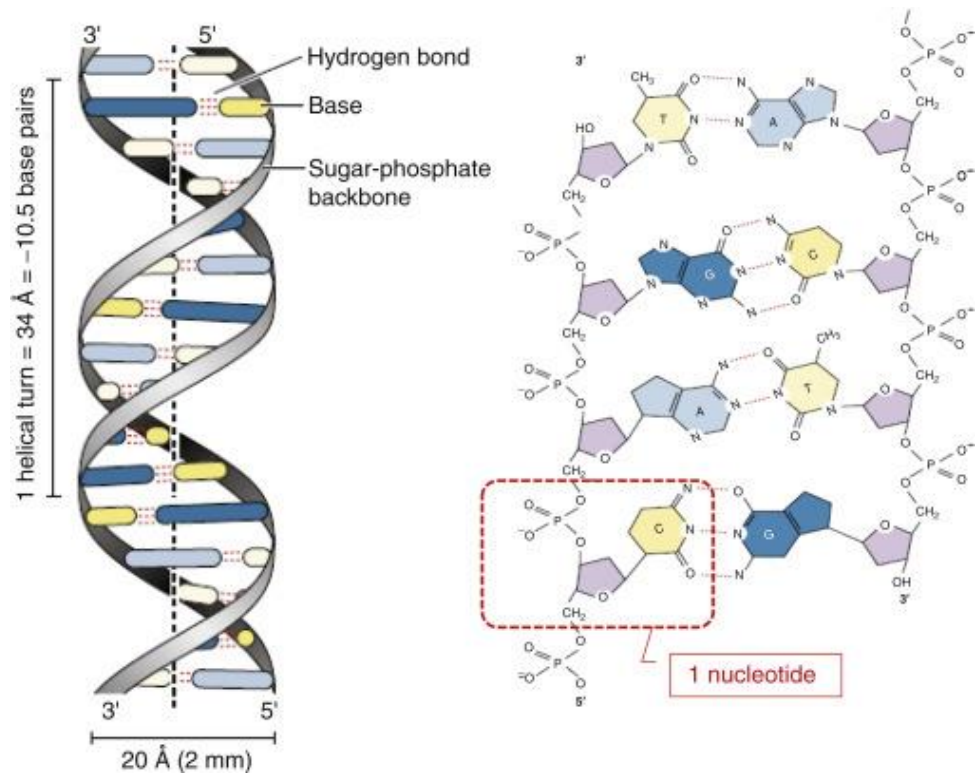


**Figure 2.5.** Schematic illustration of the DNA double helix model (Bano et al., 2016)

A sugar and a base are defined as nucleoside and in the addition of a phosphate group the nucleoside become a nucleotide and the differences are presented in the table and figure below.

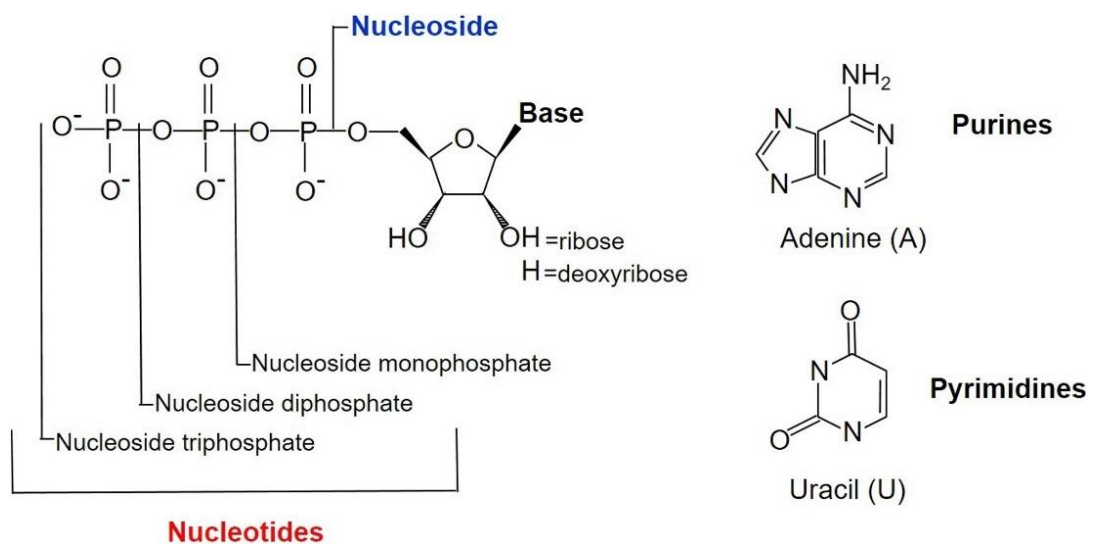


**Figure 2.6.** Biochemical structure of nucleotides and nucleoside's structure (Giuliani et al., 2019)

The stability of the DNA is impacted by different environmental conditions and factors. In the literature, the more guanine and cytosine bonds the more DNA become stable, this is related to the fact the C-G bonds have three hydrogen bonds instead of only two bonds for the A-T bonds. Many factors can impact the stability of DNA added to G-C content, chain length, presence of ions, temperature, etc. ...

### **2.4.3. The structure of RNA**

The RNA is another category of nucleic acid generally present in synthesis of proteins. In RNA the nitrogenous base is slightly different from the DNA. adenine (A), cytosine (C), guanine (G), and uracil (U) instead of thymine (T). RNA exists in single-stranded form and can have a varied length and structure, two hydrogen bonds between adenine and uracil, and three bonds form between cytosine and guanine and this base pairing is the basis of RNA structure.

The RNA polymerase synthesizes RNA from DNA through a transcription process, in the case of prokaryotes, for all the types of RNA, transcription is catalyzed by a single RNA polymerase. In eukaryotes case, multiple types of polymerases are present, each responsible for a synthesis of a specific RNA, RNA polymerase I synthesizes rRNA, RNA polymerase II led to the creation of mRNA, and RNA polymerase III creates tRNA.

The main function of the RNA is to create protein via translation process or simply to convert the information stored in the DNA into proteins, by carrying genetic information translated by ribosomes into proteins indispensable for the cellular processes.(Wang and Farhana, 2021)

The main types of RNA are rRNA is the ribosomal RNA and is defined to be as a crucial element forming ribosomes, mRNA which is the messenger RNA copied DNA in nucleus and carries the information to the ribosome in the cytoplasm, and tRNA the transfer RNA is responsible for the mRNA translation into proteins, it plays the role of carrying amino acids to the ribosome where they are joined to form proteins.(Wang and Farhana, 2021).



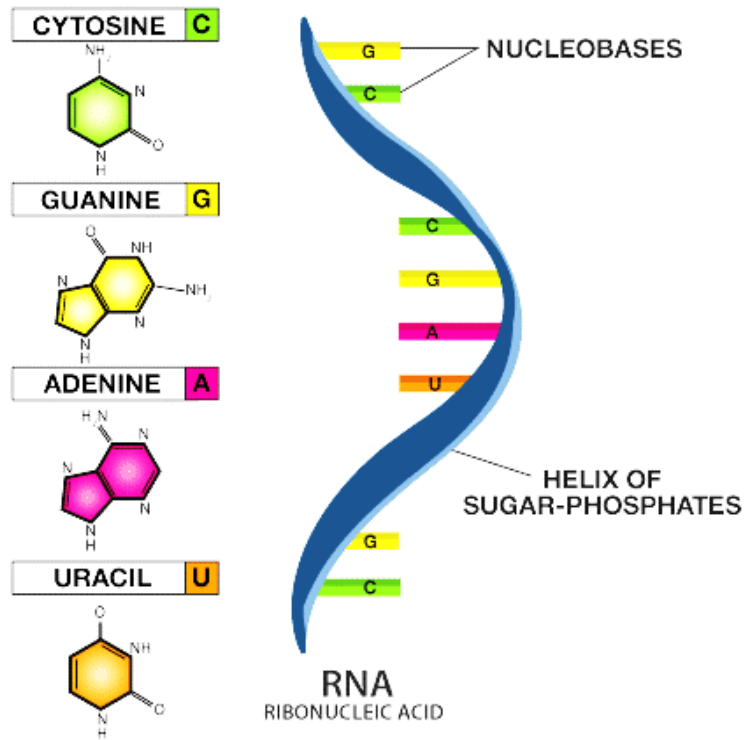


**Figure 2.7.** Basic structure of RNA (Thies, 2015)

#### 2.4.4. The structure of miRNA

In this part of research, the mechanism of the molecules is presented and studied for an efficient performance and an optimal condition of study. In this thesis the miRNA is used as a part of the project.

The literature presents a panoply of studies aiming to develop the use of small RNA in a biosensor. Multiple types of small RNA exist in eucaryotes and plays a role of gene expression's regulators in the cytoplasm and nucleus, they are known as a suppressor of undesired genetic materials and transcripts by regulatory mechanism:

- a- Post transcriptional gene silencing (PTGS).
- b- Chromatin- dependent gene silencing (CDGS).
- c- RNA activation

And this is why they have a primordial role in health and diseases diagnosis and need to be focalized on to understand the metabolism for a better use (Ha and Kim, 2014).

The terminology of small RNA was widely present in the literature as non-coding RNA molecules with a length varying about 18-30 nucleotides and can inhibit the expression of the target genes, the small RNAs are present in three classes: miRNAs (micro-RNA), siRNAs (small interfering RNA) and piRNAs (piwi-interacting RNAs). A plethora of studies in the literature were reported about the association of these molecules with biological functions and proved to be prominent and efficient. The small RNA sequence is inserted due to its ability of regulating the expression of multiple genes by binding to target genes as complement (Ha et al., 2008). The small RNA are able to regulate directly more than 30% of the genes in the cells, therefore they are involved in the regulation of the most important cellular functions as cell differentiation, proliferation, migration, growth, apoptosis, death, metabolism and defense (Wang et al., 2007; Zhang, 2008), these properties lead to give a pivotal role for the small RNAs as regulators in development, physiology and disease (Wang et al., 2007).

In the case of eucaryotes, miRNA are defined as small, non-coding and endogenous RNAs controlling the expression of genes by managing their target mRNAs (Zhang, 2008), their length is approximately about ~22 nucleotides, produced via Drosha and Dicer which are RNase III proteins dominating the classes of small RNAs, the miRNA binding regions is located in the 3' untranslated-region (UTR) of mRNA sequences (Bartel, 2009; Huntzinger and Izaurralde, 2011). Studies have shown that miRNAs can function like hormones. These properties lead the researchers to prove these extracellular miRNAs as a perfect biomarkers for a wide range of diseases and investigating the circulating miRNAs in cancer researches through its important role in the oncogenes control and as tumor suppressors (Condrat et al., 2020; Wang and Farhana, 2021). More than 60% of the human protein-coding genes pairs with miRNAs and results that most proteins-coding genes are under control of miRNAs (Huntzinger and Izaurralde, 2011). It is important to note that in addition that miRNAs is regulating the expression of genes, the expression of miRNAs are regulated by specific regulatory system (Gulyaeva and Kushlinskiy, 2016). The dysregulation is an important signal related to human diseases, including disorders and misfunction in neurodevelopment as fragile X syndrome and Rett,

complex behavior disorders such schizophrenia, depression and drug addiction, and also cardiovascular diseases, cancers, diabetes, livers and infectious diseases, a proper understanding of the miRNAs mechanisms influence fundamental insights into the causes of these fatal diseases and leads to develop targets for therapeutics methods (Im and Kenny, 2012).

#### 2.4.5. miRNA transcription

the transcription of miRNAs genes are processed by RNA polymerase II (pol II) and it generate a primary transcripts (pri-miRNAs) forming a hairpin secondary structure of approximately 50-120 nucleotides length, then, via multiprotein complex (Drosha and DGCR8 complex), a cleavage of the pri-miRNAs is accomplished, this process yields the pre-miRNAs exported from the nucleus to the cytoplasm by Exportin-5 by binding from the 3' overhang, in the cytoplasm, Dicer cleaves the hairpin loop in order to generate a miRNA duplex having approximately ~22 nucleotides single-stranded miRNA made from one arm of the pre-miRNA, the obtained mature miRNA is induced into the RNA-induced silencing complex (RISC) in a sequence event controlled by Dicer, TAR RNA-binding protein (TRBP). Once incorporated into RISC the miRNAs guide the ribonucleoproteins complex to specific mRNAs transcripts through complementary base pairing interactions with in the 3'UTR of the target mRNA transcript, named as MREs: miRNA response elements as presented in the figure below (Im and Kenny, 2012)

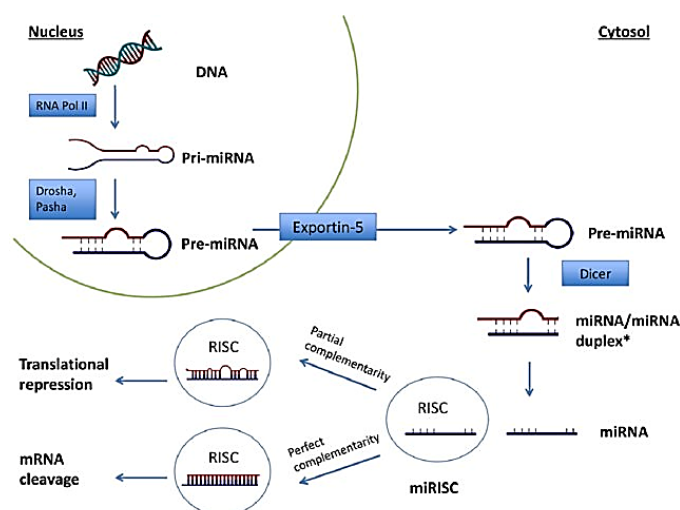


**Figure 2.8.** miRNAs biogenesis and functions (Magri et al., 2018).

The miRNAs gene is one of the widely propagated genes family and are observed in animals, plants, protists and viruses (Ha and Kim, 2014). miRBase is the international database for all investigated miRNAs and associated annotations with aiming to assign stable and consistent standard name to newly discovered miRNAs. The latest upload of the miRBase has enumerated 2588 miRNAs in humans, although the functional importance and performances of the cited miRNAs annotations is still a research gate and need to be investigated (Chiang et al., 2010; Kozomara and Griffiths-Jones, 2014).

The process of transcription of miRNAs is carried out by RNA pol II (Cai et al., 2004; Ha and Kim, 2014; Lee et al., 2004), in addition RNA pol III has been studied to transcribe a class of viral miRNAs (Pfeffer et al., 2005), the transcription of tRNA by RNA pol III and derivation of small RNAs can occurs and a type of endogenous miRNAs are obtained (Babiarz et al., 2008). The main role of the transcription factors is regulating the miRNA's expression (Graves and Zeng, 2012), p53, MYC, ZEB1, ZEB2, and myoblast determination protein 1 (MYOD1) are defined to be a transcription factors regulating (positively or negatively) miRNA expression as presented is the figure below (Kim et al., 2009; Krol et al., 2010). It is also important to note that the miRNAs genes regulations can also be contributed by a methylation of DNA and histone modifications (Davis-Dusenbery and Hata, 2010; Ha and Kim, 2014).

#### **2.4.6. miRNA nuclear processing**

In the nucleus stage, following transcription and formation of the primary miRNA (pri-miRNA) transcripts they need to be modelled to undergoes several levels of maturation. The pri-miRNA is about 1 kb long and containing local stem-loops, in which mature miRNA is embedded. Pri-miRNA stem length consists of 33-35 bp and has a terminal loop and a single stranded RNA sites at the 3' and 5' sites. The nuclear RNase III Drosha initiate the process of maturation by cropping the stem-loop and a small hairpin-shaped RNA of f ~65 nucleotides in length named as pre-miRNA is released. the microprocessor complex is defined in the literature as the protein complex formed of Drosha with its cofactor DGCR8. Drosha is the nuclear protein of ~160kDa, like the dicer it belongs to a family of RNase III types endonucleases that are efficiently acting on double stranded RNA (dsRNA). Drosha and DGCR8 are cited to be conserved in mammals ( fractionating

about 650 kDa) (Ha and Kim, 2014). the pri-miRNA processing is very important due to its effect of defining the miRNA abundance.

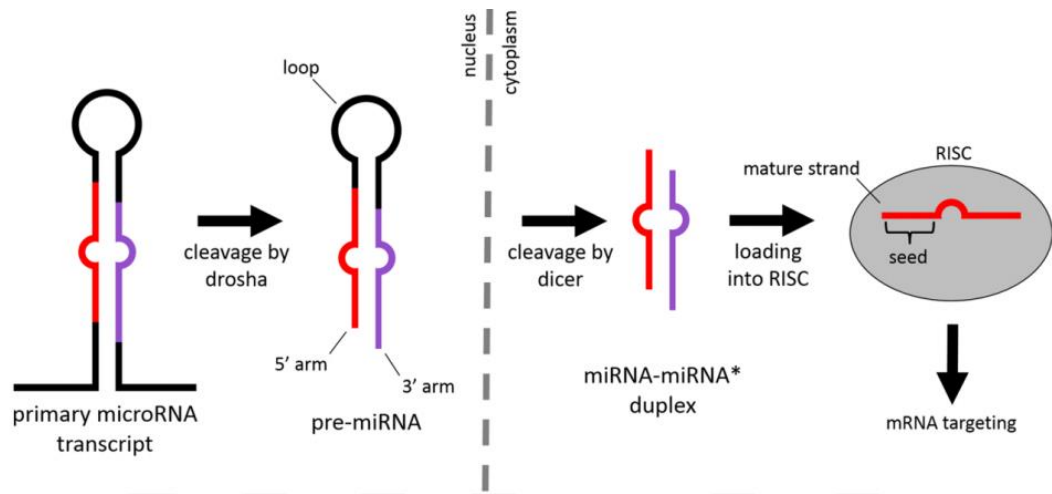


**Figure 2.9.** Schematic illustration of translocation occurring in microRNA from nucleus to cytoplasm (Durası, 2018)

Upon Drosha processing, a translocation of the pre-miRNA from the nucleus to the cytoplasm via exportin 5 (EXP5) process is realized as presented in the figure 2.10.

The EXP5 with GTP-binding nuclear protein form RAN.GTP and with the pre-miRNA combines to form a protein owing the role of transportation of pre-miRNA. After the process of translocation, pre-miRNA is released and GTP is hydrolysed and the complex of transport disassembled (Bohnsack et al. , 2004).

The transcriptional factors (TFs) as present in the literature defined as an important element contributing to biological mechanisms during the phase of gene's transcription, and are not just limited in the regulatory role of genes expression.

Compared to transcriptional regulators, miRNAs play an important role as a posttranscriptional regulator, for their activity in the cytoplasmic part as regulating transcripts in different special tissues, and causing a disturbance and even cancel out the process of upstream process in the transcriptional phase in the nucleus (Durası, 2018).

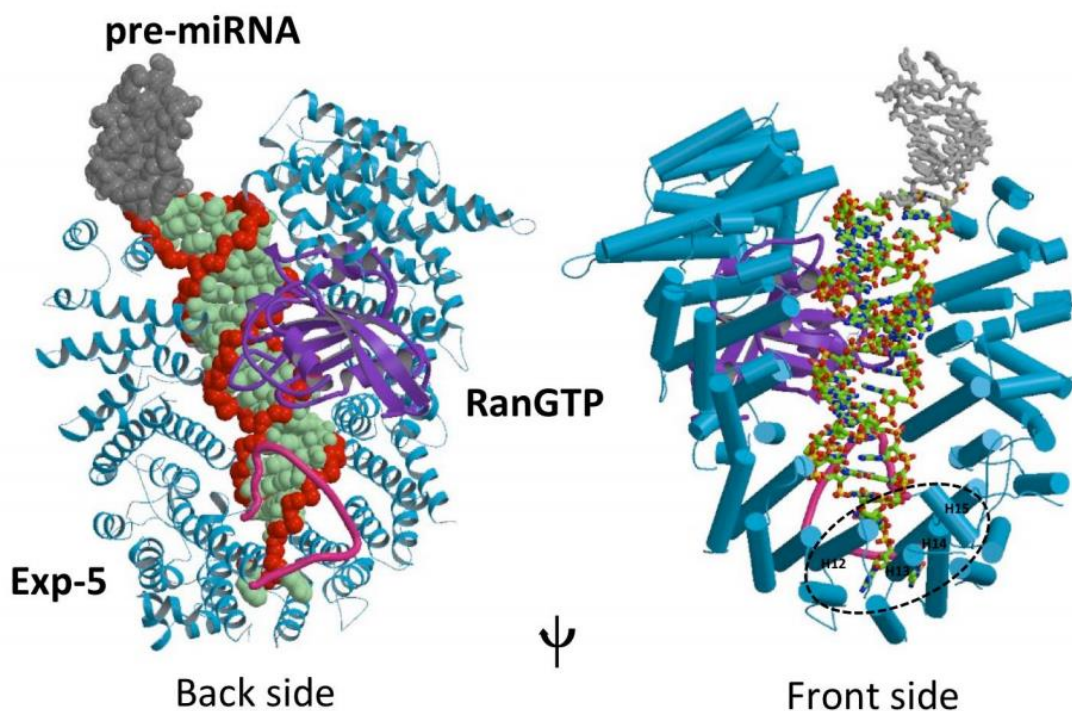


**Figure 2.10.** Schematic illustration of pre-miRNA exported by EXP5-RAN•GTP transport complex (Durası, 2018)

## 2.5. Electrochemistry

### 2.5.1. General view

Electrochemistry is defined as a branch of science studying the movement of the electron during the reduction and oxidation reaction at a surface of an electrode. Every analyte is susceptible to an oxidation or a reduction at a particular potential and the measurement is proportional to the concentration and is very efficient towards bioanalysis due to its wide use for measurement of multiple types of analytes and its ability and flexibility to be used in a plethora of techniques and sensors that can be made in-vivo, ex-vivo and also in-vitro (Patel, 2020). The electrochemistry activities play an advantageous role in the investigation of nerve's impulses transmission for integrated biological systems, electron's transfer and redox chemistry reactions and their analysis and in a wide range of electrochemical applications offering a flexibility of use with a secured repeatability.

Electrochemical reaction can be defined as a chemical reaction in which electrons flows between an interface electrode and a substance, this flow involves a charge transfer and triggers an electric current through the electrodes causing a liberation or absorption of heat.

The electrochemical unit usually includes 3 main electrodes: a reference electrode, a working and auxiliary electrode. The reference electrode is generally made of Ag/AgCl and is always kept distant from the reaction apparatus in order to keep the potential in a stable level. The working electrode is the transduction element during the biochemical reaction. While the reference electrode is in an interconnection with the electrolytic solution in which a current can be applied to the working electrode. It is primordial to note that the electrodes have to be conductive and maintain chemical stability (Grieshaber et al., 2008).

The electrochemical techniques are generally based in the measurement of the signal of an electrochemical cell integrating an ion-conducting phase. The electroanalytical techniques are classified into different categories based on the applied potential or current for a measurement of an impedance, current or potential etc.(Bakirhan et al.,2021).

Generally, the electroanalytical methods are compared with the atomic absorption spectroscopy (AAS) and inductively coupled plasma (ICP), but the electroanalytical methods give more advantages to be used as the rapid response without any pre-treatment procedures needed. In this side a simple basic principle is applied, the analyte that have to be measured should react directly. The important benefits of the electroanalytical measurements are grouped in the literature as (Bakirhan and Ozkan, 2018):

1. Higher specificity.
2. Selectivity in function of the chosen material.
3. Noticeable level of sensitivity and low detection limits.
4. Possibility of real time results.
5. Possibility to be designing in a small sized sensor.

In the biosensing field, the obtention of the desired measurement from the biological system is generally electrochemical in nature, although the biosensing devices use wide types of recognition elements, the electrochemical detection techniques use generally enzymes, due to their higher binding potential (Grieshaber et al., 2008). The electroanalytical measurements can be performed by different types according to the electric parameters that are measured and can be classified mainly as potentiometry, amperometry, conductometry, electrogravimetry, voltammetry (and polarography), and coulometry. Most of the electroanalytical methods are relying the flow of the electrons between the electrodes and the analytes, the analyte have the ability of accepting electrons (reduction) or donating electrons (oxidation) to the electrode (“Chemical analysis - Electroanalysis | Britannica,” n.d.). in this thesis the project was using the voltammetric methods in the electrochemical part of the biosensor’s performance.

### **2.5.2. Voltammetry**

Voltammetry is a branch of the electrochemistry, developed earlier in 1922 by y Czech scientist Jaroslav Heyrovský, who received the Nobel prize in chemistry in 1959 for his works in the field of voltammetry, then the scientific researches highly advanced between 1960-1970 aiming to improve the performances, sensitivity and range of analytical techniques for a wide range of use especially in biologic and pathologic applications.

Voltammetry is reported to be an electrochemical technique with a working principle of applying a varying potential to a working electrode and the corresponding obtained current after an electrochemical measurements is then plotted and calculated, voltammetry is a technique generally used in bioanalysis, these methods are called active methods in the reason of the change that happen due to applied potential lead to a concentration’s difference of an electroactive species occurring in the surface of the electrode, this is a result of an electrochemical reduction or oxidation (Sharma & Mehtab, 2020). the result that comes from the voltammetric experiment in the form of voltammogram as curves,  $I=f(E)$  (Roy and Pandit, 2018).

Voltammetry technique can be used for the analysis of a plethora of molecular and ionic materials. In this method the electrochemical cell composed of three electrodes defined as a working electrode, reference electrode, and counter (auxiliary) electrode and



assembled with a device named potentiostat that control the applied potential at the electrolyte/working electrode interface as a function of the reference electrode potential. the potentiostat has an important role of generating accurate and control of the potential applied with a higher flexibility due to its internal electronic system that include converter, electrometer circuits, a microprocessor with internal memory and amplifier(Sharma and Mehtab, 2020).

The electrochemical cell:

The electrochemical cell in the case of the voltammetric system is named as a sample holder in the fact that its where a proper dissolution of the analyte in a specific solvent occurs and is placed into an ionic electrolyte. The typical arrangement of a voltammetric electrochemical cell is composed of four elements as below:

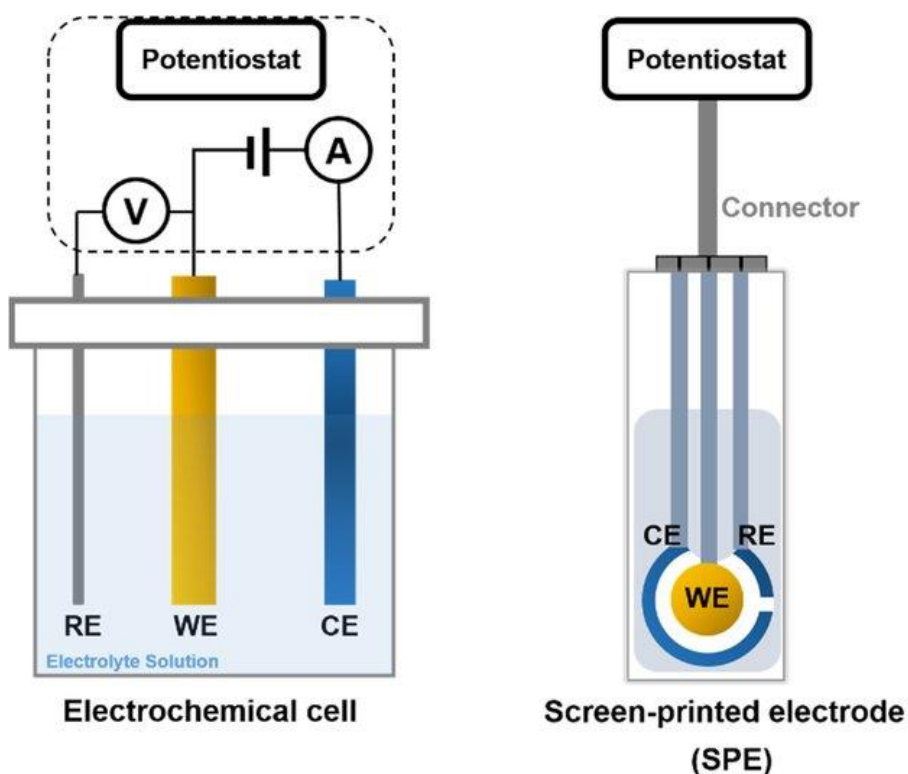


**Figure 2.11.** The schematic representation of electrochemical biosensors types with three main electrodes: working (WE), reference (RE) and counter (CE) connected to a potentiostat.(Damiani and Schuster, 2020)

## Working electrode (WE)

The working electrode is an important part of the voltammetric electrochemical cell affecting the sensitivity and the quality of the obtained signal, it is important to choose the right working electrode for a better performance of the system. This electrode is defined as the element in which the reaction of interest occurs, the composition of this element in electrochemical cell is redox-inert material and this is one of the most important property, the choose of the working electrode can vary depending on the experiment to be suitable to provide potential possibilities or to promote the surface adsorption performances of the species of interest (Elgrishi et al., 2018a).

Different electrodes materials can be used: Mercury, gold, platinum and various forms of carbon are some metals which are used widely in literature and leads to obtain a variety of electrochemical responses. The modification and changement of the material used in electrode is a challenging part to diagnose in the conception of the electrochemical cell. It is also important to note that during the electrochemical event occurring at the surface of the working electrode, it is primordial that the electrode surface be totally clean and maintained for an optimal performance. The presence of impurities in the solvent, the risk of adsorbing to the carbon electrode surface is higher and lead to changement of voltammograms and affect the quality of the obtained results. To avoid this kind of situation a treatment of the surface is required.

As cited above, a wide range of material is used in the working electrode, the case of mercury exhibits a wider negative potential due to the surface reduction in hydrogen ion or water in it. The case of platinum is cited as durable and flexibly used in an anhydrous organic solvent, this is not the case for gold being less useful due to its surface undergoes oxidation even at a lower amount of positive potential, carbon is the widely nowadays used in different forms as working electrode and offering a wide potential range with high conductance, stability, flexibility and economically advantageous. this project of thesis is also using this carbon material for enhancing the electrochemical property of the surface of the biosensors.

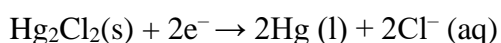
Reference electrode (RE):

The reference electrode is an independent, stable electrode and defined to be an electrode potential used as the third electrode electrochemical cells systems for voltammetry application. The composition of this electrode must respect the characteristics of higher stability and reproducibility of potential all along the electrochemical analysis and measurements. The purpose of this electrode is to provide a maintained and stable potential for an optimum controlled regulation of the working electrode potential. Owing zero impedance or nearly is an expected characteristic of an ideal reference electrode. This is determined by the resistance (that must be high) of its isolation junction. In order to limit the Ohmic drop occurring between the reference and working electrode, it is recommendable to be nearly placed (Ossila, n.d.).

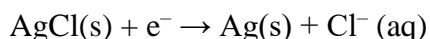
A large variety of reference electrodes for an aqueous media applications have been reported in the literature as standard hydrogen electrode (SHE), saturated calomel electrode (SCE) and the AgCl/Ag electrode. It is also noted that via a porous frit, a proper separation of the solution can be applied and advised to minimize the junction potential. In the case of the nonaqueous solvents the reference electrodes have been reported to be made from the Ag<sup>+</sup>/Ag couple are generally used and they consists of a silver wire immersed in a solution containing Ag<sup>+</sup> salt, standardly AgNO<sub>3</sub> (Elgrishi et al., 2018a).

The working electrode's importance in the voltammetry experiments is generally bounded with some critical conditions as the reference electrode. The isolation of the counter electrode and the sample is not required all the time as the electrode to be referenced have to result in a reversible half-reaction following a Nernstian behavior and the insulation of these electrodes from the samples is done in the aim to prevent any contamination of the solution to be done and to be affecting the quality of the analyses (Sharma and Mehtab, 2020).

- Half reaction for SCE:



- Half reaction for "silver-silver chloride" or "Ag/AgCl" electrode:



Counter electrode (CE):

A counter electrode (auxiliary electrode) is a special electrode used in the electrochemical cells for voltammetric analysis and used to make connection to the electrolyte in the aim of applying a current to the working electrode. The potential applied to the working electrode a followed reduction or oxidation of the analyte can be observed, the current begins to flows and the main role of the counter electrode is completing the electrical circuit, the current is calculated between the working and the counter electrode as electrons flows. The counter electrode is generally ensured by the use of platinum wire or disk and recently the use of carbon-based counter electrode is also available due to the wide range of advantages of these materials that will be detailed in this thesis. The counter electrode should be chosen to be as inert as possible (Elgrishi et al., 2018a).

Electrolytic solution:

The electrolytic solution in the electrochemical cells for a voltammetric use must be at the room temperature and having sufficiently the solubility for ionic substances to form an electrolyte. The electrolytic solution's main characteristic is its ability for dissolving the electro-active species with a high potential region for the redox process of interest and this means that the solvent itself must not undergo oxidation or reduction in the potential region and must hold the properties of required acid-base. The wide example used solvent is water and Salts like tetraalkylammonium are used in organic solvents but also depending on the species interests and when the pH is an obligation to be maintained at a stable reaction, a plethora of buffer are used as phosphate, acetate, citrate and Britton-Robinson buffers (Sharma and Mehtab, 2020).

### **2.5.3. Types of voltammetric techniques**

The electrochemical cell, where the voltammetric analysis occurs, consist of an amalgam of elements chemically and physically coordinated. The occurred oxidation or reduction of a substance at the surface of the electrode at an appropriate potential applied lead to a changement and a transport of a mass of new material to the electrode surface with a generation of a current that can be interpreted as a form of graph. The voltammetric

techniques are owing one fundamental principle are issued from the same electrochemical laws common to all the voltammetric techniques, the reported difference between these techniques by the material chosen for the working electrode and the applied potential. These cited differences can lead to an obtention of a variety of electrochemical, physical and chemical information such rates constants for chemical analyses, electrons investigated during the redox reactions and constants of diffusion (Sharma and Mehtab, 2020; Kounaves, 1997). The most used voltammetric techniques are presented in the following part.

#### Cyclic voltammetry (CV):

The cyclic voltammetry is considered one of the powerful and popular reported electrochemical technique in a wide range of chemistry, this technique have been used for its large advantages for the analysis of the redox reactions occurred for molecular species and become an indispensable tool for analysing electrochemical reaction and electroanalytical measurements in a variety of fields especially in pharmaceutical analysis and biological materials (Elgrishi et al., 2018b).

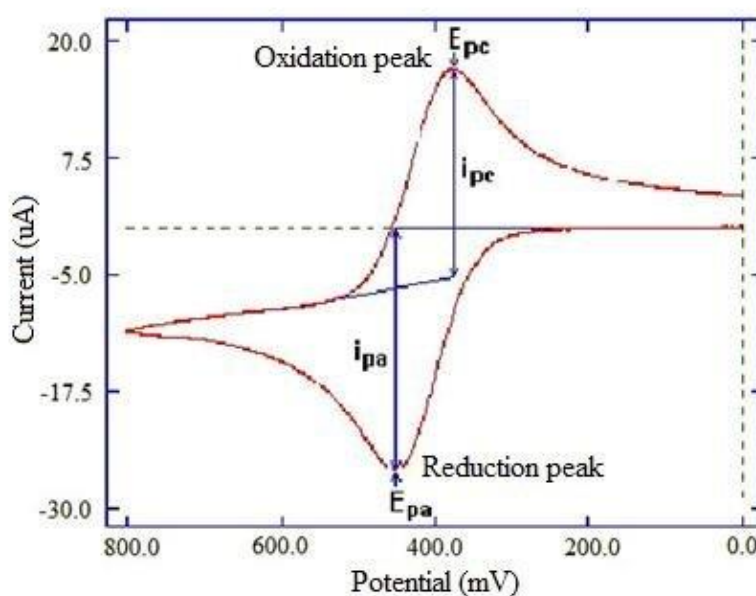


**Figure 2.12.** A typical cyclic voltammogram showing oxidation and reduction current peaks (Kumar and Bankoti, 2009)

The cyclic voltammetry was first reported in 1938 by Randles to analyse the electrochemical behavior of a substrate in electrolytic medium. The principle of this method is based on the variation of the potential applied at a working electrode with a preliminary fixed scan rate while observing the current and depending on the analysis, one or a series of cycles can be studied, the final obtained results are performed in a cyclic voltammogram (Kounaves, 1997).

The main important parameters in a cyclic voltammogram are the peak of potentials: anodic peak potential ( $E_{pa}$ ), cathodic peak potential ( $E_{pc}$ ) and peak of currents: magnitudes of anodic peak current ( $I_{pa}$ ), the cathodic peak current ( $I_{pc}$ ).

A cyclic voltammetry CV circuit's main elements are a potentiostat, data acquisition system, an electrolysis cell and a current-to-voltage converter. The applied potential during the cyclic voltammetry CV measurements controls the concentrations of the redox species at the electrode surfaces and is described by the Nernst equation:

$$E_{cell} = E^0 - \left(\frac{RT}{nF}\right) \ln Q$$

where  $E_{cell}$  is the cell potential and  $E^0$  represent the cell potential under standard conditions,  $R$  is the universal molar gas constant,  $n$  is the number of electrons transferred,  $Q$  is the reaction quotient,  $T$  is the temperature,  $F$  is the Faraday's constant (96.485 C/equivalent) and  $E^0$  is the standard reduction potential for the redox couple.

In order to report the data from the cyclic voltammetry, the literature present two conventions widely used, the US and the IUPAC conventions, as seen in the figure below the graphics appears being rotated by  $180^\circ$  and the difference resides in the potential axis. Each traces contains an arrow mentioning the direction in which the potential is scanned to record the data as indicated in the figure below (Elgrishi et al., 2018b):

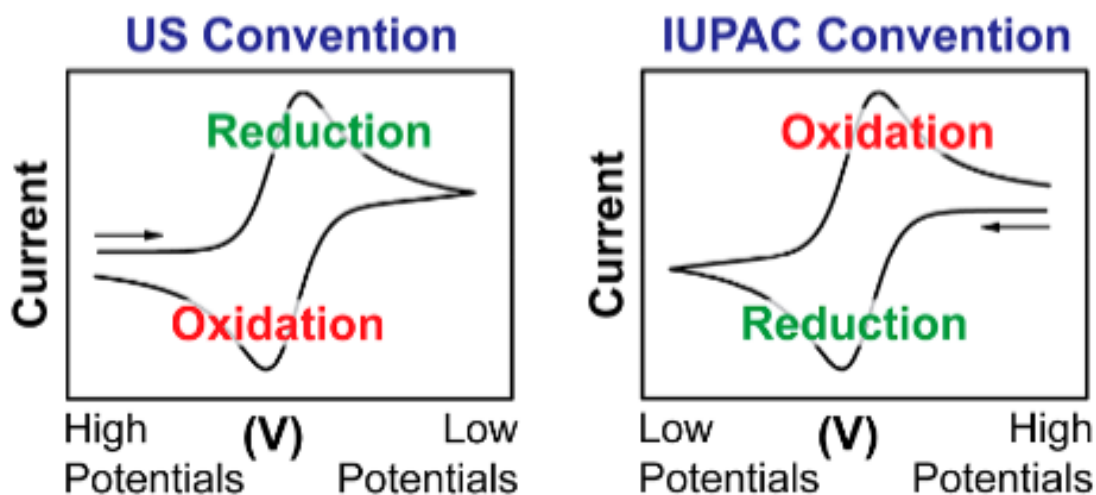


**Figure 2.13.** IUPAC and US convention for Cyclic voltammogram (Elgrishi et al., 2018b)

Differential pulse voltammetry (DPV):

In the order to enhance the sensitivity and performance efficiency, many techniques were involved in the literature by changing the parameters controlling the progress of the analyses and also many forms of modulations have been investigated and analysed over the years ( Kounaves, 1997).

The pulse voltammetric techniques are one of the most used in the electrochemical analysis characterized of a frequently potential and the main principle of the reported pulse techniques is the rate of the decay's differences of the changing and the faradaic currents following the potential step named as pulse.

It is also important to note that the charging current decays exponentially, whereas the faradaic current decays as a function of  $1/(\text{time})^{1/2}$  and in this way the rate of decay of the charging current  $I_c$  is faster than the decay of the faradaic current  $I_f$  and the charging current is considered negligible at a time of  $5R_uC_{dl}$  after the potential step ( $5R_uC_{dl}$  represent the time constant for the electrochemical cell and ranges from  $\mu\text{s}$  to  $\text{ms}$ ) (Mendoza et al., 2015).

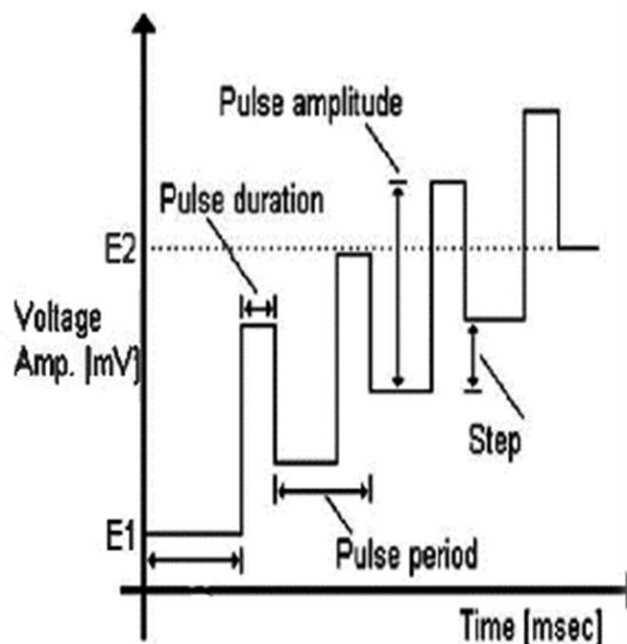


**Figure 2.14.** The important parameters in pulse voltammetry (Amin et al., 2016)

The most important parameters for the pulse techniques are cited as:

1. **The pulse amplitude** is attributed to the calculated height of the potential pulse.
2. **The pulse width** convenient to the duration of the potential pulse.
3. **Sample period** is the time at the end of the pulse during the which the current is measured.
4. **The pulse period** or also named as drop time must be specified for some pulse techniques and defines the time required for one complete potential cycle.

In the pulse voltammetry techniques, three techniques are the most widely used (Normal, square wave and differential voltammetry) and differs in their waves forms, sampling points numbers and also whether an electrode (voltammetry) or a mercury drop electrode (polarography) is used. These techniques are convenable in the case of quantitative analysis (BASi®, 2018). The main common principle of pulse voltammetry is the difference in rate of decay of faradaic and capacitive current (Sharma and Mehtab, 2020).



The differential pulse voltammetry was introduced by Barker and Gardner and have the ability of impacting higher sensitivity, the efficient resolution of a wide range of species and the peak-shaped response with a higher minimization of double layer and background effects. This technique has been applied for the quantification of drug, biomolecules

## **2.6. Electrochemical DNA biosensors**

### **2.6.1. General aspect**

The electrochemical DNA biosensors have been reported in the literature taking advantages from the characteristics (affinity) of the single strand DNA for complementary strands of DNA and are largely deployed in the detection and analyses of specific sequences of DNA and aiming to enhance the quality of the analytical devices in a wide range of species and applications. A great progress was noted in the literature in this field and numerous challenges are still overcoming especially in the bio electrochemical detection of some diseases (Odenthal and Gooding, 2007). Compared to enzymes or antibodies bioreceptors, nucleic acid recognition layers can be synthesized and regenerated and this in an advantage for its use however the DNA damage is an important factor to be noted when nucleic acids bioreceptors are used. The use of chemical can cause an irreversible damage to DNA by changing the morphological structure of DNA and also the base sequences that lead to disturb the DNA replication (Velusamy et al., 2009). In order to minimize the instrumentation's sizes of the DNA detection and the costs of the purpose, the use of the electronics improvements leads to developing a chips performing for the detection of target with an interpretable electrical signal, in fact, the miniaturization of the electrochemical devices facilitate their use in a plethora of application and domain and make them one of the most used tools for DNA diagnosis (Cagnin et al., 2009).

The principle of the electrochemical DNA biosensors is centered on the hybridization of nucleic acids sequences an the electrochemical detection of the DNA hybridization includes a control of current response based on a complementary matching recognition under a controlled potential beforehand fixed (Dođru, 2017). An immersion of the probe-modified electrode in the solution including the target DNA (the DNA sequences that have to be measured) is carried out. In the case of the target DNA contains a sequence

matching that of the immobilized probe DNA, a hybridization is occurred and a hybrid duplex DNA is formed at the electrode surface (figure 2.15). It is important to note that the hybridization is generally detected and interpreted through a change in the current signal of an electroactive indicator, linked to the use of enzymes or redox labels or also from the hybridization-induced alterations in electrochemical parameters as conductivity or capacitance (Dođru et al., 2017). The preparation and conception of an efficient and highly sensitive electrode with a higher selectivity of electrochemical probes are the most important key in developing and enhancing the quality of performance of an electrochemical DNA biosensor (Liu et al., 2012a).

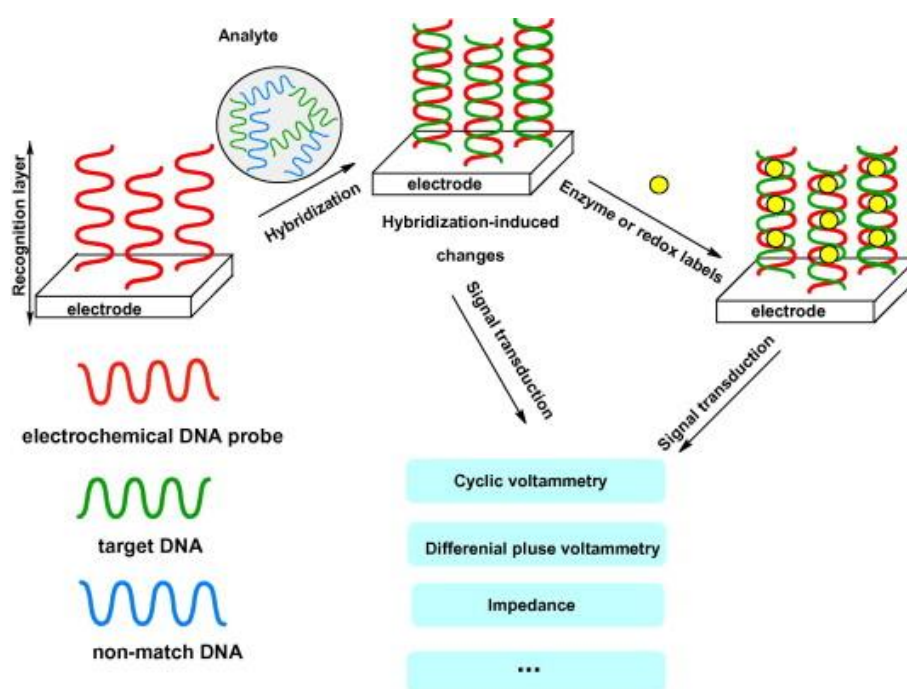


**Figure 2.15.** General design of DNA biosensor (Liu et al., 2012b)

### 2.6.2. Methods of DNA immobilization onto sensor surfaces

In the last decades, the researches in the fields of electrochemical DNA biosensor owed a large interest due to its facility of application and its flexibility for different materials, the researchers converged the efforts on the applicability of the DNA in the biosensory system and its integration in the sensor surface taking advantages from its ability of detecting target DNA reported as very sensitive, therefore the DNA hybridization process had become the main part in the conception and construction of the DNA biosensor device

based on a single stranded DNA (ssDNA) probes layer that must be immobilized on a transducer surface in order to recognize its complementary DNA target to obtain a DNA double helix that can be later converted, quantified and interpreted in the following part.

The immobilization of DNA probes on the working electrode surface is a crucial part in the construction of an electrochemical DNA sensor and affect the performance of the final obtained results and interpretations, an efficient DNA probe immobilization leads to promote an higher orientation and reactivity of the immobilized DNA probe for an efficient hybridization (Rashid and Yusof, 2017). The literature reported several procedures for probe immobilization techniques on the transducer surface that have been investigated in electrochemical DNA sensing as detailed below.

#### Adsorption:

This method is defined to be a simple technique used for the DNA probe immobilization on the working electrode surface, because it doesn't require any modification of DNA or any chemical reagents. The principle of this methods is based on the immobilization of the DNA probes on the surface of the working electrode via an electrostatic adsorption occurring between the positively charged films-modified electrodes and negatively charged phosphate group of DNAs (Rashid and Yusof, 2017).

The simplicity of this method resides in the fact that the DNA didn't require any preliminary modification so that these moieties can be absorbed by dipping surface in DNA-containing solution for a preconized time and following it by rinsing to remove the unabsorbed species, this physical adsorption and electrostatic accumulation is studied to be an easy and fast method to immobilize DNA onto carbon transducers (Erdem et al., 1999; Erdem et al., 2004; Marrazza et al., 1999; Ozkan et al., 2002; Singh et al., 2011; Wang et al., 1996). The adsorption method don't require reagents or labeled nucleic acids and complicated process but disadvantages as the uncontrolled immobilization of DNA and a weak bound of the nucleic acid to the surface can be obtained in this technique (Ozkan-Ariksoysal et al., 2012; Doğru, 2017).

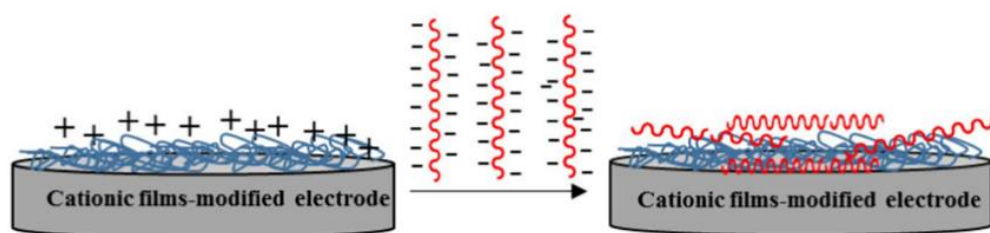


**Figure 2.16.** DNA probe immobilization via electrostatic adsorption (Rashid and Yusof, 2017)

Covalent immobilization:

The covalent binding process of biomolecules and especially of DNA onto solid substrates attract the interest of a large scale of scientist due to its use and in bio-analytical and medical applications, using carbodiimide molecules, DNA bound to a pre-treated electrode via a covalent attachment (Dođru, 2017; Millan and Mikkelsen, 1993). after this reaction the occurred bounding of DNA to surface is investigated from the guanine bases and this technique was then improved and used by the addition of reagent N-hydroxysulfosuccinimide (NHS) in order to enhance the activity of the carboxyl groups on the carbon electrode (figure 2.17) The covalent agent is generally used in this application and plays an important role and are also used for the untreated carbon surfaces directly before DNA immobilization onto activated sites of carbodiimides compounds (Yang et al., 1997).

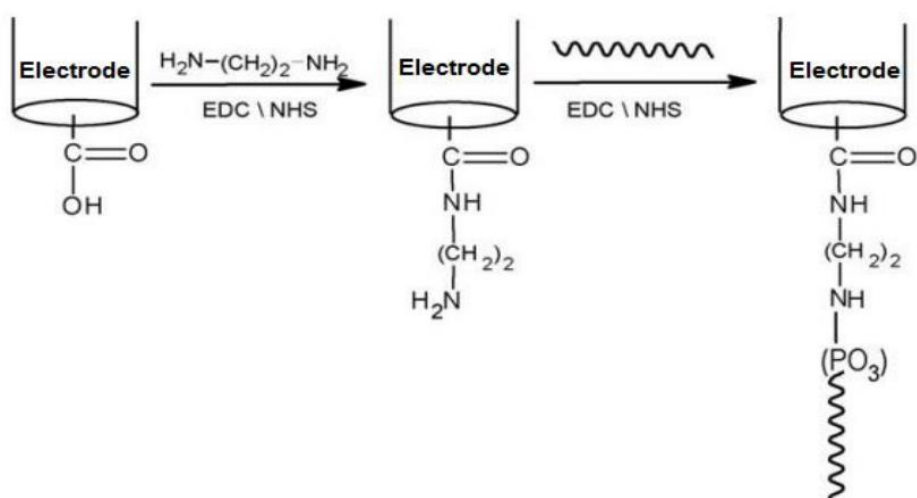


**Figure 2.17.** Covalent binding to the electrode surfaces (Ligaj et al., 2006)

Unlike the adsorption method, the DNA immobilization technique through covalent bonding showed a higher stability, flexibility and good bending strength. Moreover, the covalent bonding technique has an important role in an efficient DNA hybridization by providing a good vertical orientation in the case where the end of the DNA was grafted on the surface of the electrode. In this method, the DNA probe is coupled with the group of thiol or amines at the end of the 3' or 5' for a proper covalent binding to the metal surface or specific functional group to the electrode surface, and lead to an efficient immobilization of DNA probe onto the surface of the electrode with preventing the non-specific binding (Rashid and Yusof, 2017).

Avidin/streptavidin-biotin interaction:

In the aim of an efficient immobilization of DNA, the help of affinity reaction is used in this strategy and is one of the most used. The Avidin/streptavidin-Biotin interaction is defined as a technique of non-covalent DNA probe's immobilization on the surface of the electrodes based on an Avidin-biotin formation. The binding between avidin and biotin glycoproteins is one of the strongest protein-ligand interactions, this fact is explained with the fact that the biotin molecule is small and has the potential of interacting with the binding site of the avidin/streptavidin with a higher affinity ( $K_a = 1 \times 10^{-15}$  M) nearly to a covalent binding (Rashid and Yusof, 2017). This interaction is strong and irreversible, the non-covalent bond between avidin and biotin is due to a superposition of different interactions (hydrogen bonds, van der Waals reactions and forces coupled to the order-disorder transition) (Dođru, 2017).

The binding occurring in avidin/streptavidin to biotin molecules is analyzed to be owing higher stability and resistance to different factors as temperature, pH and organic solvents. In addition, for the avidin/streptavidin a tetrameric protein is tested providing four binding sites of biotin molecules and these interactions can be then exploited for an efficient immobilization of DNA probes onto the surface of electrodes by experimentally changing the end of 3' or 5' of DNA probes sequence with biotin molecule and including it to the modified electrodes (Rashid and Yusof, 2017). Various studies were converged in the same aim as the study done by (Chung et al., 2011) that prepared an electrochemical DNA biosensor by chemical reduction and avidin-biotin coupling in the surface of an

GCE for the case of influenza virus detection as presented in the figure 2.18 below. The most widely used immobilization technique is the EDC/NHS coupling interaction acting between avidin/streptavidin and activated carboxyl groups.

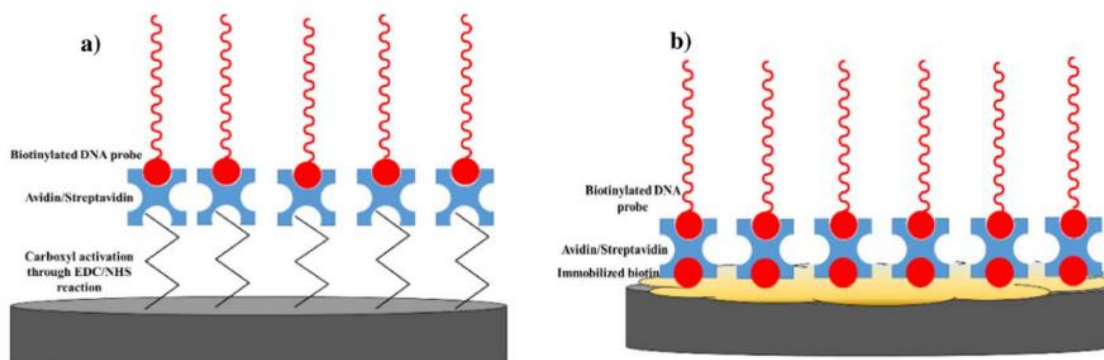


**Figure 2.18.** Schematic representation of the immobilization strategies of biotinylated DNA probe; a) avidin/streptavidin-functionalized electrode activated with carboxyl groups; b) biotin/avidin (streptavidin)/biotin as sandwiches technique representation (Rashid and Yusof, 2017)

### 2.6.3. Molecular binding interaction to DNA

The last 30 years of researches, electrochemical DNA biosensors for the analyses of DNA compounds interactions have been attracting different fields with a large number of experiments and methods aiming to enhance the quality and the efficiency of the detecting quality and the stability of the purpose. In this regards the voltammetric methods appeared to be the most used techniques and the safely giving good interpretable results with a higher flexibility and have been largely investigated for the detection of the DNA strand breakage and damages which is very important in some diseases analyses and also have been used for the identification of binding compounds to DNA (Paleček and Jelen, 2002).

As cited in the previous parts, the electrochemical DNA biosensors have been used for their high selectivity, flexibility, sensitivity, low-cost and their rapid-analysis in molecular biology solving a panoply of obstacles. Different methods have been developed as Numerous voltammetric that aim to integrate and investigate the electrochemistry of both DNA bases and DNA-specific electroactive mediators in order to obtain efficient performances (Drummond et al., 2003). The last past decades of studies reported a large

type of interactions investigating the binding occurring between DNA and compounds as presented in the paper by (Ozkan et al., 2012) as intercalation, covalent and groove binding, and electrostatic interaction, etc.

#### The groove binding interactions

Looking in the structure of DNA, the minor grooves take part of its structure and are described to be an attractive zone for positively charged and flat molecules as metal complexes due to their flexible and electrostatic structures (Neidle, 1994). After the interactions occurs, a formation of electrostatic and hydrogen bonding occurs between the minor groove bases/phosphate groups and the compounds as the study of Mithramycin investigated in the paper by (Erdem and Ozsoz, 2001). It is also reported that the minor-groove binders are owing unique chemical structure of aromatic compounds with amide or vinyl groups as linking elements (Goodsell and Dickerson, 1986). After a proper binding interaction between the DNA and compound, the obtained structure on DNA is held for a stabilization condition by Van der Waals forces. The important advantage of this interaction is its ability to don't cause any damages or harmful effect on DNA structure (Marrington et al., 2004).

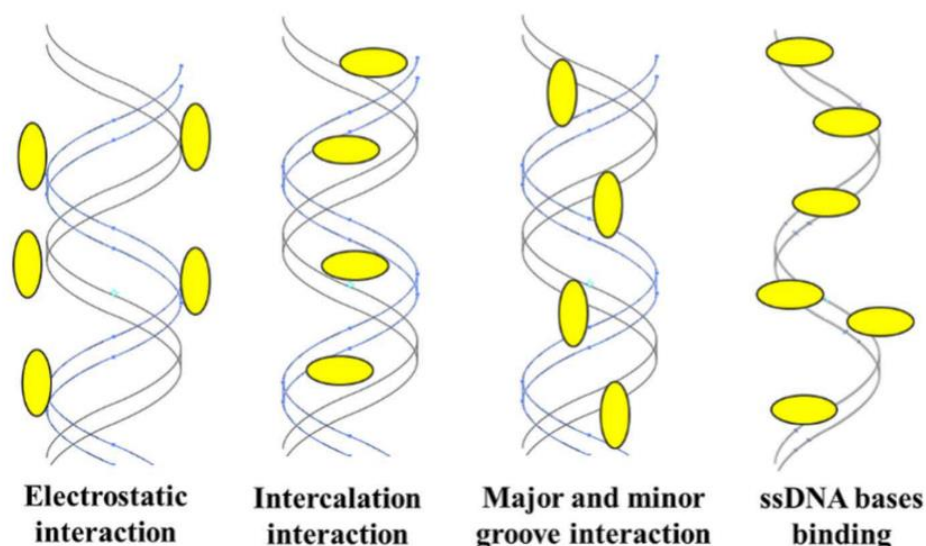


**Figure 2.19.** Schematic representation of binding mode of redox indicator to DNA (Rashid and Yusof, 2017)

The applications of this interactions start with investigating the proper compounds that can bind to DNA via hydrogen bonds and as presented in the literature review by (Rosenberg et al., 1965) that studied on of the most widely used anticancer compounds named as c/s-platin and was used in various biosensors applications for the detection of the DNA damages (Rosenberg et al., 1965). The compounds bind to the DNA from its own purine bases via covalent bonds (Boulikas and Vougiouka, 2003).

#### The intercalation mode

The intercalation concept was introduced earlier in 1982 to prove the efficacy and affinity of the intercalators to dsDNA structures, due to their location between two adjacent pairs of bases (Dođru, 2017). The intercalators molecules are characterized by the planar aromatic rings (like phenanthroline and terpyridine) and can then stack in between the DNA base pairs, stabilized through the dipole-dipole interactions (Bertini et al., 1994). Some intercalators destroys the deoxyribose-phosphate structures as the example of antibiotics (Bertini et al., 1994).

The study of the intercalators characteristics and applications possibilities leads to a plethora of results converged to their high DNA-binding constants which is very important in some electrochemical applications, after the interactions between the intercalators compounds and the double-helix a noticeable can be note onto DNA and lead to a propulsion of a free energy from complex formation. In the case of bis-intercalators, through a covalent bonding occurring between DNA and the aromatic rings of the molecules, the integration of two intercalators performs via this bonding like the case of Echinomycin (Palecek and Fojta, 2005).

#### Electrostatic interactions

This type of interaction related to compound-DNA binding is also named as a non-specific external association, in which an electrostatic binding is maintaining the interaction between metal ions and DNA (Eichhorn and Shin, 1968). As known in the mononucleotides along a nucleic acid polymer, a variety of sites for interactions with metal ions exists in the mononucleotides and range from electrostatic interactions (occurring with anionic phosphate backbone) to nucleophilic interactions (case of



purines) as detailedly described in the paper published by Barton (Bertini et al., 1994). Different factors affect the strength of these interactions as the charge of the compounds, hydrophilic-hydrophobic structures of the molecules and also the size of the ions (Dođru, 2017). Once the interaction between the compounds and the DNA is done, the structure of the double-helix DNA knows a separation which is described as a damage of the structure (Ozkan et al., 2012).

#### **2.6.4. The electrochemical DNA biosensors investigation in detection for compounds DNA binding reactions: label-free and label-based electrochemical DNA detection.**

In this part, the mechanism of electrochemical DNA detection will be investigated due to its major application in this project. The electrochemical detection of DNA hybridization was always a subject of research and development attracting interest of different fields especially for detection of some several diseases, this fact is typically in factor with the changement of electrochemical response with or without the presence of an complementary DNA target (Rashid and Yusof, 2017)..

The oxidation-reduction of a compound or the oxidation signals of guanine/adenine shows a higher efficiency and affinity to DNA and reported as the mostly used for detection of the interaction compounds-DNA occurring in the surface of the studied sensor (Erdem and Ozsoz, 2001). As described in the literature, the DNA hybridization detection is reported in two approaches: the label based and label-free electrochemical DNA detection methods.

Electrochemical label-free DNA detection approach:

Starting from the analyses of the DNA structure to its life cycle investigations and its molecular changement in different environment, the literature presents a plethora of scientific research and project approving that the DNA changes occurring via its own metabolites or by a chemical are one of the most important carcinogenic processes (Miller, 1994). The precocial phases in the carcinogenesis is affected by the combination of multiple factors as the carcinogen's stimulators, drugs or even the metabolized chemical with the cellular DNA. The analysis of the DNA damages leads to cause the

genetic mutations which can be an important cause of several effects on the normal living process and its functions.

The label-free electrochemical DNA detection are nowadays based on the analyze of the changement in the redox properties of the DNA electroactive bases (Rashid and Yusof, 2017). Historically, the electroactive DNA bases properties was reported by the research group of Palecek (Paleček and Jelen, 2002), in which, after the application of a potential at the electrode, the DNA bases perform an reduction or oxidation as the hybridization was accomplished. They also studied that from the bases of DNA, only guanine and adenine show an efficient electroactivity with an easy absorption and oxidation on multiple electrodes as gold and carbon. The oxidation signal of both guanine and adenine carbon electrodes is respectively obtained around 1.0 and 1.3 V in 0.50 M ABS (pH 4.80), (Rashid and Yusof, 2017). The changement occurring during reduction/oxidation of guanine current have been widely used in the label-free based electrochemical DNA detection. The main purpose of this approach is relied to the interaction of free guanine and adenine with its complementary base thymine and cytosine of DNA target during the process of hybridization. The redox reaction's current signal obtained of guanine and adenine after hybridization is always lower than the signal obtained before the hybridization.

It is also important to note that the increase or decrease of the guanine oxidation signal can enable the analysis and control of the DNA-molecule interactions in the electrochemical level, and this lead to make the light on the DNA damage. If an additionally new peak in the is obtained, it can be explained by the extent of an adduct formation (Kerman et al., 2001). Some synthetically made polynucleotides of guanine and adenine are nowadays produced and used for experiments to analyse the interaction of one compound with the guanine and adenine bases (Meric et al., 2002).

The study of the compound-DNA interaction, in the case of a decrease noted in the guanine oxidation signal can be presented by three assumptions, a: if the peak's height of guanine tends to decrease is related to the presence of oxidizable guanine's groups during the interaction of a molecule with DNA, b: the binding occurring of a chemical compound to guanine bases and this lead to facilitate the formation of a damage in guanine and also

c: after interacting with the compound, a change in the charge-transfer properties of DNA can be a cause of the decrease of the signal obtained after the guanine's oxidation at the electrode surface (Fojta, 2002; Wang, 2002).

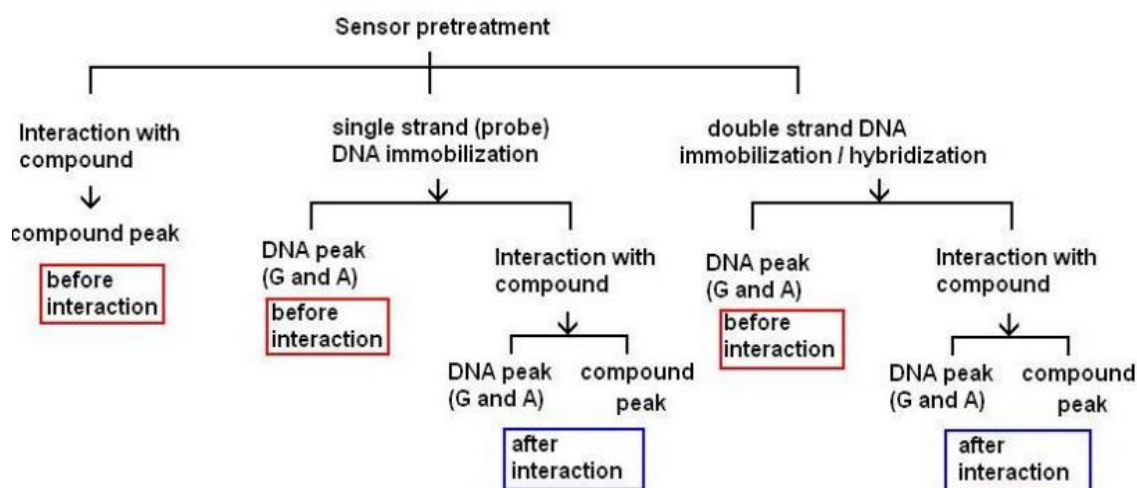


**Figure 2.20.** Electrochemical detection schemes for compound-DNA interactions (Ozkan-Ariksoysal et al., 2012)

The main advantage of the label-free electrochemical DNA method is its ability to be flexible for multiples compounds and also providing simply a hybridization assays by skipping the implementation of hybridization markers procedures. However this method's drawback is the requirement of high potential for the detection of guanine oxidation's signal with a high background signal frequently occurred caused by the adsorption of DNA target that contain guanine bases (Rashid and Yusof, 2017).

The label based electrochemical DNA detection interaction (redox indicator-based detection)

In this method, and in order to generate an electrochemical signal. Indirect or also named label-based approach for DNA hybridization detection's main principle is the integration of a redox-active indicator to the DNA sequences, these molecules are also named as DNA hybridization indicator. This method facilitated the development of the DNA genosensors and some drugs for a future efficient microchips' device. The literature discussed a wide range of indicator-based electrochemical biosensors but the main cited and used are the electroactive compounds as the methylene blue (Ozkan et al., 2002),

ferrocenylnaphthalene diimide (Takenaka et al., 2000), the metal complexes as osmium, cobalt phenanthroline and ruthenium (Steel et al., 1998). The paper elaborated by (Kelley et al., 1999) in which, for this application, electroactive intercalators were investigated and resulted an non-covalently bound to DNA for a detection of changes occurring in single-base nucleotides. The study of redox-active DNA markers (amino and nitro-phenyl tags and ferrocenes) was reported by (Brázdilová et al., 2007; Cahová et al., 2008). The carbon-based transducers have also gained the attention of different researchers for its efficient use with a plethora of covalent or noncovalent binding labels on DNA (Labuda et al., 2003).

## **2.7. Electrochemical miRNA biosensors**

### **2.7.1. General view**

The combination of researches in the field of nanotechnology and biosensing and its application in medicines technology and biomedical diagnostics is taking huge advancements every year. Enhancing the properties of the nanomaterials and their efficiency and applying it in electrochemical nanobiosensors have been reported in a wide range of studies, and applied for quantification of different types of biomarkers for a detection and follow up of some diseases (Azimzadeh et al., 2017). miRNAs are one of the popular studied biomarkers used for biomedical diagnosis of some cancer types.

The miRNAs are defined as small non-coding, post-transcriptional gene regulators of genomes with approximately 22 nucleotides long. More than 1200 miRNAs have been detected and studied in the literature, but the traditional methods deployed for DNA does not works efficiently for miRNA and push the researches to converge the efforts in this sense because of their morphology as short strands and their low expression in biofluids.

In a typical electrochemical miRNA biosensor, cyclic voltammetry (CV), differential pulse voltammetry (DPV), and square wave voltammetry (SWV) are the main technique used because of their sensitivity and flexibility. In the miRNA biosensors, the detection process is investigated on the hybridization of miRNA target with a complementary probe. The fabrication of an electrochemical miRNA biosensors can be divided into 3 important steps: immobilization of the complementary probe on the electrode surface.

Hybridization of the miRNA molecules with the probe and electrochemical measurement to analyze the interaction's peaks, the efficiency and performance obtained depends directly on conception of the biosensory system including the immobilization process, the biosensing setup and the electrode surface (Azimzadeh et al., 2017).

### 2.7.2. Electrochemical label-based biosensing for miRNA analysis

Electrochemical genosensors (DNA and RNA) principle is on hybridization in which a nucleic acid recognition probe is immobilized on the transducer surface and the recognition of target is occurring by hybridization and converted to an interpretable signal (Keshavarz et al., 2015).

The label-based electrochemical miRNA detection is axed on the changes in the voltammetry signals after hybridization. This method is widely applied for miRNA detection and gives directly the value of RedOx current response related to miRNA hybridization. The label-based offers multiple advantages due to the small-size of miRNAs (Keshavarz et al., 2015).

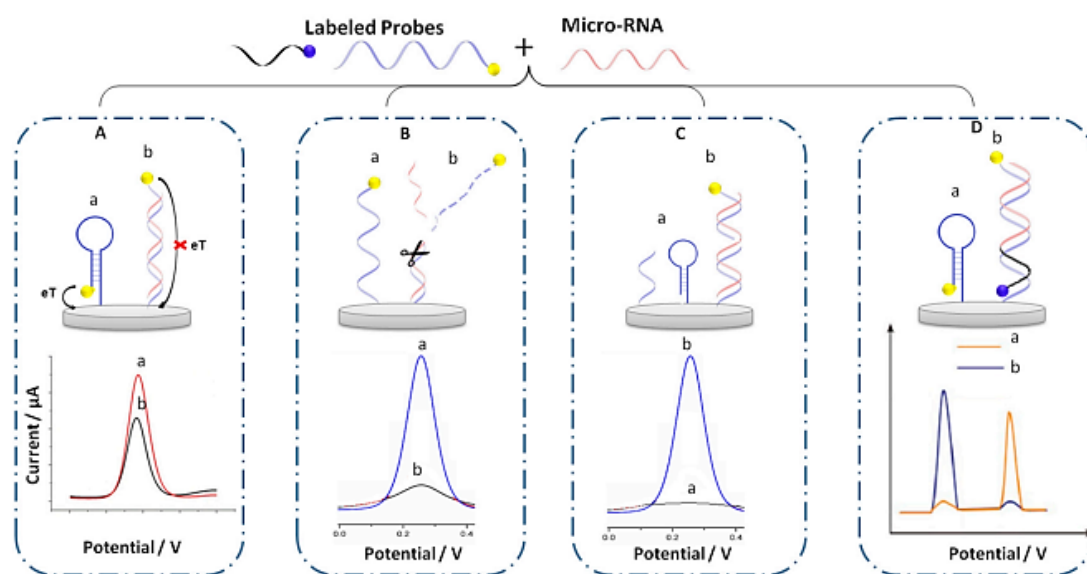


**Figure 2.21.** Schematic illustration of an electrochemical biosensors based on labelled probe with RedOx molecules before and after hybridization. (A) Basic design; (B) elimination of labelled probe sequence; (C) the use of secondary probe labelled with

RedOx molecule; (D) the use of two-probe labelled sequence, (a) before and (b) after hybridization (El Aamri, Yammouri, Mohammadi, Amine, & Korri-Youssoufi, 2020)

The used electroactive species in this method can be organic or inorganic as silver nanoparticles, gold nanoparticles, cadmium, ferrocene and methylene blue. In this purpose, the RedOx molecule can be labeled to the probe sequence directly or by using linker (El Aamri et al., 2020) as demonstrated in the figure 2.21 and figure 2.22. below.

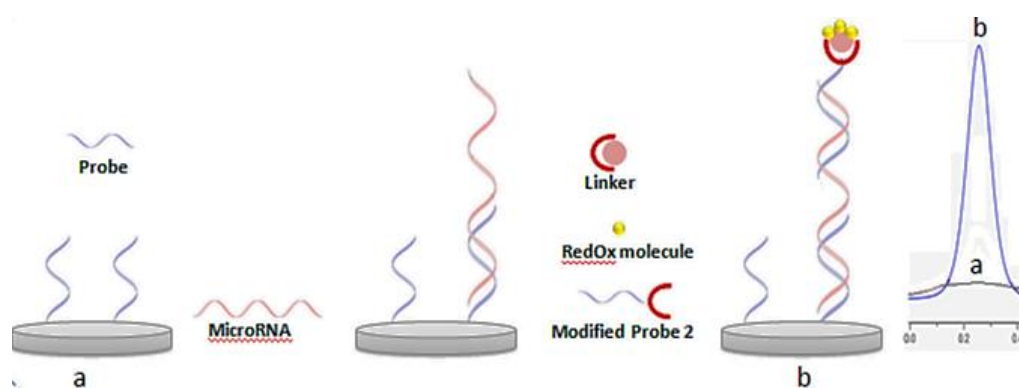


**Figure 2.22.** Schematic illustration of electrochemical biosensor based on a RedOx molecule labelled probe via a linker molecule (a) before and (b) after hybridization (El Aamri et al., 2020)

### 2.7.3. Electrochemical miRNA biosensors based on catalysts

In this part, the catalysts include DNA enzymes, chemical catalysts and enzymes. The enzymes are biomacromolecules are known for the highly selective catalytic performance and have been investigated in a wide range of studies.

Nanomaterials can be used as chemical catalysts and play similar role as enzymes catalysis and can perform as alternatives for enzymes. Due to their higher properties discovered in the last decades, nanomaterials are owing good physico-chemical properties and size near to enzymes which led to be used comparably to natural enzymes.

The nanosized properties allows high catalytic efficiency (El Aamri et al., 2020) as presented in the figure below.

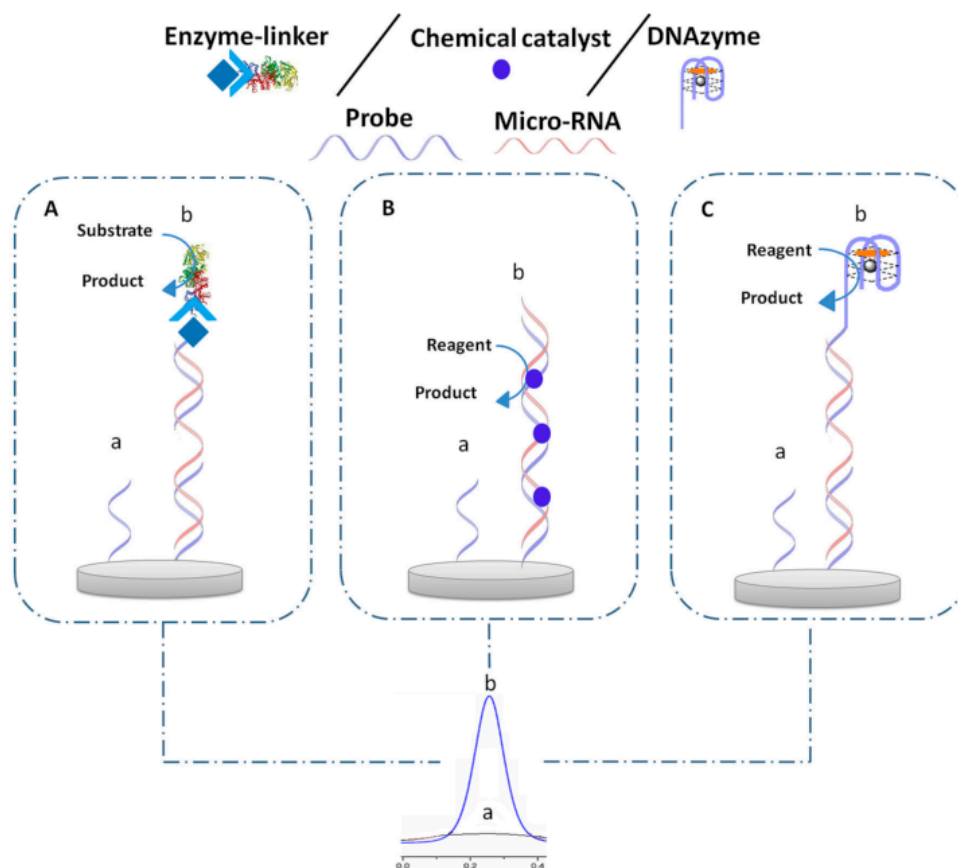


**Figure 2.23.** Electrochemical biosensor based on different types of catalysts before (a) and after hybridization (b) with micro-RNA, (A) enzyme, (B) chemical catalyst, (C) DNAzyme (El Aamri et al., 2020)

DNA enzymes or DNAzymes are defined to be ssDNA molecules enhancing the catalytic effect and widely used in a large type of applications. Increasing the efficiency of these molecules lead to enhance the performance of the electrochemical miRNA biosensor.

Enzymes are used for the amplification strategies for miRNA detection, a plethora of enzymes have been used as reported in the literature including enzymes that lead to obtain electroactive species that can be electrochemically detected and measured. alkaline phosphatase (ALP) and horseradish peroxidase (HRP) are widely used enzymes and extremely important in order to impact the accessibility of the active sites (El Aamri et al., 2020)

#### 2.7.4. Electrochemical Biosensor Based on RedOx Intercalating Agent

As cited in the DNA part of study, the intercalation is an insertion of a molecules between two other molecules. In this case, the RedOx molecules are investigated by intercalation in the biomolecule strand binding. A panoply of molecules was used as intercalators for miRNA analysis. This process of intercalating on biosensing can be directly to the target DNA strand or indirectly by immobilizing intercalating molecules in specific sites called template (El Aamri et al., 2020; Keshavarz et al., 2015).

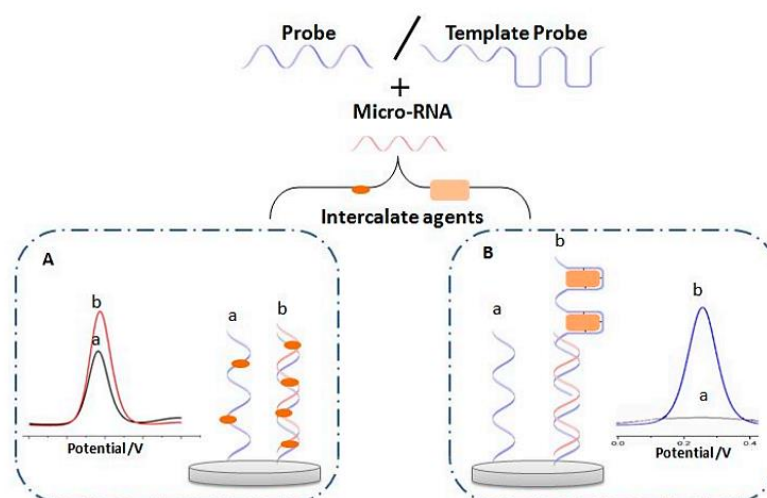


**Figure 2.24.** Electrochemical biosensor based on RedOx intercalating agent before (a) and after hybridization (b) with micro-RNA, (A) direct intercalation, and (B) intercalation via the template (El Aamri et al., 2020)

#### 2.7.5. Oxidation of guanine method for electrochemical miRNA biosensors

Guanine is a nucleobase present in the miRNA's strands. As studied in the approach of oxidation of guanine in the case of electrochemical DNA biosensor, the same process can be applied for miRNAs. In this case, the probe is immobilized on the electrode's surface and the oxidation of guanine can be measured. After hybridization, guanine's electrochemical signal decrease can be observed. Even if this method can appear easy but it has many limitations, admitting that the oxidation of guanine base as free molecules is uncomplicated than in DNA and this could generate non-interpretable results. In some studies, the replacement of guanine by inosine was investigated, but does not show the same performance as guanine oxidation after hybridization process, and this is explained



by the binding cytosine-guanine is highly prominent than the guanine-inosine's binding and lead to a lower level of binding compared to the case of DNA. Also its important to note that the irreversibility of this method is also a limitation of use (El Aamri et al., 2020).

## **2.8. Carbon nanofibers in biosensors**

### **2.8.1. General view**

The tune of the nanomaterial's properties within the biosensing field lead to an efficient result with an optimization of the biosensors structure. Carbon nanomaterials are nowadays classified to be in the forefronts of research in this field, for approving the performance in a wide range of physical and chemical disciplines. In the light of some scientific papers, few nanostructures are suitable for the electrochemical biosensor's conceptions and applications, the importance of the sensitivity and fast signal responding criteria of the electrochemical sensing to quantify purine bases is always in correlations with the enhancement of the surface characteristics of the working electrodes since the electrochemical detection is investigated in this surface. Carbon electrodes have attracted attention and have been a subject of study in different field in electrochemical sensing because of their panoply of promising characteristics and advantages. Also, the modification of the carbon electrodes surfaces with carbon nanocomposites has proved an effectives outcome with attractive sensitivity, reproducibility and stability for the purine bases quantification via the electrochemical methods. The main advantages of using carbon nanocomposites including the carbon nanomaterials, metal/metal oxides nanoparticles and polymer is their high conductivity and surface volume ratio allowing an efficient immobilization of high amount of molecules in the surface (Singhal et al., 2021). Particularly, the carbon nanotubes and carbon nanofibers have been deployed and demonstrated to be the most used due to their exceptional physical and chemical and physical characteristics for a better performance and analytical properties of the developed biosensors. The area of electrochemical biosensors has been revolutionized because of the inherent, induced functionalities and biocompatibility of this materials.

The last decades of researches in the branch of electrochemical biosensing for the improvement of the performance and early detection of some critical diseases in

combination with the nanotechnology researches has enabled the development of an autonomic nano-systems based on actively modified electrodes on new nanomaterials overcoming many obstacles of analysis and calculus especially for the bio-analytical systems (Vamvakaki et al. , 2007).

### **2.8.2. Carbon nanofibers**

The nanomaterials with a critical dimension ranging of 100 nm are used for their advantageous large surface to volume ratio and their specific surface area, displaying unique physical and chemical characteristics, plays a primordial role in the biosensing fields, also, their electron transfer properties and catalytic activities and makes them the most usable materials (Vamvakaki et al., 2007), this projects focused on the investigation of this materials to enhance the electrochemical properties of the surface of the transducer for a better performance of the biosensor using activated carbon nanofibers and will be detailly discussed in the following chapters. It is also important to note that the higher sensitivity and stability of a biosensor can be improved by incorporating nanomaterials to the biosensing systems as nanoparticles, nanowires and nano-porous structures.

Among the plethora of nanomaterials developed nowadays, the carbon nanostructures have been studied to be suitable for biosensing applications, the biocompatibility, conductivity and porous properties of this material facilitated their incorporations in the enhancement of the quality of the transducer surfaces. The literature presents a wide range of publications using the carbon nanomaterials for a biosensing systems and were successfully efficient.

Carbon nanofibers with diameters in the range of submicron and nanometers scales owing and 1D nanostructures, are cylindrical shaped graphite layers composition packed around the fiber's axis in a well-organized structure. The diameter of the nanofibers is from 5 to 200 nm with a length of micrometers and are considered of great interest because of their chemical similarity to CNTs and fullerenes and have been widely used in different areas such as supercapacitors, catalysts support materials and battery applications.

The study of the properties of carbon nanofibers lead to show that their mechanical and electrical characteristics that are similar to carbon nanotubes, during the manufacturing

processes, chemical and physical treatment can reduce the diameters and the length of nanofibers that leads to improve of the electrochemical properties of the final material. The oxidation process can increase the hydroxyl or carboxylic sides functional groups and the edge of every graphite layer is functionalized with a higher interaction with the surrounding environment. Compared to carbon nanotubes CNT the carbon nanofibers are studied to be owning a large number of chemically active groups on their surface in the same set volume of a material with a lower resistivity and these properties are highly searched for an electrochemical signal transduction. It is also important to note that the variety of oxygen containing functional groups on the surface of the carbon nanofibers can be flexibly modified and lead to an efficient immobilization and stabilization of biological molecules such DNA, enzymes and proteins (Vamvakaki et al., 2007).

Polyacrylonitrile (PAN) has been reported to be the principal precursor material for obtaining carbon nanofibers with a diameter of nanometers and exhibit good properties as high electrical conductivity and high surface area, also the nanofibers can be investigated with a polymeric structures to make composites materials aiming to enhance to efficiency of the electrochemical properties of the polymeric structures, the obtained nanofibers-reinforced polymeric structures in studied to be improving mechanical properties due to their interactions nanofibers-matrix materials.

Although any material containing carbon back-bone can be investigated as a precursor of carbon basically. The carbon nanofibers generally produced from three polymeric precursors: polyacrylonitrile PAN, cellulose and pitch detailly present in the literature, but the PAN has been the most used by scientists due to its high carbon yield and mechanical properties of the resultant carbon nanofibers, nowadays the PAN is considered to be the precursor for approximately 90% of the carbon nanofibers manufactured, also, an efficient and highly performance carbon nanofibers have been produced exclusively from PAN copolymers precursors containing 0.5–8 wt% comonomers as acids and vinyl esters (Zhang et al., 2014b).

The chemistry of concretization of PAN into carbon nanofibers are generally divided on three steps:

1. Cyclization in low temperature process

2. High temperature oxidative treatment of carbonization
3. Process of graphitization where chains are joined into graphite planes (figure 2.27)

## **2.9. Production of carbon nanofibers from electrospun PAN**

### **2.9.1. Electrospinning of nanofibers**

The nanomaterials are nowadays in forefront of research in a wide range of discipline especially biological and chemical fields. Some nanofibrous structure were proved efficient in some electrochemical biosensor's applications. Carbon nanomaterials are considered efficiently used in the electrochemical biosensory systems, providing a high biocompatibility and conductivity.

Nanofibers are cylindric nanostructure of graphite layers around a fiber axis in an organized structure. Nanofibers are owing a cross sectional diameter in the range of 5 to 200 nm and a length up to micrometers. These nanostructures can be produced with different methods depending on the desired characteristics. The production process impacts the total morphological, chemical and mechanical properties of the nanofibers and can be used in a wide range of applications from agricultural to medical technologies.

The literature presents a variety of nanofiber's production methods that have been used for years and proved their efficacy as: self-assembly, drawing, electroblowing, template synthesis, phase separation and electrospinning.

Electrospinning method is defined to be a multipurpose process providing a high flexibility of applied materials (polymers, ceramics, metallic and composites) and control of adaptable parameters. The principle of electrospinning method is related to the electrostatic spinning of a polymer in an electrical field. The electrospinning process was mathematically modeled and studied by Taylor in 1969 in which the conical shape of fluid droplets (Taylor cone) was investigated. Once the polymer solutions were under a high voltage, a formation of Taylor cone under occurs and are initiating to a formation of nanofibers in different morphologies and characteristics.

The last decades of researches have been using more than 100 of synthetic and natural polymers to produce nanofibers via electrospinning process. The spinnability of the polymer solution and the produced nanofiber's characteristics are relative to the fixed parameters as applied voltage, distance from collector to capillary and flow rate of the polymer solution, also the nanofiber's morphology is affected by the solution parameters as viscosity, solvent volatility conductivity, polymer concentration and surface tension (Inagaki et al., 2012). the nanofibers obtained by electrospinning process are generally smooth fibers, the use of volatile solvent in the solution preparation leads to a formation of porous nanofibers structure as studied in this project.

**Table 2.3.** Morphology of fiber affected by electrospinning parameters

Parameters	Impact on fiber morphology
Applied voltage ↑	The fiber diameter decreases first then tend to increase (not monotonic).
Flow rate ↑	The fiber diameter increase (if the flow rate is too high a beaded morphologies occur).
Collector and capillary distance ↑	The fiber diameter decrease (if the distance between the collector and capillary is too short a beaded morphologies can be obtained).
Polymer concentration (viscosity) ↑	The fiber diameter increase (in an optimal range).
Solution conductivity ↑	The fiber diameter decrease (broad diameter distribution).
Solvent volatility ↑	The fibers exhibit a microtexture (porous structure on the surface and increase of the surface area).

As cited above, the fixed parameters affect directly the fibers characteristics, but it is also important to note that this relationship must be studied separately for each polymer-solvent case. In the same electrospinning setup and polymer, different nanofiber's formation can be produced depending on the solution characteristics. A study of Sill and von Recum's investigated the production parameters and their impact on the nanofibers formations as presented in the table above.

Depending on the expected nanofiber's morphology and structures, different types of electrospinning process were developed in the last years of researches as Centrifugal Electrospinning, Bubble Electrospinning, Conjugate Electrospinning, Magneto Electrospinning, Co-axial Electrospinning, Needleless Electrospinning, Gas-Jacket Electrospinning, Melt Electrospinning and Solution based Electrospinning that have been investigated in this study.

### **2.9.2. Solution based electrospinning**

In this electrospinning type, the polymer solution is placed in a syringe and placed on a micropump in order to hydraulically press the syringe needle. Once an electrical field is applied, the droplet of the solution at the spinneret tip that deforms from the shape due to the surface tension and a formation of cone-like surface shape called Taylor cone occur (Yarin et al., 2001).

Once the electrical field reach a critical value and the resulting electrical field in the on the droplet solution surpass its surface tension and viscoelastic force, a jet of the solution occurs and ejects from the tip of Taylor cone and be followed by a bending, winding and spiraling in 3D (Zhang et al., 2014a). the solidification occurs when the solvent is evaporated (approximately 99% of the solvent can be removed) during the electrospinning process by providing a convenient ventilation. During this process, the drawing of the nanofibers in the collector surface occurs randomly and the formation of nanofibers be assembled in a thin layer's nonwoven mat structures using a metallic plate as collector or by using a rotating collector in a constant speed to obtain continuous aligned nanofibers (Inagaki et al., 2012).

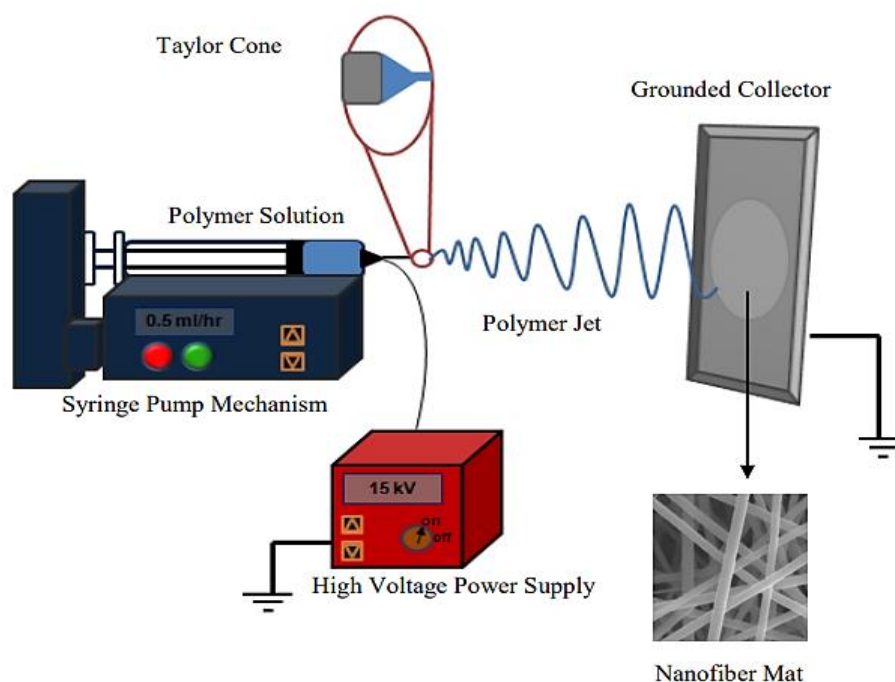


**Figure 2.25.** Schematic representation of electrospinning process (Aykut, 2011)

The spinnability of polymer solution for this type of electrospinning can't be investigated without controlling environmental and procedural condition to obtain the expected structures and performances, the distance of needle tip and collector is generally in the round of 10-25 cm, interfacial viscosity of streaming solution within air must be controlled, viscosity, electrostatic repulsion force applied voltage, temperature and humidity are the main factors affecting the obtained morphologies (Aykut, 2011) as presented in the figure 2.4.

### 2.9.3. Carbon nanofibers derived from electrospun PAN

Carbon nanofibers, as defined have attracted researchers' attention in the last decades, due to their flexibility of use and high morphological, mechanical and thermal properties. In the addition of the traditional methods of nanofiber's production, electrospinning has been widely used and reported in a plethora of literature papers.

Carbon nanofibers are produced from polymers precursors as polyacrylonitrile (PAN), poly-imide (PI), poly (vinyl alcohol) (PVA), poly (vinylidene fluoride) (PVDF) and pitch.

PAN is defined to be a versatile man-made polymer used in a wide range of product as water purification, air filtration, supercapacitors and especially its value-added is in manufacture as precursor for the production of carbon nanofibers, in a process of electrospinning followed by a thermal treatment of stabilization and carbonization. The produced carbon nanofiber's properties depend on the quality of PAN precursor and the process parameters (especially the stage of stabilization) (Khayyam et al., 2020). The literature presents the PAN as the main precursor of carbon nanofibers production due to its efficiency to grow into a well structure of carbon network after carbonization.

For electrospinning process, PAN is dissolved in DMF and waited for a proper homogenization, as presented in the electrospinning process principle, the solution is feed in a syringe and a high voltage is applied for the purpose, during the electrospinning process DMF is evaporated and nanofibers formation on the collector surface is obtained in a form of a web. A panoply of collectors can be used for the fabrication of PAN-based nanofibers to achieve the expected alignment for the future applications. As presented in the figure bellow, an aligned and non-aligned nanofiber imaging can be compared in which the rotating collector allow a production of an aligned nanofibers web with a decrease of the nanofiber's diameters and this result is inversible for the non-aligned nanofibers obtained from a fixed collector (Gergin et al., 2017). The morphologies of the electrospun PAN nanofibers differs depending on the electrospinning process parameters, environment parameters and solution parameters.

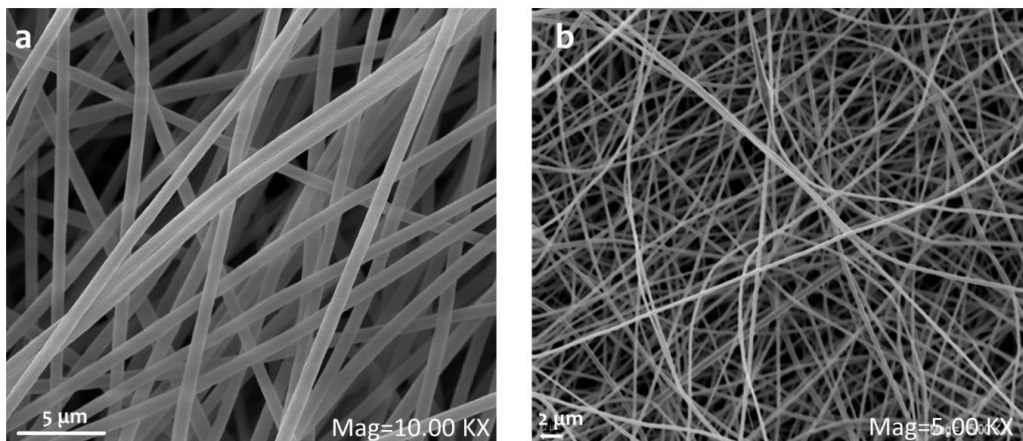


**Figure 2.26.** a) Aligned PAN nanofibers produced with rotating collector b) PAN nanofibers produced with fixed collector (Gergin et al., 2017)



The phase of stabilization is extremely important to produce carbon nanofibers from PAN nanofibers, due to the formation of cross-link during this process, and the structure can be prepared for the following carbonization heat treatment, the parameters must be controlled in this step. Stabilization prevent fusion, melting and minimizes volatilization of elemental carbon in the carbonization. This heat treatment consists on dehydrogenations and cyclization of nitrile groups and crosslinking of chain molecules – C=N–C=N–. in this part of process, it is extremely important to control the temperature, tension of the fiber, heating rate, air flow rate, stabilization time parameters to assure the expected structure and performances.

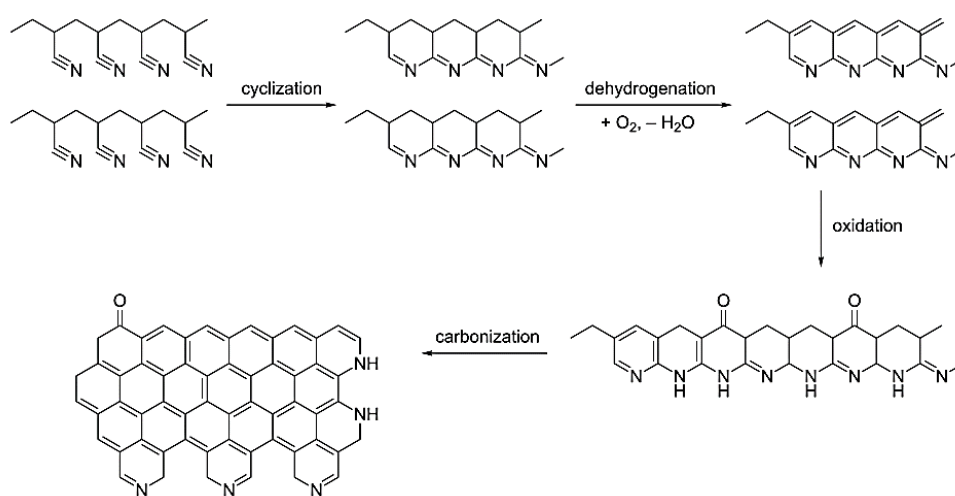


**Figure 2.27.** Representation of carbonization process starting from polyacrylonitrile (Gergin et al., 2017)

The carbonization is the last step of the heat treatment process, in which the stabilized PAN nanofibers are immersed under nitrogen atmosphere to prevent burning and under high temperature, in this process a total elimination of impurities and elements like (N<sub>2</sub>, O<sub>2</sub>, H<sub>2</sub>) occurs and an increase of the carbon concentration with a decrease of the nanofiber's diameter is observed.

The obtained carbon nanofibers after carbonization process are morphologically investigated and the surface of the nanofibers is not smooth and porous which is an important advantage for biosensory system's application for a better immobilization of probes. The use of this material will be investigated in this study for an electrochemical miRNA biosensor application.

### **3. MATERIALS and METHODS**

#### **3.1. Materials**

##### **3.1.1. Raw and chemical materials**

For the electrospinning solutions preparations, Polyacrylonitrile (average Mw 150000) was purchased from Sigma Aldrich. N,N-Dimethylformamide was provided from Carlo Erba. lawsone (2-Hydroxy-1,4-naphthoquinone) (Mw 174,15) and Hemoglobin (from Bovine blood) were both provided from Sigma Aldrich. All the chemicals were used without any purification.

For the electrochemical analysis part of the project, the buffer solutions were prepared by using ultra-pure water (DNase and RNase free).

Potassium phosphate monobasic  $\text{KH}_2\text{PO}_4$ , Sodium hydroxide, NaOH, analytical-grade, hydrochloric acid fuming 37% for analysis HCL and Glasiyel acetic acid %100, analytical-grade were provided from SIGMA.

Potassium phosphate dibasic  $\text{HK}_2\text{O}_4\text{P}$  was provided from SCHARLAU. Tris-Hydrochloride, Tris-HCl, analytical-grade from WISENT. Both of EDC and NHS were provided from TCI Tokyo Chemical Industry.

The used primers were purchased from Genaxxon bioscience.

##### **3.1.2. Sequences of oligonucleotides**

The nucleotides used in this study were purchased from Genaxxon bioscience (Germany) and oligonucleotides sequences are presented in the table below.

The purchased synthetic miRNA, PolyT(I), PolyA, PolyT(G), NC. miRNA, and SM. miRNA molecules were first dissolved in ultra-pure water and stored as the stock solutions.

**Table 3.1.** Sequences of the miRNA and anti-miRNA molecules used in this study

Name	Features	Sequences (5'→ 3')
<b>miRNA</b> (miR451)	22mer RNA, Scale RM27 inclusive HPLC	AAA CCG UUA CCA UUA CUG AGU U
<b>SM. miRNA</b> (SM-miR451)	22mer RNA, Scale RM27 inclusive HPLC	AAA <u>CCC</u> UUA CCA UUA CUG AGU U
<b>NC. miRNA</b> (NC-miR21)	22mer RNA, Scale RM27 inclusive HPLC	UAG CUU AUC AGA CUG AUG UUG A
<b>PolyT (G)</b> polyT- antimiR451(G)	28mer DNA, Scale M inclusive HPLC	TTT TTT AAC TCA GTA ATG GTA ACG GTT T
<b>PolyT (I)</b> polyT- antimiR451(I)	28mer DNA, mit 5=2'-dInosin, Scale M inclusive HPLC	TTT TTT AAC TCA 5TA AT5 5TA AC5 5TT T
<b>PolyA</b> NH <sub>2</sub> -poly A	6mer DNA, mit 5'-AminoC6, Scale M ink. HPLC	AAA AAA

SM: Single-base mismatched of the miRNA, and NC: Non-complementary of the miRNA. PolyT(G) and PolyT(I) are anti-miRNA.

### 3.1.3. miRNA and anti-miRNA solutions

In this study and for both Lawson and Hemoglobin added CNFs parts, the same stock solutions were prepared. The oligonucleotides stock solutions were prepared as adjusting to 1000 ppm.

The previously purchased synthetic miRNA, PolyT(I), PolyT(G), PolyA, NC. miRNA and SM. miRNA molecules were dissolved in ultra-pure water and stored for stock solutions preparation. The stock solutions were poured in the PCR tubes as 50µL and stored at -18 °C until they are used.

The oligonucleotide solution for the electrochemical measurements were prepared by diluting 10 µL of the prepared stock solution in 50 µL of PBS in an empty sterilized PCR tube. Both of stock and measurement solutions were prepared using a vortex mixture.



**Figure 3.1.** The purchased oligonucleotides PolyA, miRNA and anti-miRNA

#### **3.1.4. Buffer solutions for electrochemical measurements**

##### Preparation of 0.05 M phosphate buffer solution (PBS)

For this purpose, 1.36 gr (0.01 mol)  $\text{KH}_2\text{PO}_4$  and 6.96 gr (0.04 mol)  $\text{HK}_2\text{O}_4\text{P}$  were dissolved in 1 lt ultrapure water by magnetic stirring to obtain 0.05 M PBS solution. 0.1 N NaOH and/or 0.1N HCl was gradually added in the prepared solution to adjust the pH 7.4. finally, 1.168 gr NaCl was added into the final solution to set the NaCl as 0.02 M in the solution.

##### Preparation of 0.5 M acetate buffer solution (ABS)

The acetate buffer solution (ABS) was prepared by setting .5 M glacial acetic acid in 500 mL ultra-pure water. 0.1 N NaOH and/or 0.1 N HCl was gradually included to the solution to set the pH 4.8. Finally, 0.584 gr NaCl was added into the prepared solution to set the NaCl as 0.02 M in the solution.

### 3.1.5. Testing station for the electrochemical miRNA biosensor system

The electrochemical measurements were performed on the electrochemical workstation suitable for the purpose with a Potentiostat - AUTOLAB AUT204 (Eco Chemie, Nederland) by using NOVA 1.11 software was used in a typical Screen-printed electrodes (SPE) system.

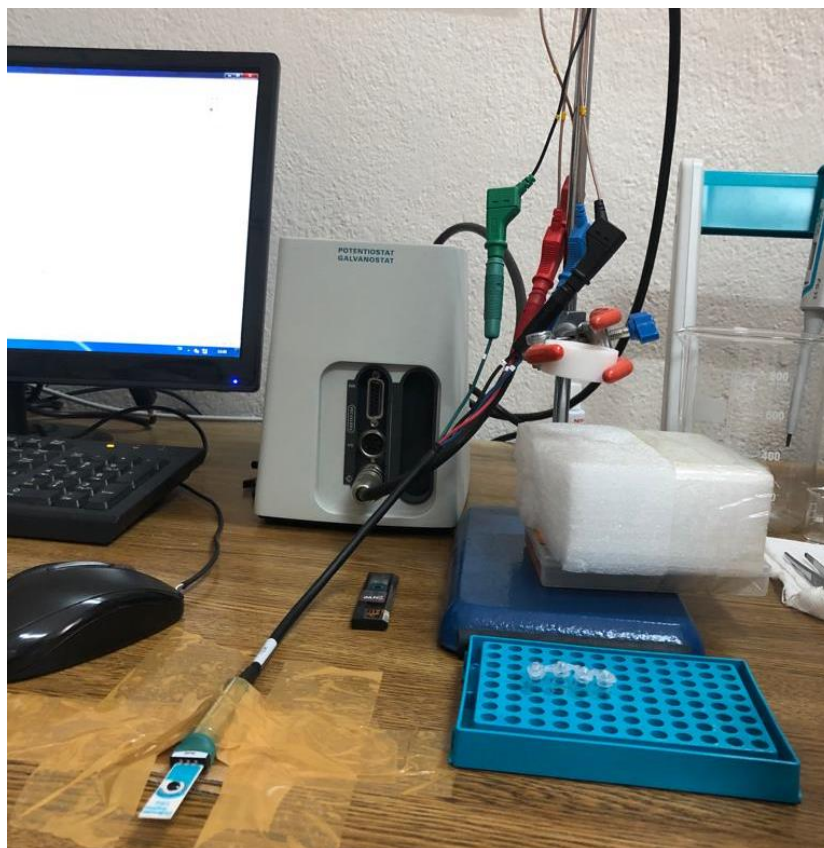


**Figure 3.2.** Testing station for electrochemical measurements

For the Lawsonite added CNFs part of the study, Metrohm DropSens - Screen-printed Carbon electrodes (SPE) DS 150 in which the working electrode is carbon, auxiliary electrode is platinum and the reference electrode is silver were purchased and used at all the measurements.

For the Hemoglobin added CNFs part, Metrohm DropSens - Screen-printed Carbon electrodes (SPE) DS 110 with both of the working and auxiliary electrodes are carbon and reference electrode are silver were purchased and used at all the measurement process.



**Figure 3.3.** Screen printed electrodes used in the study.

### **3.2. Preparation of precursor nanofibers**

#### **3.2.1. Preparation of precursor Lawsons/PAN nanofibers**

The preparation of the solutions for the nanofibers production was applying the chart testing the efficient and applicable concentrations for the purpose, for this, 8 wt. % of polyacrylonitrile was dissolved in N,N-Dimethylformamide by magnetic stirring at ambient condition for 24 hours, the obtained PAN/DMF solution was removed into sterilized vials.

A defined amount of lawsons was added into the prepared solution separately and stirred for 24 hours for an homogenous amalgam. 1, 3, 15, 30, 50, 70 and 100 wt.% of Lawsons was added into PAN/DMF solutions and symbolized as L<sub>1</sub>, L<sub>3</sub>, L<sub>15</sub>, L<sub>30</sub>, L<sub>50</sub>, L<sub>70</sub> and L<sub>100</sub>. Subscript “x” at L<sub>x</sub> is referred the amount of Lawsons added in the solution as the wt. % of PAN in the final solution.





**Figure 3.4.** The prepared PAN/DMF/Law solutions

The prepared stock solutions were transferred into 10 ml medical plastic syringe (metal blunt needle with a 21-gauge number). The syringe was placed on a micropump system (New Era, NE-300) with fixing the distance parameter of the tip of needle with grounded collector system at 10 cm for the whole electrospinning process as presented in the figure 3.5. The feeding rate during the production was set at 0,5 ml/hour with an applied voltage of 12 kV to the metal needle from Gamma high Voltage Research power supplier. The electrospinning of the PAN nanofibers was made in the conventional conditions reported in the literature.

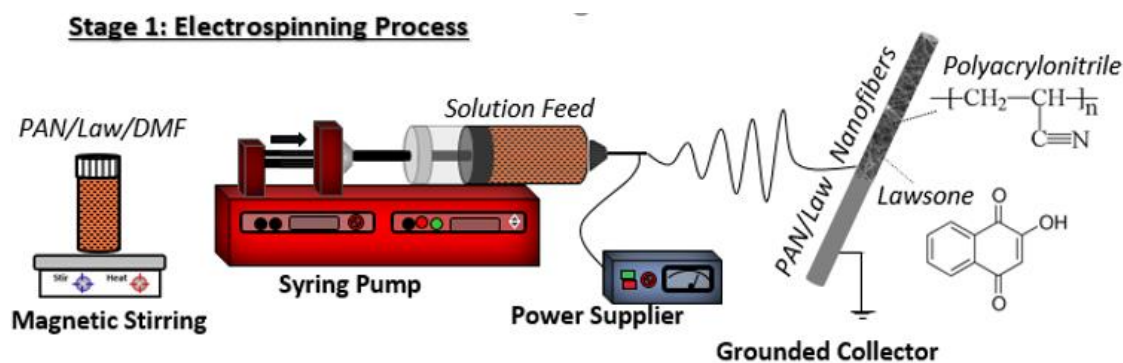


**Figure 3.5.** solution preparation and electrospinning process of PAN/Law nanofibers

For the phase of determination of the electrospinning solution parameters, the prepared PAN/DMF and Law/PAN/DMF solutions parameters were determined and analyzed under an ambient condition, firstly the viscosity measurement was performed in the aBrookfield DV-II+Pro, 100 rpm by the use of a thermosel spindle, then the surface tension measurements were carried out with Attension Theta Tensiometer. The solutions

conductivities were an important analyse that were measured with a Hach-HQ40d portable digital multimeter.



**Figure 3.6.** Prepared precursor PAN/Law nanofibers

### **3.2.2. Preparation of precursor Hemoglobin/PAN nanofibers**

The preparation of the precursor Hemoglobin/PAN nanofibers was made by the preliminary preparing 8 wt. % of PAN solution that was by dissolving PAN in N,N-Dimethylformamide (DMF) via magnetic stirring at the ambient conditions.

This first step was important for obtaining a homogenous amalgam for the further solutions, an appropriate amount of the prepared solution was transferred in an equal amount into the empty vials and Hemoglobin powders were added into these vials in different amounts. .5, 1, 3, 5, 15 and 30 wt.% of Hb respect to PAN were added into PAN/DMF solutions and labelled as H<sub>0.5</sub>, H<sub>1</sub>, H<sub>3</sub>, H<sub>5</sub>, H<sub>15</sub>, and H<sub>30</sub>. Subscript “x” at H<sub>x</sub> is referred the amount of Hb added in the solution as the wt. % of PAN in the final solution.





**Figure 3.7.** The prepared PAN/DMF/Hb solutions

To assure a proper homogenization of the solutions, the mixtures were stirred in the ambient conditions for 24 hours. Once the prepared solution is ready for the electrospinning process, a proper amount of 10 ml from each concentration was transferred into the plastic syringe and adjusted on a micro pump feeding system (New Era, NE-300). The electrospinning process parameters were fixed as 10 cm for the distance between the grounded conductive metal collector and the needle, the feeding rate was fixed as 0.5 ml/hours feeding rate and 12 kV voltage applied (Gamma High Voltage Research power supplier) to the metal needle (with a metal blunt needle, gauge number 21) of the syringe as presented in the figure 3.5.

As the case of lawsone presented above, the characterization of the precursor PAN/Hb and CNF, the electrospinning solution parameters were analyzed by determining the viscosity, surface tension and conductivity of the prepared solution PAN/Hb/DMF.

### **3.3. Heat treatment of the precursor nanofibers**

#### **3.3.1. Heat treatment of the precursor Law/PAN nanofibers.**

The step of stabilization is highly important and crucial to prevent melting and fusion of the nanofibers, minimizing the volatilization of the elemental carbon in the carbonization steps maximizing the carbon yield are the mainly important role of this treatment process. The literature reported a wide range of PAN stabilization studies consisting mainly on the dehydrogenation and cyclization of the nitrile groups ( $C\equiv N$ ) and crosslinking of chain molecules in the form of  $-C=N-C=N-$ . this process performances can be controlled by

different parameters as the pyrolysis temperature, tension of the fibers, process time, air flow and heating rate (Gergin et al., 2017).

The prepared precursors pure PAN and Law/PAN nanofibers were stabilized first by feeding a dried air gas into a tube at 280°C for 1 hour to allow an efficient cross-linking of the PAN chains during this process and the obtained polymeric structure can be able to face the high temperature of the following treatment.

For this process a Protherm (STF 12/60/300 model) tube furnace with PC442T temperature control unit and 60 cm diameter ceramic tube was chosen, from the room temperature to 280 °C the increase was with a heating rate of 10 °C/min.

Once the samples were stabilized, the cooling was in room temperature before the following process of carbonization.

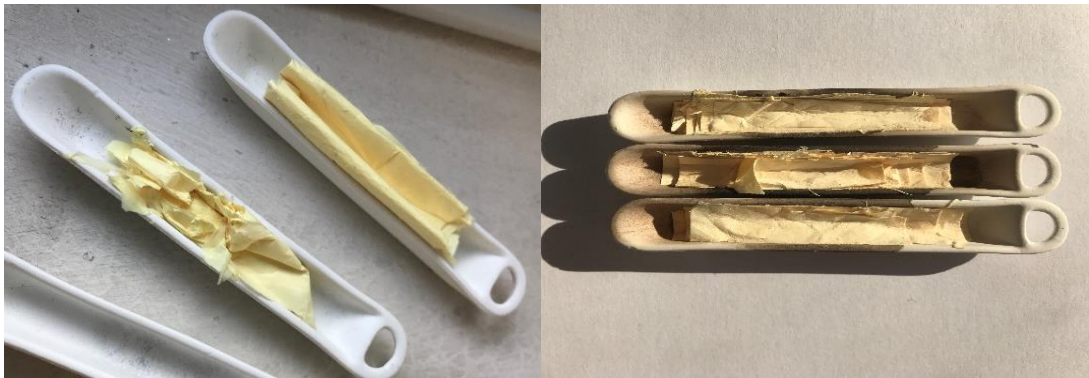


**Figure 3.8.** A: prepared as-spun PAN/Law precursor nanofibers. B: stabilized PAN/Law precursor nanofibers

The carbonization of the PAN nanofibers was reported in a plethora of scientific researches and articles, this process should be conducted under nitrogen gas to prevent burning of the nanofibers, during this process the elimination under high temperature of other elements ( $N_2$ ,  $O_2$ ,  $H_2$ ) and impurities is guaranteed and the obtained structure's carbon concentration is increased with a higher decrease of the structure's diameters.

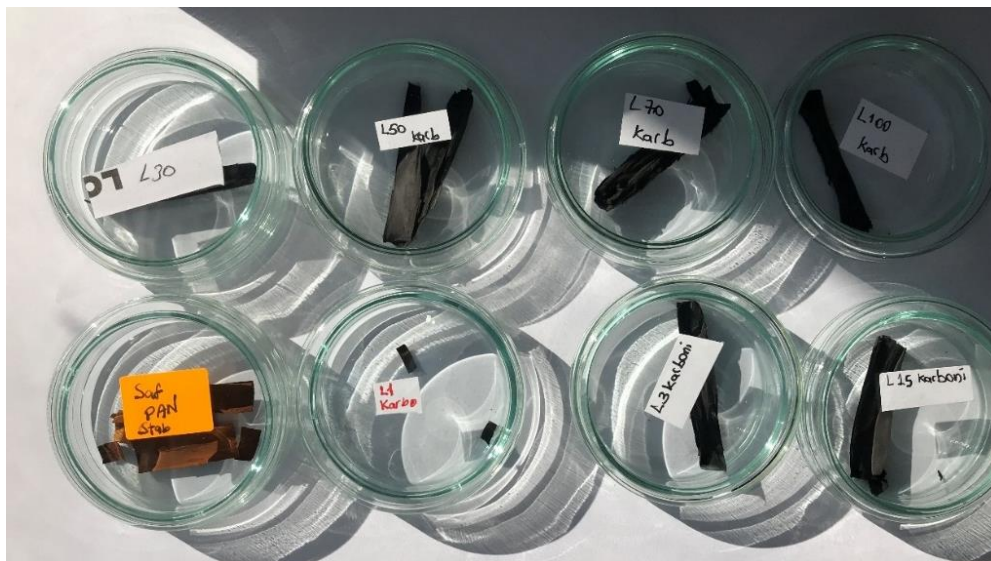


**Figure 3.9.** Carbonized PAN/Law samples

Once the stabilized samples were totally cooled in the room temperature, a carbonization process was done in the same furnace in a temperature up to 800 °C with a heating rate of 10 °C/min, once the temperature reached it higher value, the samples were maintained at this temperature for 2 hours for an efficient carbonization of the nanofibers. Both of stabilization and carbonization processes were schematically illustrated in the figure 3.10.

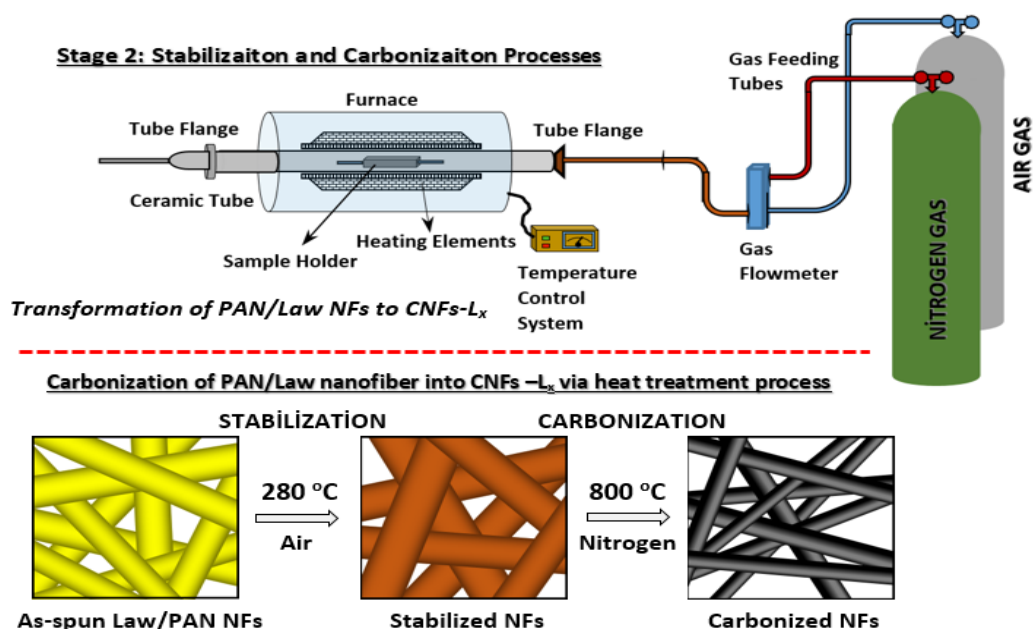


**Figure 3.10.** Schematic illustration of electrospun precursor nanofiber preparation (Stage 1) and stabilization and carbonization of as-spun precursor nanofibers (Stage 2), and transformation of Law/PAN NFs into Law enriched CNFs

### 3.3.2. Heat treatment of the precursor Hb/PAN nanofibers.

The thermal analysis of the prepared precursor Hb/PAN and pure PAN were investigated in two steps of stabilization and carbonization and aimed to transform and convert the precursor nanofibers into Hb-CNFs as schematically illustrated in the figure 3.12.

The stabilization process, as introduced in all the research papers, was applied in a standard condition for all the samples, the prepared as spun Hb/PAN precursors nanofibers were stabilized in air environment at 280 °C with a heating rate of 10 °C/min for 1 hour in a tube furnace system to make the samples prepared for an efficient following carbonization step.



**Figure 3.11.** Stabilized and carbonized PAN/Hb nanofibers samples

Once the process of stabilization was completely done, the samples were cooled for 24h in the room temperature and integrated for the carbonization process.

The carbonization started with a progressive heating in the same furnace by feeding nitrogen gas to prevent any burning. Nanofibers were carbonized at 800 °C for continuously 2 hours with a heating rate of 10 °C/min.

The obtained nanofibers were analyzed and characterized in the following parts of the project.



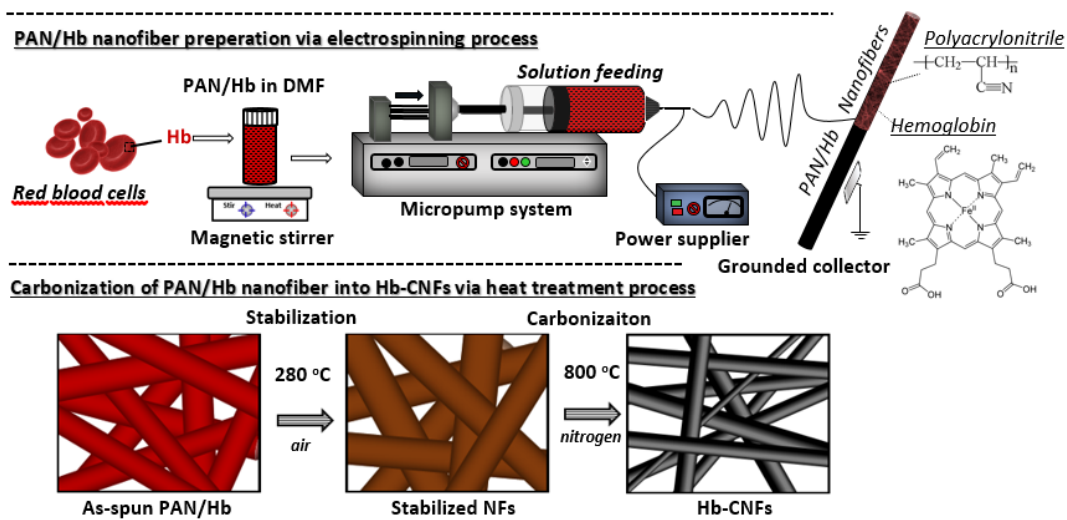


**Figure 3.12.** Schematic illustration of the electrospinning of PAN/Hb hybrid nanofibers, and their carbonization into Hb-CNFs via heat treatment processes.

### 3.4. Characterizations of the prepared nanofibers

#### 3.4.1. Characterizations of the prepared Law/PAN nanofibers.

The processes of electrospinning and heat treatment were efficiently investigated and the obtained samples were carefully maintained from any contamination sources, in this part, the characterizations of the nanofibers are primordial to analyse the chemical and morphological changes present for a better advancements and efficiency.

For this purpose, the samples were gently collected from the surface of grounded collector and prepared in similar amounts, the morphological analysis was investigated with a scanning electron microscopy (SEM, ZEISS EVO 40), the nanofibers samples were firstly coated with gold palladium (60/40) for 60 seconds (using a Baltec Sputter Coater) to prevent any charge accumulation on their surfaces. As-spun, stabilized and carbonized Law/PAN nanofibers morphological images were taken in this stage then the fiber diameter was measured afterwards using ImageJ program (The National Institutes of Health, USA). In a standardized process, 100 nanofibers from each sample and its corresponding heat treatment grade were measured in the SEM images and average nanofibers diameters were determined. The collected data were directly organized for a nanofiber diameter distribution chart and built as fiber diameter vs frequency in MS Excel.

The chemical analysis was accomplished for as-spun precursor Lw/PAN nanofibers with Fourier transform infrared spectroscopy (FTIR) (Perkin Elmer, Spectrum100 model, USA).

Differential Scanning Calorimetry (DSC) tests were carried out with Differential Scanning Calorimetry Analyzer (TA Instruments/ Discovery DSC251, New Castle, USA) at  $10^{\circ}\text{C min}^{-1}$  of heating rate from 20 to  $400^{\circ}\text{C}$  with a continuous Nitrogen gas feeding into the DSC test chamber during the whole process of measurement.

Thermalgravimetric (TGA) tests were conducted with a simultaneous thermogravimetric analyser for the investigation of the weight loss under nitrogen gas atmosphere with a heating rate of  $10^{\circ}\text{C min}^{-1}$  from 30 to  $800^{\circ}\text{C}$  (TA/STD650).

Surface area and pore sizes of the carbonized nanofibers were also analyzed by using the Brunauer-Emmett-Teller (BET) technique to investigate the physical adsorption of nitrogen molecules on the surface at a Micrometrics-Tristar II instrument, the degassing temperature was  $120^{\circ}\text{C}$  for 24 hours.

Raman spectroscopy measurement were made to provide detailed information about the chemical structure, crystallinity and the molecular interaction of the samples using the interaction of the chemical bounds within the material with a scattered light, these measurements were conducted with a Renishaw inVIA with the laser line at 532 nm.

X-Ray diffraction (XRD) analysis was carried out with a Bruker/D8 advance X-ray diffractometer to analyse the crystallographic structure of the material.

#### **3.4.2. Characterizations of the prepared Hb/PAN nanofibers.**

As presented in the preceding part and following the chronology of the project, the electrospinning solutions parameters were investigated by the viscosity measurement, conductivity and surface tension of the prepared Hb/PAN/DMF solutions. The obtained electrospun nanofibers were carefully prepared for characterizations analysis. The samples were gently collected from the surface of the grounded collector without destroying their physical morphology. Scanning electron microscopy (SEM) was performed with a ZEISS EVO 40 for a morphological investigation of as-spun, stabilized

and carbonized prepared nanofibers. Before the analyse, the nanofibers were conductively coated with gold-palladium (60/40) for 60 seconds for an enhanced imaging with preventing any charge accumulation on the surface of the nanofibers and homogenous surface for analysis and imaging quality by using Baltec Sputter Coater.

Once the images were generated, nanofibers diameters were measured following a standard methodology of selecting 100 nanofibers from each concentration and heat analogy, and using an open-source program, ImageJ program (The National Institutes of Health, USA) for average nanofiber diameter determination and diameter distribution chart preparation, the collected diameters were transferred to MS Excel and organized for a nanofiber diameter distribution chart and built as fiber diameter vs frequency.

Chemical analysis of as-spun Hb/PAN nanofibers was carried out with Fourier transform infrared spectroscopy (FTIR) (Perkin Elmer, Spectrum 100 model, USA).

The samples were thermally analyzed with Differential Scanning Calorimetry Analyzer (DSC) (TA Instruments/Discovery DSC251, New Castle, USA) and Thermalgravimetric (TGA) (TA/SDT650) methods, during these processes, nitrogen gas was fed into measurement chamber continuously and the temperatures were increased with a heating rate of 10 °C/min for an exhaustive analyse of the weight loss and heat flow of the samples over a temperature range for an efficient following measurement.

In order to analyse the microstructure of the carbonized nanofibers, the X-Ray diffraction (XRD) method was conducted with Bruker/D8 Advance X-ray diffractometer.

Raman spectroscopy measurement was investigated to analyse the chemical structure, crystallinity and the molecular interaction of the samples using the interaction of the chemical bounds within the material with a scattered light, these measurements were carried out with a Renishaw inVIA with the laser line at 532 nm.

Interaction of Phosphate-Buffered Saline on the Surface of Carbon Nanofiber Electrodes was studied, in this regard, after morphological analyses of the prepared PAN/Law and PAN/Hb nanofibers with a scanning electron microscope, contact angle measurements were conducted by dropping PBS on the carbon nanofibrous mat surfaces.

Physical interaction of phosphate-buffered saline with the surface of carbon nanofiber mats were investigated via contact angle measurements. When the droplet of PBS was touched the surface, the angle was about 120° at pure carbon nanofibers as seen in APP 10.

When lawsone was presented in the precursor nanofibers then carbonized, the contact angle were 49.39 °, 72.44 °, and 111.64 ° for L<sub>15</sub>, L<sub>30</sub> and L<sub>100</sub> samples as seen in APP 11. The PBS droplet was directly sucked by the L<sub>70</sub> sample.

For the Hemoglobin added samples (see APP 12), the droplet was directly sucked by H<sub>0.5</sub> and H<sub>3</sub> samples, and the contact angles were 32.07°, 124.02 °, and 100.97 ° for H<sub>1</sub>, H<sub>15</sub> and H<sub>30</sub> samples.

As it is seen the contact angles at the carbonized nanofiber mat surfaces were decreased at the initial addition of lawsone and hemoglobin into their precursor nanofibers, and the angle increased again with increasing lawsone and hemoglobin ratio in the fibers.

The results are revealed that the affinity of the PBS at the lawsone and hemoglobin added carbonized fiber samples were fluctuated due to surface properties and the added materials in the precursor fibers.

Contact angle measurements of electrospun PAN derived neat carbon nanofibers and PAN/lawsone and PAN/hemoglobin derived carbon nanofibers with PBS were carried out. Highest contact angle was measured with neat carbon nanofiber mat surfaces.

Even though initial addition of lawsone and hemoglobin reduced the contact angle and increasing lawsone and hemoglobin content also increased the contact angle at carbonized nanofibers mat surfaces, since PBS droplet was directly sucked by some samples (L<sub>70</sub>, H<sub>0.5</sub> and H<sub>3</sub>) it is concluded that the contact angle is not only depend on the lawsone and hemoglobin content, it is also depended on the surface properties of the carbonized nanofiber mat.



### **3.5. Experimental procedure for the electrochemical miRNA biosensor measurements**

#### **3.5.1. Electrochemical activation of the SPEs surfaces**

In this part of the study, a proper preparation of the SPEs surface was firstly done by electrochemically cleaning the electrodes and activating by dropping 100  $\mu\text{L}$  of ABS on the surface and applying a differential pulse voltammetry DPV method for a complete activation. In this part, along 60 sec, 1.4 V deposition potential was applied with 600 number of points, a continuous measurement is applied then in the scale of 0.7-1.4 V with 10 mV/s scanning rate with keeping the ABS on the SPEs surfaces. Finally, the ABS were removed from the surface of the SPEs and the SPEs were washed with 300  $\mu\text{L}$  of PBS by a careful drop by drop method. After the activation process, the SPEs were totally dried at ambient conditions at least 1 hour and can be ready for the following step of electrochemical measurements.

#### **3.5.2. Immobilization of CNFs on the SPEs surfaces**

The prepared continuous CNFs from the electrospinning process followed by a suitable stabilization and carbonization were dispatched in a proper amount to glass vial after a mechanical broke into short fibers as in the powder form in order to immobilize the CNFs on the working electrode of the SPEs. The CNFs web were transferred to the glass vials and magnetically stirred and vibrated using a vortex mixture in order to obtain a homogeneous result.

The immobilization of the CNFs on the SPE surface was a critical step in the electrochemical part of the study. For this purpose, two different approaches were applied and tested.

In the first approach, the shortened CNFs were directly immobilized. For this purpose, the CNFs powders suspended in ethanol and the obtained solutions were dropped on the surface of the working electrodes part of the SPEs, dried and used without any washing step with PBS.

In the second method, a covalent bond modification was assured by chemically modifying the SPEs surfaces with N-hydroxysuccinimide/1-ethyl-3-(3-dimethylaminopropyl)-carbodiimide (NHS/EDC) solution. To prepare the NHS/EDC solution, 9.21 mg NHS (8 mmol. l<sup>-1</sup>) and 9.59 mg EDC (5 mmol. l<sup>-1</sup>) were put in 10 mL PBS solution and magnetically stirred at ambient condition until obtaining a homogeneous amalgam. From the prepared NHS/EDC solution. For the surface modification, 10 µL of the prepared NHS/EDC was dropped on the SPEs surfaces and held for 1 hour in the ambient condition and be ready to use.

On the other part, CNFs were prepared by mixing 1g of the CNF powders of every sample with 100µl dimethyl sulfoxide (DMSO) at 1500r/min for 30 s using a vortex mixer, the obtained CNFs suspensions were hold in the laboratory conditions for 1 hour before being immobilized on the SPEs surfaces.

For a proper immobilization process, 5µl of the prepared CNF suspensions were carefully dropped on the working electrode part of the SPEs and kept for 6 h for an efficient immobilization which is one of the most important parts of the biosensing performances. The final prepared SPEs were washed with 300µl of PBS and dried at ambient condition for at least 1h.

### **3.5.3. Immobilization of anti-miRNA and miRNA molecules on the SPEs**

After the preparation of the SPEs surfaces, firstly NH modified PolyA molecules were attached on the NHS/EDC modified and CNFs immobilized SPEs before the anti-miRNA attachment and the PolyA molecules were not used for the samples without NHS/EDC modification. For this purpose, 5µl of the prepared PolyA measurement solution was carefully dropped on the CNFs immobilized SPEs surfaces and waited for 1 h for a proper attachment, then the electrodes surfaces were gently washed with 300µl of PBS and dried for at least 1 h at the ambient conditions.

Once the prepared electrodes were totally dried and ready for the anti-miRNA immobilization, the PolyT(G) and PolyT(I) were attached on the electrodes surfaces by dropping 10µl of the previously prepared measurement solutions on the working electrode part and for 1 h for an optimal attachment phase, to remove the unattached molecules a

Carefully washing of the samples with 300 $\mu$ l of PBS was done and the electrodes were dried for 1h before the following hybridization step of miRNA molecules.

The process of hybridization of miRNA was investigated by separately dropping 10 $\mu$ l of miRNA, SM. miRNA, and NC. miRNA on the previously prepared anti-miRNA attached samples at the ambient temperature and waited 1h for a proper hybridization. This process was followed by a gently washing of the electrodes surfaces with 300 $\mu$ l of PBS and dried for 1h in order to remove all unattached molecules before the electrochemical measurement.

#### **3.5.4. Electrochemical measurements**

After a proper activation of the electrodes and the immobilization of the genetic molecules on the working electrode surface, SPEs were carefully connected to the potentiostat via a cable having a port suitable to the SPEs.

For the measurement process, ACB solution was dropped on the SPE surface and the measurements were carried out via differential pulse voltammetry in which the change of guanine oxidation signal peaks were obtained and evaluated from the plots. The effects of adding both of Lawson and Hemoglobin as catalysts to the CNFs were investigated and analyzed by a comparison of the guanine peaks intensities.

## 4. RESULTS and DISCUSSION

### 4.1. Morphological investigation of PAN/Law and PAN/Hb nanofibers

#### 4.1.1. Morphological analysis of PAN and PAN/Law nanofibers

The morphological investigation of the prepared as spun precursor pure PAN and PAN/Law nanofibers was carried out via SEM imaging that present a general view of the nanofiber's diameters and continuities. As shown in the figure bellow, the images collected for each sample was projected to an interpretable chart.

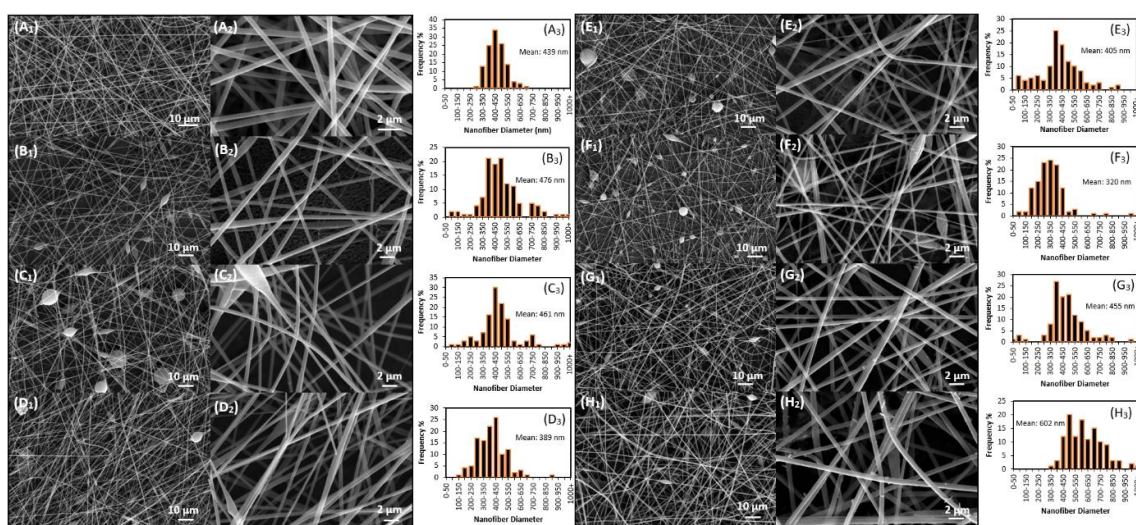


**Figure 4.1.** SEM images (subscript 1 and 2) and diameter distribution (subscript 3) of electrospun PAN/Law precursor nanofibers with different wt.% of Lawsonsone respect to PAN content: (A<sub>1-3</sub>) 0, (B<sub>1-3</sub>) 1, (C<sub>1-3</sub>) 3, (D<sub>1-3</sub>) 5, (E<sub>1-3</sub>) 30, (F<sub>1-3</sub>) 50, (G<sub>1-3</sub>) 70, and (H<sub>1-3</sub>) 100

As-spun pure PAN nanofibers present a random orientation fashion in the 3D nanofibrous mat structure with a smooth structure observed. The addition of Lawsonsone molecules leads to an apparition of beads defects in all the concentrations. The diameters of the beads were big in comparison with the diameter of the nanofibers. From the result of the viscosity, surface tension and conductivity measurements given in table 4.1 to interpret the effect of complex interactions in the prepared solution on the diameter of the nanofibers during the electrospinning process and confirm that, compared to PAN/DMF solutions, the viscosity and conductivities increased after the Law addition with a decrease on the surface tension except for the low Law added sample L<sub>1</sub>. The addition of

Law lead to a few increases of the average nanofiber’s diameters. It could be revealed that whichever the solution parameters outweigh, its effect on the nanofibers diameters tends to be more determinative. Analysing the obtained diameters distribution chart leads to conclude that nanofibers diameters distribution manifested a changement from narrow to broader fashion with Law addition and this result is homogenously converging with the standard deviation measurements. It is also important to note that the higher concentration of Law addition into the electrospinning solution led to a formation of nanorod-like particulate and their amount were proportionally increasing by the increase of the Law content in the nanofibers as presented in figure 4.1 (F<sub>2</sub>-H<sub>2</sub>).

**Table 4.1.** Characteristics of Measured Electrospinning Solution Parameters and Diameters of Electrospun PAN and PAN/Law<sup>a</sup> Nanofibers

Samples	Viscosity (cP)	Surface Tension (mN m <sup>-1</sup> )	Conductivity (μS cm <sup>-1</sup> )	As-spun-diameter <sup>b</sup> (nm)	Stb-diameter <sup>c</sup> (nm)	CNFs-diameter <sup>d</sup> (nm)
PAN	265.6	43.99	96.3	439±72	451±127	322±62
L1	332.5	53.48	115.4	476±163	383±115	232±79
L3	284	40.92	111.9	461±163	435±127	267±84
L15	291.2	41.91	111.5	389±113	387±137	249±86
L30	232.2	42.20	113.9	405±162	480±112	293±83
L50	294.4	41.47	113.2	320±121	466±107	305±108
L70	288	41.39	113.4	455±145	933±364	506±149
L100	297	40.68	110.7	602±144	500±147	293±71

<sup>a</sup>Precursor Polyacrylonitrile/Lawsone (PAN/Law) nanofibers, <sup>b</sup>Diameters of as spun PAN/Law precursor nanofibers, <sup>c</sup>Stabilized nanofibers of “b”, <sup>d</sup>Diameters of carbonized nanofiber of “c”. The values of nanofiber diameters were expressed as means ± standard deviations.

The electrospun PAN and PAN/Law nanofibers were induced for a proper stabilization process at 280 °C for 1 h before a following carbonization. The obtained stabilized samples were also morphologically investigated and SEM images of the nanofiber’s diameters were collected and plot as diameter distribution chart to be analyzed. The nanofibers kept their uniformity and continuity without any change in their 3D nanofibrous mat structure. As presented in the Table 4.2, the average diameter of the stabilized nanofibers was calculated for a proper analyze and showed an increase of 2.73% of the pure PAN nanofibers after the stabilization process.

The average diameter of the stabilized nanofibers compared to their as-spun diameters were  $-19.5\%$ ,  $-5.6\%$ ,  $-0.5\%$ ,  $18.5\%$ ,  $45.6\%$ ,  $100.2\%$ , and  $63.9\%$  respectively for the samples L<sub>1</sub>, L<sub>3</sub>, L<sub>15</sub>, L<sub>30</sub>, L<sub>50</sub>, L<sub>70</sub>, and L<sub>100</sub> as presented in the Figure 4.2 The literature reported in a plethora of studies that stabilized PAN nanofibers in air atmosphere shows an increase of their average diameter compared to their as-spun counterparts.

The analyse of the diameter of PAN/Law nanofibers after stabilization showed a decrease with low Law addition and increase at high concentration of Law addition into the precursor nanofibers.

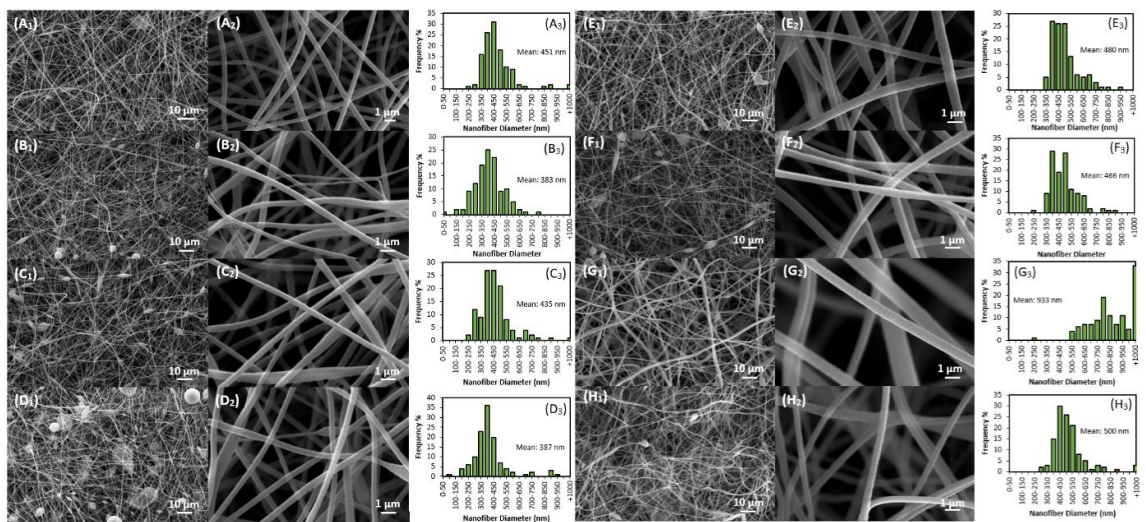


**Figure 4.2.** SEM images (subscript 1 and 2) and diameter distribution (subscript 3) of stabilized PAN/Law precursor nanofibers. The contents are in the precursor PAN/Law nanofibers before the stabilization process as wt.% of Lawsone respect to PAN content: (A<sub>1-3</sub>) 0, (B<sub>1-3</sub>) 1, (C<sub>1-3</sub>) 3, (D<sub>1-3</sub>) 5, (E<sub>1-3</sub>) 30, (F<sub>1-3</sub>) 50, (G<sub>1-3</sub>) 70, and (H<sub>1-3</sub>) 100

The stabilized nanofibers were cooled in the ambient conditions and carbonized at  $800^{\circ}\text{C}$  in the nitrogen atmosphere for 2 h. The investigation of morphological changement of carbon nanofibers was carried out via the same process above by a SEM imaging and nanofibers diameters charts graphs were plotted.

Nanofibers kept their continuities and 3D nanofibrous mat structure after carbonization, small nanoparticulate and macropore were identified (figure 4.3. G<sub>2</sub>, B<sub>2</sub>, F<sub>2</sub>). As recapitulated in the table 4.2, the nanofibers diameters were significantly decreased after being carbonized for PAN and PAN/Law nanofibers.



The comparison and analyse to pure carbon nanofibers led to conclude that the diameters of Law enhanced carbon nanofibers were lower and carbon nanofibers diameters exhibited a broader distribution with Law enhancement.

Compared to their as-spun precursor, the average nanofibers diameters showed a reduction of 26.6%, 51.2%, 42%, 35.9%, 27.6%, 4.6%, and 3.9% respectively after carbonization process of the precursor PAN and PAN/Law ( $L_1$ ,  $L_3$ ,  $L_{15}$ ,  $L_{30}$ ,  $L_{50}$ , and  $L_{100}$ ) nanofibers with a noticeable increase of 8.5% after carbonization of the  $L_{70}$  sample.

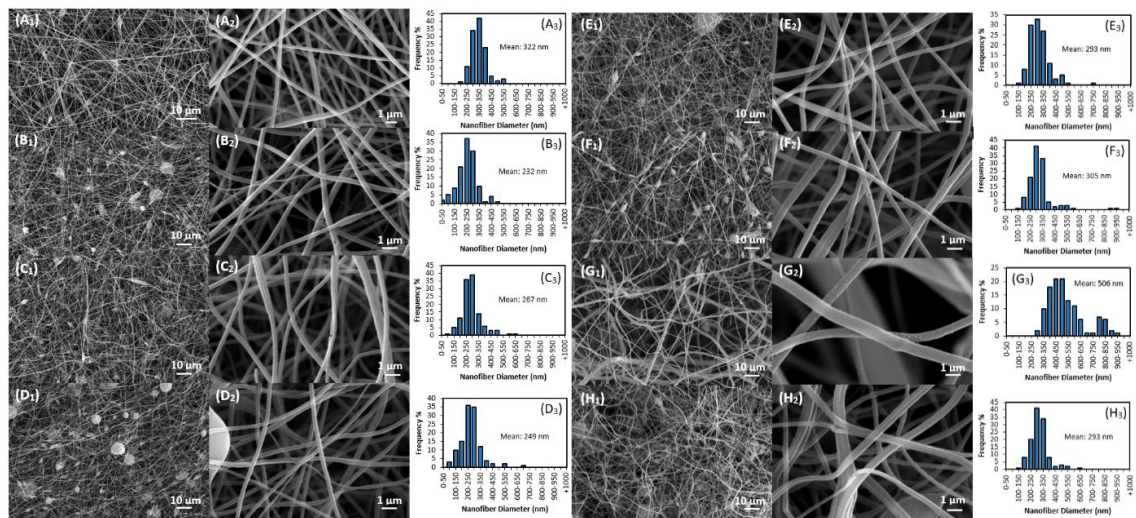


**Figure 4.3.** SEM images (subscript 1 and 2) and diameter distribution (subscript 3) of the carbonized nanofibers. The contents are in the precursor PAN/Law nanofibers before the stabilization process as wt.% of Lawsone respect to PAN content: (A<sub>1-3</sub>) 0, (B<sub>1-3</sub>) 1, (C<sub>1-3</sub>) 3, (D<sub>1-3</sub>) 5, (E<sub>1-3</sub>) 30, (F<sub>1-3</sub>) 50, (G<sub>1-3</sub>) 70, and (H<sub>1-3</sub>) 100

#### 4.1.2. Morphological analysis of PAN and PAN/Hb nanofibers

In this part of study, after the electrospinning process, the nanofibers were directly characterized to analyse the effect of Hemoglobin loaded PAN/Hb precursor nanofibers. The morphological investigations were carried out via SEM imaging as showed in the figure 4.4 bellow.

For a better analyse, pure PAN nanofibrous mat were also integrated in the figure as reference. The obtained imagery showed a 3D nanofibrous mat morphology for all the precursor nanofibers, with a smooth morphology.

**Table 4.2.** Characteristics of Measured Electrospinning Solution Parameters and Diameters of Electrospun PAN and PAN/Hb<sup>a</sup> Nanofibers

Samples	Viscosity (cP)	Surface Tension (mN m <sup>-1</sup> )	Conductivity (μS cm <sup>-1</sup> )	As-spun-diameter <sup>b</sup> (nm)	Stb-diameter <sup>c</sup> (nm)	CNFs-diameter <sup>d</sup> (nm)
PAN	265.6	43.99	96.3	439±72	451±127	322±62
H <sub>0.5</sub>	236.8	37.02	95.9	480±218	399±118	310±101
H <sub>1</sub>	240	31.82	95.1	372±133	380±99	262±92
H <sub>3</sub>	240	32.99	93.9	485±223	450±135	303±67
H <sub>5</sub>	246	39.03	91.4	346±136	437±112	300±93
H <sub>15</sub>	249	36.63	84.2	286±148	436±67	340±80
H <sub>30</sub>	256	39.16	82.3	483±159	442±105	341±112

<sup>a</sup>Precursor Polyacrylonitrile/Hemoglobin (PAN/Hb) nanofibers, <sup>b</sup>Diameters of as spun PAN/Hb precursor nanofibers, <sup>c</sup>Stabilized nanofibers of “b”, <sup>d</sup>Diameters of carbonized nanofiber of “c”. The values of nanofiber diameters were expressed as means ± standard deviations.

As-spun PAN nanofibers exhibited a perfect uniformity with no defect structure identified. The addition of Hemoglobin into the electrospinning solutions led to the formation of beaded defects structure in the mat after the electrospinning process. The beads formation could be related to the low solubility of Hemoglobin in the PAN/DMF solution. A homogenous dissolution of the hemoglobin particles in the solution, the defect level could be transferred to nanofibers more and the beaded defect could be detected on nanofibers frequently as a bead-on-string morphology defect structure. The quantity of the beads was unproportionally changed with the hemoglobin concentration as in the electrospinning solution. As seen from the table 4.2 the average nanofibers diameters were 439 for pure PAN, and 480, 372, 485, 346, 286, and 483 nm respectively for PAN/Hb (H<sub>0.5</sub>, H<sub>1</sub>, H<sub>3</sub>, H<sub>5</sub>, H<sub>15</sub>, and H<sub>30</sub>) nanofiber samples. The average nanofiber diameters were not proportionally changing with the increasing the Hb amount in the solutions. Nanofiber’s diameters distributions were broader when Hb was added to the PAN nanofibers compared to pure PAN nanofibers as illustrated in figure 4.4.

The characterizations of nanofibers were investigated by measuring viscosity, surface tension and conductivity of the electrospinning solutions for an efficient interpretation of the nanofiber diameters. The calculated viscosity of the solution decreased with the first amount of added Hb and increased again with increasing Hb amount in the solution and these results were almost similar in surface tension measurements results. The solution



conductivity showed a decrease in a regular fashion by increasing the Hb amount in the solutions. Even though this results an irregular trend in viscosity and surface tension led to a non-uniform change in average nanofibers diameters at PAN/Hb nanofibers. The Hb particles were not perfectly dissolved in PAN/DMF solution and some Hb were remained as undissolved particular form in the solution. Even though this limitation, the solution viscosity increased proportionally with increasing the amount of Hb in the solution and consequently the limited solubility of Hb in PAN/DMF solution at ambient condition didn't allow to project the efficient properties of the solution to nanofibers structures.

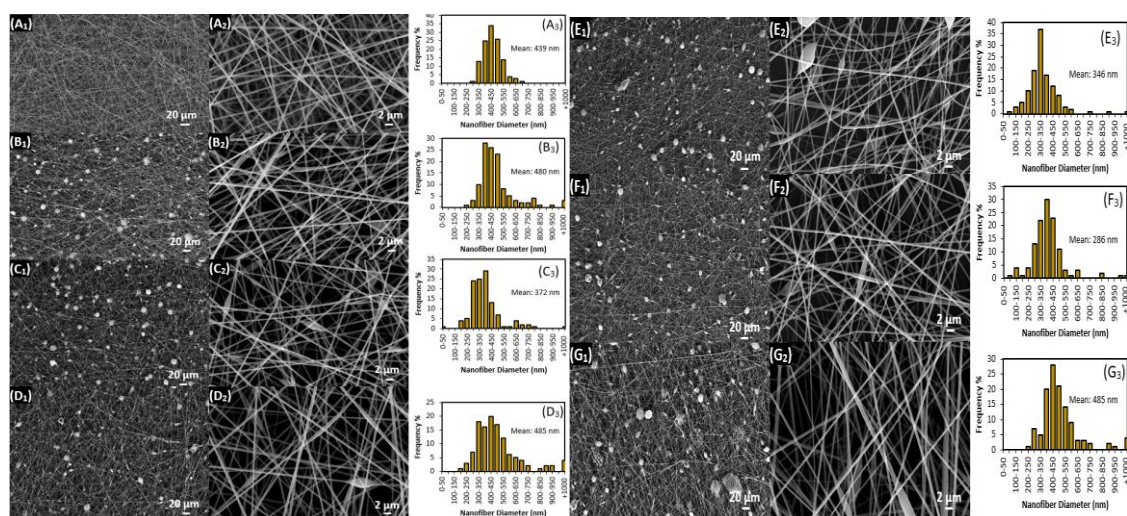


**Figure 4.4.** SEM images of as-spun PAN/Hb nanofibers and their diameter distribution charts: (A<sub>1-3</sub>) pure PAN, (B<sub>1-3</sub>) PAN/H<sub>0.5</sub>, (C<sub>1-3</sub>) PAN/H<sub>1</sub>, (D<sub>1-3</sub>) PAN/H<sub>3</sub>, (E<sub>1-3</sub>) PAN/H<sub>5</sub>, (F<sub>1-3</sub>) PAN/H<sub>15</sub>, and (G<sub>1-3</sub>) PAN/H<sub>30</sub>.

The stabilization is a crucial phase of the obtention of thermal analysis. In this study the nanofibers were stabilized in 1 hr in air atmosphere at 280 °C for the necessary reactions (e.g., cyclization, dehydrogenation) before being carbonized. The obtained 3D nanofibrous mat structure was morphologically analysed with SEM methods to compare the effect of the stabilization process on the physical morphology of the nanofibers.

After the stabilization process, the 3D mat structure did not change and no defect was detected as illustrated in figure 4.5. The average nanofiber diameter of pure PAN increased but it was noticed that Hb added precursor PAN/Hb nanofiber diameter decreased. Contrary, the standard deviation increased at pure PAN nanofibers after stabilization, it reduced when the precursor nanofibers were loaded with Hb as presented

in the table 4.2. compared to the stabilized pure PAN nanofibers, the average diameter of the Hb added samples were lower at all samples after stabilization process. In this phase, the average diameter of pure PAN was approximately about 450 nm and respectively 399, 380, 450, 437, 436, 442 nm for PAN/Hb (H<sub>0.5</sub>, H<sub>1</sub>, H<sub>3</sub>, H<sub>5</sub>, H<sub>15</sub>, and H<sub>30</sub>) nanofiber samples.

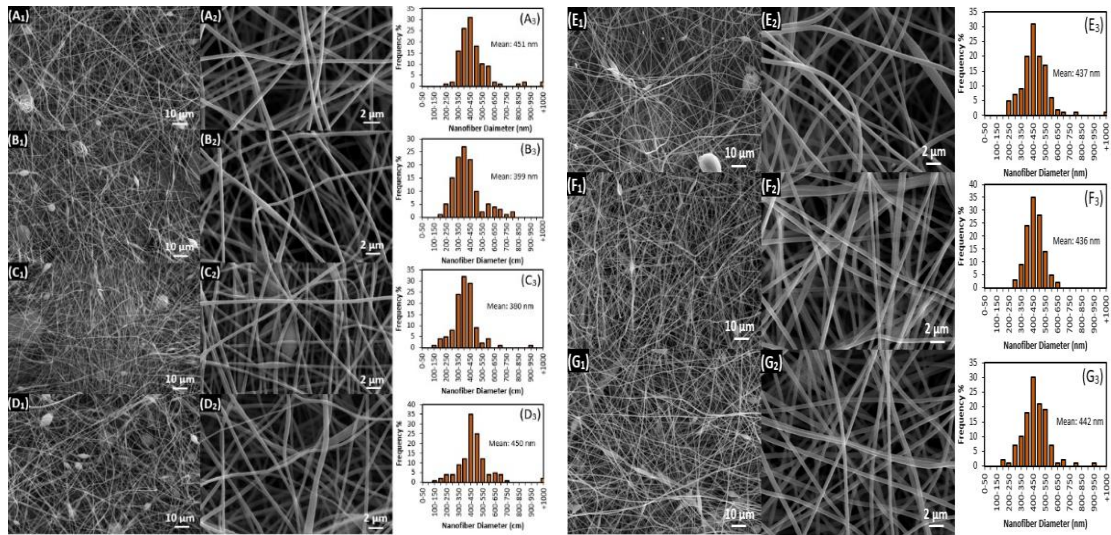


**Figure 4.5.** SEM images of stabilized PAN/Hb nanofibers and their diameter distribution charts: (A<sub>1-3</sub>) pure stb-PAN, (B<sub>1-3</sub>) stb-PAN/H<sub>0.5</sub>, (C<sub>1-3</sub>) stb-PAN/H<sub>1</sub>, (D<sub>1-3</sub>) stb-PAN/H<sub>3</sub>, (E<sub>1-3</sub>) stb-PAN/H<sub>5</sub>, (F<sub>1-3</sub>) stb-PAN/H<sub>15</sub>, and (G<sub>1-3</sub>) stb-PAN/H<sub>30</sub>

The process of stabilization was followed by a proper carbonization in which the samples were carbonized at 800 °C for 2 h in the nitrogen atmosphere. The literature reported similar study and can be referenced for the obtained results and their analysis.

The morphologies of the obtained samples were investigated after carbonization process via SEM imaging and plotted for an interpretable result illustrated in the figure below. The nanofibers kept their uniformity and continuities after carbonization. Referred to the table 4.2 the calculated average nanofibers diameters dramatically decreased and the same results were obtained in all the literature studies. Also, it was noticed that some pore formations were detected on the nanofibers Hb enhanced carbon nanofibers for the samples C<sub>2</sub>, E<sub>2</sub>, and F<sub>2</sub>. The structure of pure PAN nanofibers was perfectly seen without any breakage but with the addition of Hb amount, a breakage was clearly seen after carbonization process. The formation of porous structure in the carbon nanofibers can be

explained by the presence of iron in the precursor nanofibers. The activation effect of iron atoms in hemoglobin led to a macropore formation and an apparition of fiber breakage.

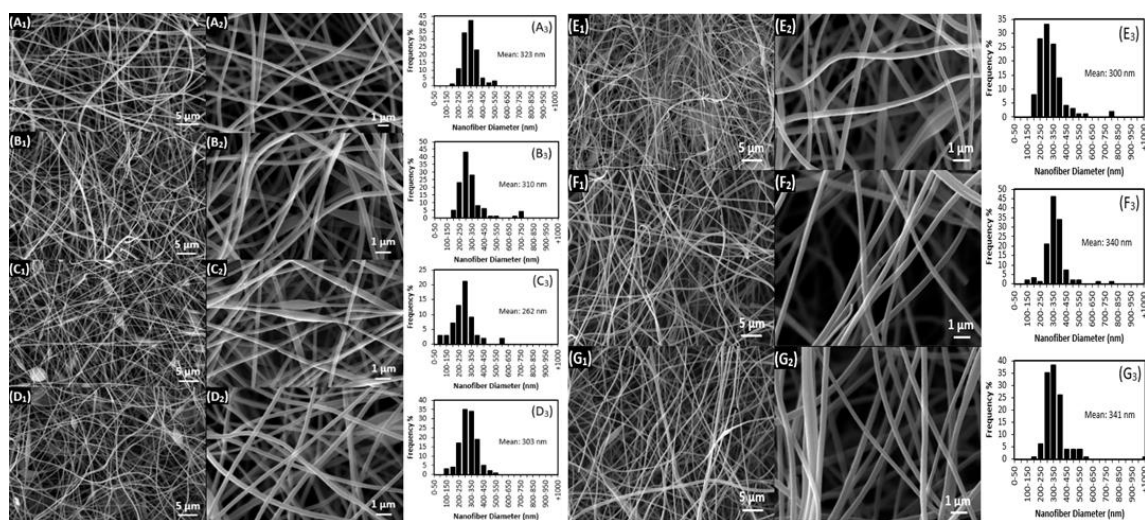


**Figure 4.6.** SEM images of carbonized PAN/Hb nanofibers and their diameter distribution charts: (A<sub>1-3</sub>) pure CNF, (B<sub>1-3</sub>) CNF/H<sub>0.5</sub>, (C<sub>1-3</sub>) CNF/H<sub>1</sub>, (D<sub>1-3</sub>) CNF/H<sub>3</sub>, (E<sub>1-3</sub>) CNF/H<sub>5</sub>, (F<sub>1-3</sub>) CNF/ H<sub>15</sub>, and (G<sub>1-3</sub>) CNF/H<sub>30</sub>

## 4.2. Chemical investigation of PAN, PAN/Law and PAN/Hb nanofibers

### 4.2.1. Chemical analysis of precursor PAN and PAN/Law nanofibers

In this part of study, an investigation of Law addition in PAN nanofibers was demonstrated. FTIR spectra of the pure PAN and pure Law powder was firstly analyzed and demonstrated in the figure below for a proper interpretation.

From the obtained results, prominent peaks were seen for pure PAN nanofibers. The peak at  $1357\text{ cm}^{-1}$  corresponds to C-H wagging of methyl groups. and the peak at  $1452\text{ cm}^{-1}$  relates to bending vibrations of CH<sub>2</sub> groups. A peak at  $1665\text{ cm}^{-1}$  could be related to C=O stretching of the residual excess DMF in PAN nanofibers. the functional group of PAN identified as C≡N nitrile functional group was detected at  $2244\text{ cm}^{-1}$  and stretching vibration band of C-H was observed at  $2938\text{ cm}^{-1}$ .

Lawsone peaks obtained from FTIR spectra were about  $720\text{ cm}^{-1}$  corresponded to C-H deformation in the rings structure. C-O stretching was seen at  $1214\text{ cm}^{-1}$ . C-H bending the naphthalene skeleton was observed at  $1283\text{ cm}^{-1}$ . C=C stretching of aromatic

compounds were detected at  $1458\text{ cm}^{-1}$ . The bands at  $1634\text{ cm}^{-1}$  and  $1677\text{ cm}^{-1}$  corresponded to stretching vibrations of carbonyl groups. The broad band with maximum peak point at  $3158\text{ cm}^{-1}$  was corresponded to OH stretching band. The peak  $1665\text{ cm}^{-1}$  for pure PAN nanofibers relatively decreased with the addition of Law amount and reveals that DMF molecules were held by PAN.

As illustrated in the figure bellow, the existence of all the PAN and Law peaks at PAN/Law nanofibers confirm the perfect incorporation of Lawsone into the PAN nanofibers and revealed that the molecules in the electrospinning solution and nanofibers are amalgamed and mixed properly

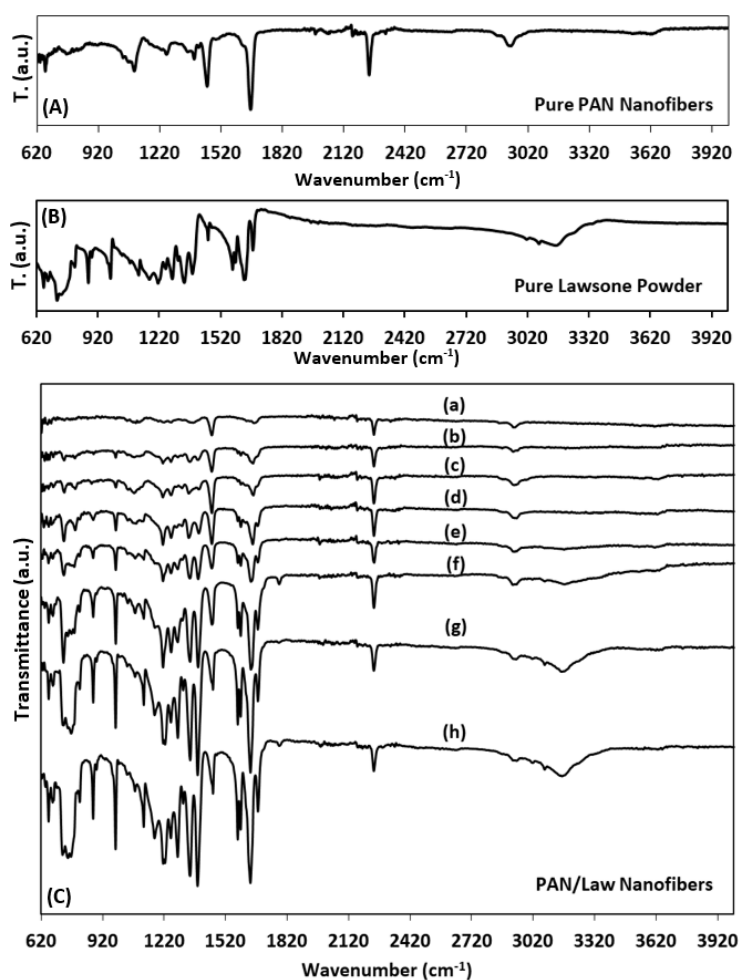


**Figure 4.7.** FTIR spectra of (A) pure PAN nanofibers, (B) pure Lawsone powder, and (C) precursor PAN/Law nanofibers with different wt.% of Lawsone respect to PAN content: (a) 1, (b) 3, (c) 5, (d) 15, (e) 30, (f) 50, (g) 70, and (h) 100 (T, Transmittance)

#### 4.2.2. Chemical analysis of precursor PAN and PAN/Hb nanofibers

The chemical properties of the prepared precursor PAN and PAN/Hb nanofibers with different amount of Hb content were carried out with ATR-FTIR method and the results were plotted for a convenient interpretation.

For pure Hb, prominent peaks were detected at 1539 and 1647  $\text{cm}^{-1}$  and corresponded to Amide-II and Amide I in hemoglobin. The peak detected at 1393  $\text{cm}^{-1}$  attributed to C-N stretching vibration of aromatic amides.

FTIR spectra of pure PAN nanofibers also obtained as reference to investigate how the Hb addition affect the chemical properties of PAN nanofibers. Prominent peaks were obtained for PAN and detected at 1357, 1452, 2244, and 2938  $\text{cm}^{-1}$  correspond to C-H wagging of methyl groups, bending vibrations in  $\text{CH}_2$  groups, stretching vibration of  $\text{C}\equiv\text{N}$  groups and stretching vibration at C-H was observed at 2938  $\text{cm}^{-1}$ .

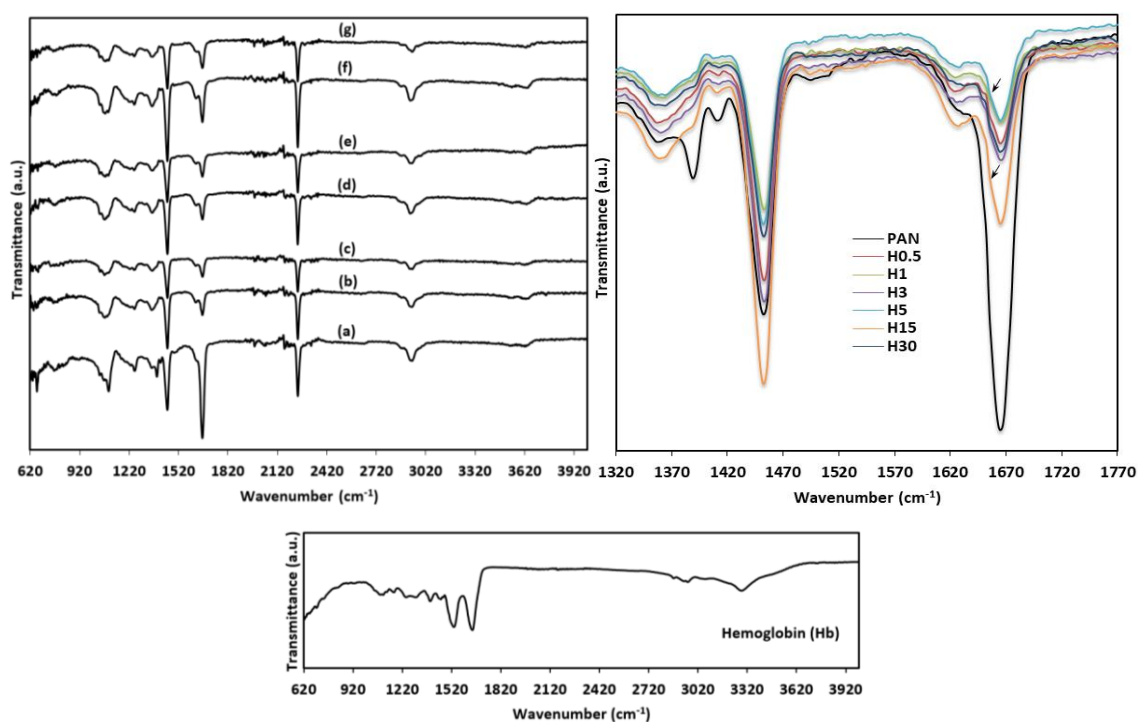


**Figure 4.8.** ATR-FTIR spectra of pure Hb powder and PAN/Hb nanofibers: (a) pure PAN, (b) PAN/H<sub>0.5</sub>, (c) PAN/H<sub>1</sub>, (d) PAN/H<sub>3</sub>, (e) PAN/H<sub>5</sub>, (f) PAN/H<sub>15</sub>, and (g) PAN/H<sub>30</sub>

The peak detected at 1650  $\text{cm}^{-1}$  corresponds to Hb and confirmed the existence of Hb in PAN/Hb nanofibers. A decrease of the peak intensity at 1665  $\text{cm}^{-1}$  with the proportional



addition of Hb to PAN nanofibers is explained that DMF molecules were less trapped by the nanofibers in the present of Hb amount.

### **4.3. Thermal investigation of PAN, PAN/Law and PAN/Hb nanofibers**

#### **4.3.1. DSC analysis of PAN and PAN/Law nanofibers**

In order to determine the glass transition  $T_g$  and melting point  $T_m$  of the nanofibers, DSC analysis of as-spun PAN/Law nanofibers were investigated. As shown in the figure bellow, two peaks were detected around 183–192 °C corresponding to the melting point of Lawsone and 284–296 °C when the plots were observed between 50 and 350 °C of the process. All the collected peak points from the DSC plots were presented in the appendix 1. The melting point of lawsone is directly proportional to increasing its ratio in PAN/Law nanofibers. More the PAN ration in PAN/Law nanofibers tends to increase, it tends to reduce the melting point and melting enthalpy of Law. An exothermic peak around 284–296 °C correspond to three main reactions, dehydrogenation, cyclization, and crosslinking taking place in PAN nanofibers. It is commonly cited in the literature that the crucial reaction is the cyclization in nitrile groups in order to form a ring system. The combination of this peak to higher temperature with the increase of the Law content could be attributed that Lawsone inhibits the occurrence of this reaction in the efficient conditions. From the figure, it is important to note that the decrease of the intensity of this peak can be directly correlated to a reduction of the cyclization reaction. We can conclude that, less graphitic degree of nanofibers can be obtained with a high amount of Lawsone addition to PAN nanofibers (the obtained carbonized PAN/Law nanofibers at higher Law concentrations were smooth and foldable which is not the expected material's performance and structure). Otherwise, it was noticeable that with a few amounts of added Lawsone (like  $L_1$  and  $L_3$ ), an increase of this peak occurs and the peak positions changed and shifted to lower temperature, it results that a low Lawsone addition in the precursor PAN/Law nanofibers leads to a catalytic effect for the stabilization process and will contribute for an efficient and optimal carbonization of the nanofibers.

The focused plot between 80 to 240 °C, showed a peak around 101–109 °C corresponds to  $T_g$  of PAN that increase with a low amount of Lawsone and decrease with its higher addition in PAN/Law nanofibers. This can be explained by the fact that with a high

amount of Lawsone leads to a formation of Lawsone crystals that penetrate into the amorphous structure of PAN and limits their molecular motions.

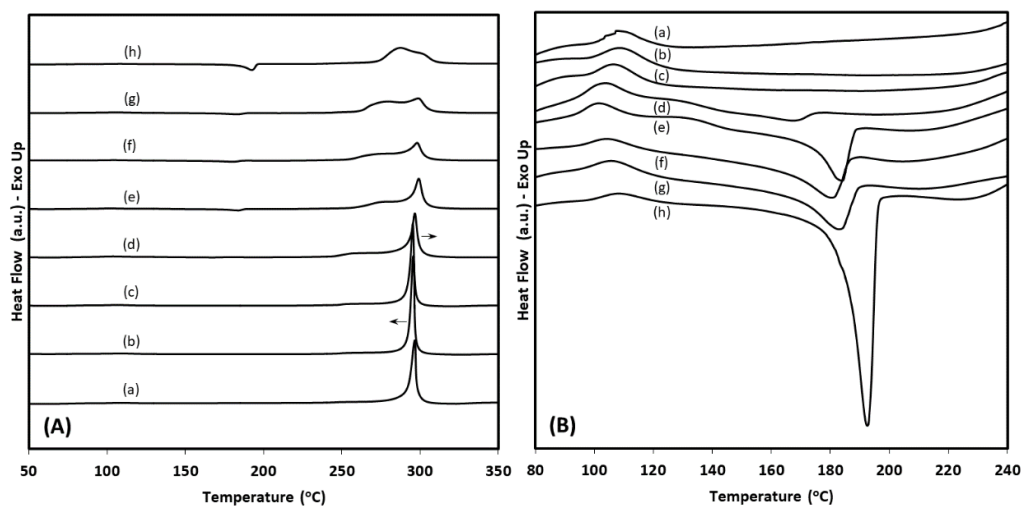


**Figure 4.9.** DSC thermograms of precursor Law/PAN nanofibers with different wt.% of Lawsone respect to PAN content: (a) 0, (b) 1, (c) 3, (d) 15, (e) 30, (f) 50, (g) 70, and (h) 100

#### 4.3.2. DSC analysis of PAN and PAN/Hb nanofibers

In this study, the same process for DSC measurements of Hb added as-spun PAN/Hb nanofibers were performed between 50–150 °C the generated plots were analyzed in accordance to the peaks detected as long range and peak focus. An extremely detectable exothermic peak at all nanofibers samples was observed around 293–301° C. the highest peak was around 296.5, 296.6, 291.9, 293.3, 296.4, 301.4, and 298.5 ° C and onset peak points 292.1, 293.1, 285, 290, 292.8, 295.6, and 295.3 ° C were attributed respectively for pure PAN and PAN/Hb samples H<sub>0.5</sub>, H<sub>1</sub>, H<sub>3</sub>, H<sub>5</sub>, H<sub>15</sub>, and H<sub>30</sub> nanofibers. As cited above. These peaks are corresponding to three reactions, dehydrogenation, cyclization, and crosslinking taking place in PAN nanofibers in which the cyclization is taking the largest attention due to its critical ability to form rings structures. The obtained results showed a chagement in the peak position that shifted to higher temperature accordingly to the addition of Hb amount and revealed that the presence of Hb in the nanofibers leads to inhibits effect and efficiency of these reactions during the process of stabilization. Also, a decrease of the intensity was also a sign of the decrease of the cyclization reaction but it was not the case for the few Hb added samples like H<sub>0.5</sub> and H<sub>3</sub> that performed an

increase of the intensity of these peaks which led to a higher graphitization degree of the structure in the following carbonization process and can be considered as a considerably point of study.

It is also important to notice that at a higher content of Hb content addition (case of H<sub>15</sub> and H<sub>30</sub> samples) a noticeable peak was observed above the main peak as a shoulder peak after a broadening of the peak and can be explained that another crystalline structure is present in the nanofibers.

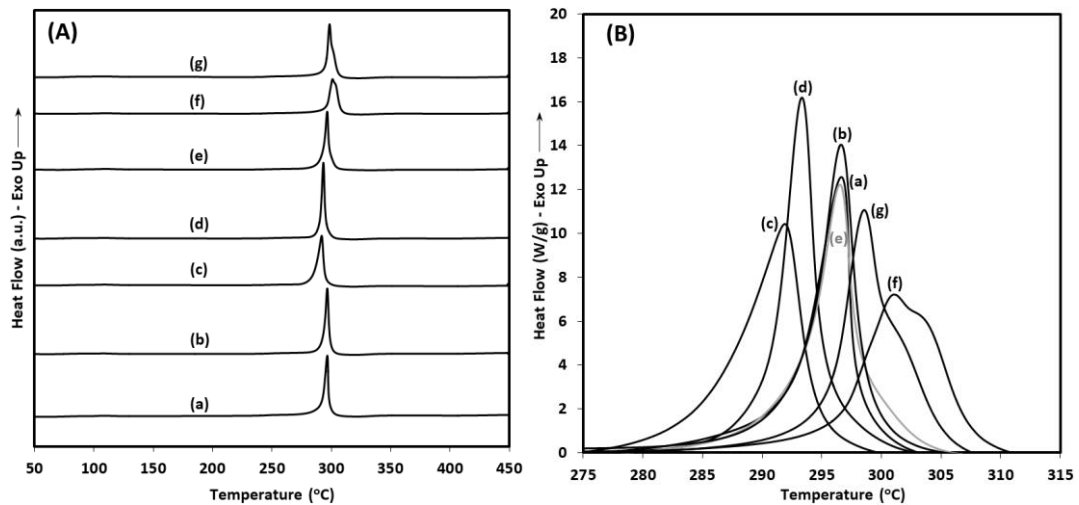


**Figure 4.10.** DSC analysis of PAN/Hb nanofibers with different ratio: (a) pure PAN, (b) PAN/H<sub>0.5</sub>, (c) PAN/H<sub>1</sub>, (d) PAN/H<sub>3</sub>, (e) PAN/H<sub>5</sub>, (f) PAN/H<sub>15</sub>, and (g) PAN/H<sub>30</sub>

#### 4.3.3. TGA investigations of PAN and PAN/Law nanofibers

TGA measurements of the samples were conducted for testing the thermal stabilities of as-spun PAN/Law nanofibers under nitrogen atmosphere. The plots generated of as-spun PAN/Law nanofibers is presented in the figure below (the points addressed on the plots are grouped in appendix 2. DTA and DTG in appendix 3 and 4).

As seen from the generated plots, an important weight loss around 100 °C was observed and corresponds to the water evaporation from the nanofibers. The pure PAN nanofibers lost an important weight occurring from point 3 3 (284.8 °C) to Point 4 (456.5 °C). The calculated rate of weight loss diminishes gradually until reaching the temperature to Point 5 (800 °C). it was noted that the residual at Point 4 was 43.1%, and at Point 5 was 31.1%



for pure PAN and can be explained that the weight loss is related to the loss of volatiles present from the system due to the complex chemical reactions cited above.

As concluded in the thermal analysis above, Lawsonsone showed its low thermal stability that leads in this measurement to an obvious weight loss at a lower temperature and this can be observed in the plot that the main weight loss occurred between the point 1 and 2 and this result is obvious and clearly obtained at the high law content in Law/PAN nanofibers due to the decomposition of Law in the PAN/Law composites nanofibrous system. The calculated residuals at Point 3 for pure PAN, L<sub>1</sub>, L<sub>3</sub>, L<sub>15</sub>, L<sub>30</sub>, L<sub>50</sub>, L<sub>70</sub>, and L<sub>100</sub> samples were 96, 95.1%, 92.8%, 86.9%, 76.6%, 72.4%, 67.3%, and 58.2% sequentially. All the samples, and due to the Law amount, reached to the plateau at early temperature as demonstrated in the point 2 in a temperature 178.6, 179.5, 199.2, 206.8, 216.6, and 219.6 °C, respectively for the samples L<sub>1</sub>, L<sub>3</sub>, L<sub>15</sub>, L<sub>30</sub>, L<sub>50</sub>, L<sub>70</sub>, and L<sub>100</sub> and a slow weight loss occurred after point 4 for all the samples.

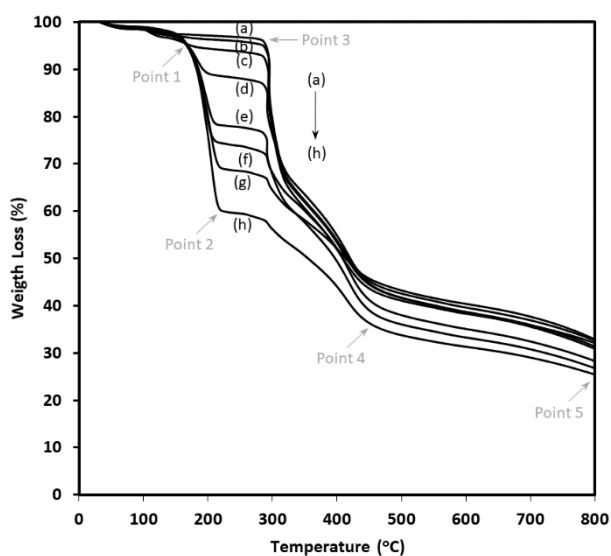


**Figure 4.11.** Thermogravimetric (TGA) analysis results of PAN/Law nanofibers with different wt.% of Lawsonsone respect to PAN content: (a) 0, (b) 1, (c) 3, (d) 15, (e) 30, (f) 50, (g) 70, and (h) 100

Compared to pure PAN nanofibers, the residuals at the end of the test at 800 °C demonstrated in point 5 tended to decrease independently to the amount of Law in the precursor PAN/Law nanofibers as 32.1%, 32.6%, 30.8%, 31.3%, 26.7%, 28.3%, 32.8%,

and 25.4% respectively for pure PAN, L<sub>1</sub>, L<sub>3</sub>, L<sub>15</sub>, L<sub>30</sub>, L<sub>50</sub>, L<sub>70</sub>, and L<sub>100</sub> nanofibers samples.

#### 4.3.4. TGA investigation of PAN and PAN/Hb nanofibers

Thermogravimetric analysis was investigated via TGA measurement under nitrogen atmosphere for the precursor as-spun PAN/Hb nanofibers and the generated plot for analysis was shown in the figure bellow. The weight loss observed around 100 °C corresponds to excess water evaporation from the nanofibers. Three stages of weight loss were observed from point 1, 2 and 3. An important weight loss Point 1 were 284.8, 285.7, 285.1, 287.4, 285.7, 287.6, and 287.6 °C respectively for pure PAN, H<sub>0.5</sub>, H<sub>1</sub>, H<sub>3</sub>, H<sub>5</sub>, H<sub>15</sub>, and H<sub>30</sub>. the thermal stability of PAN/Hb nanofibers samples was reduced by the addition of Hb amount to the nanofibers. The points illustrated in the plots are detailly grouped in appendix 6, DTA and DTG in appendix 7 and 8.

A several weight losses from the nanofibers was obtained by heating and can be related to removed volatiles after the complex chemical reactions (dehydrogenation, cyclization, and cross-linking) occurrence. When the temperature reached 800 °C at point 4, the residuals of the samples were 32.1, 31.4, 27.1, 26.7, 32.5, 32.6, and 33.5% respectively for pure PAN, H<sub>0.5</sub>, H<sub>1</sub>, H<sub>3</sub>, H<sub>5</sub>, H<sub>15</sub>, and H<sub>30</sub> samples.

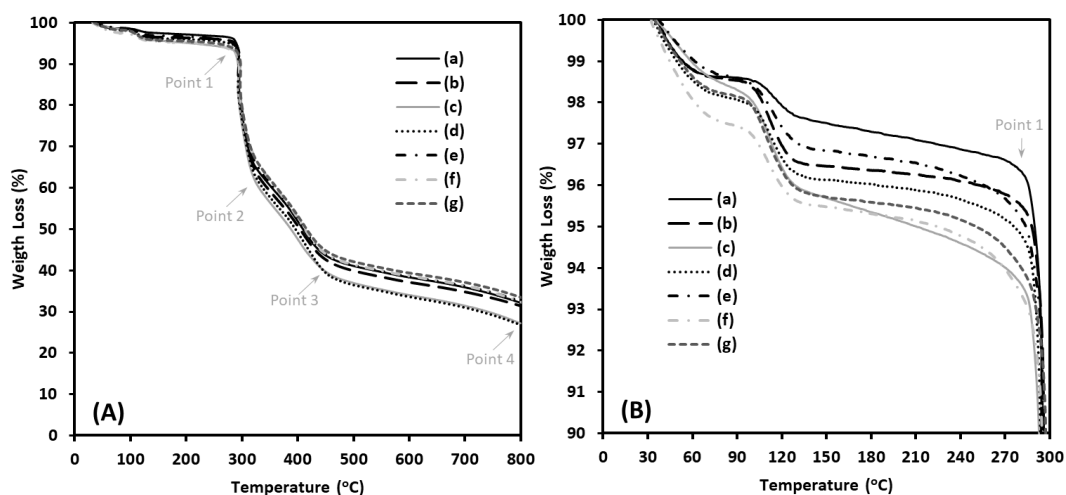


**Figure 4.12.** Thermogravimetric analysis of PAN/Hb nanofibers (A and B) TGA: (a) pure PAN, (b) PAN/H<sub>0.5</sub>, (c) PAN/H<sub>1</sub>, (d) PAN/H<sub>3</sub>, (e) PAN/H<sub>5</sub>, (f) PAN/H<sub>15</sub> and (g) PAN/H<sub>30</sub>

## **4.4. Carbonaceous investigations of PAN, PAN/Law and PAN/Hb derived carbon nanofibers**

### **4.4.1. Raman spectra analysis of Law enriched CNFs**

In order to analyze detailly the structural perfectness of the carbon-based materials, Raman spectroscopy is widely applied technique based on investigating the bands positions and intensities. The generated spectrum makes the light on two distinct peaks located ca.  $1344\text{ cm}^{-1}$  (D-band) and  $1589\text{ cm}^{-1}$  (G-band) corresponding to disordered carbons and ordered graphitic phase with calculating the intensity ratio of the peaks ( $R=I_D/I_G$ ) that represents the structural order property of the nanofibers (Huang et al., 2018). The increase of this ration is automatically related to the disordered nature of carbon structure (Chen et al., 2015).

The graphitization level is inversely proportional to the ration so it is extremely important to analyse these peaks for a better improvement of the graphitic structure of the studied materials. The figure below presents the obtained Raman spectra of both neat CNFs and lawsone enhanced CNFs (The peak positions and intensities of D and G bands of all the samples are given in appendix 5).

As seen the peak positions and intensities of D and G bands of the elaborated samples were presented with the calculated R values.

The ration R for neat CNFs was 1,0005, with a minimal addition of Lawsone amount the ration increased to 1,0155 ( $L_1$ ) and decreased with the addition of the Lawsone amount as in  $L_3$  and  $L_{15}$ , we can note that a low amount of Lawsone lead to increase the graphitization of PAN derived Carbon NFs, more Lawsone content increase more graphitization degree, Sample  $L_3$  and  $L_{15}$  present an optimal and better ordered structure compared to neat CNFs but increasing the amount as  $L_{30}$ ,  $L_{50}$ ,  $L_{70}$  and  $L_{100}$  impact the ordered structure, we can conclude that an optimal amount of Lawsone addition ( as in  $L_3$  and  $L_{15}$ ) could enhance the graphitic structure of carbon nanofibers and the obtained results confirm their matching and accordance with the thermal and chemical analysis above.

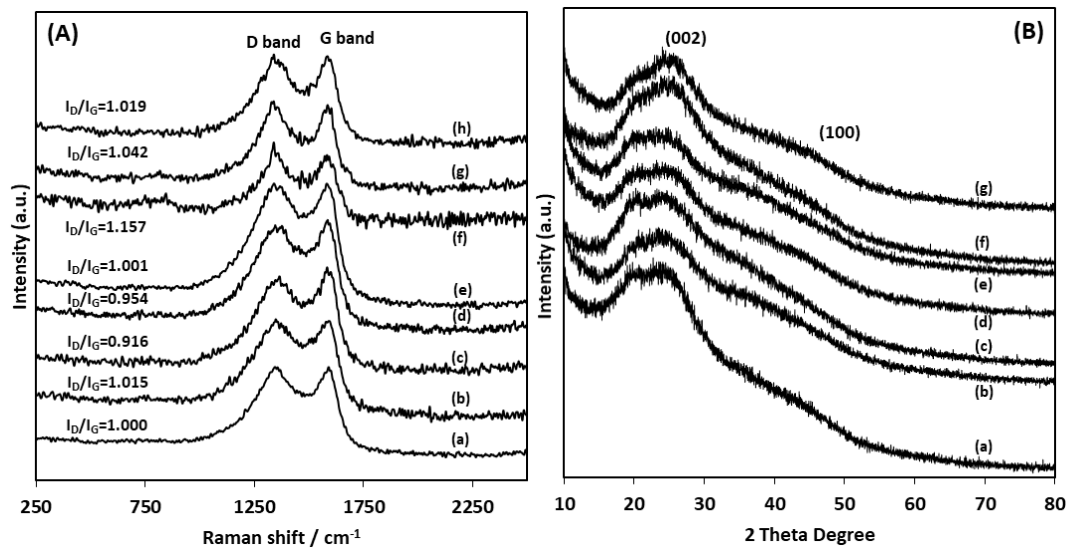


**Figure 4.13.** (A) Raman spectra and (B) X-ray diffraction patterns of carbonized nanofibers. The contents are in the precursor PAN/Law nanofibers before the stabilization process as wt.% of Lawstone respect to PAN content: (a) 0, (b) 3, (c) 15, (d) 30, (e) 50, (f) 70 and (g) 100.

#### 4.4.2. X-ray diffraction analysis of Law enriched CNFs

Aiming to assimilate details the microstructure of the nanofibers, X-Ray diffraction (XRD) analyses of carbonized precursor Law/PAN nanofibers were investigated as presented in the figure 4.13. The diffraction peak around  $2\theta = 23.5^\circ$  correspond to (002) layers of graphite parts in the carbon nanofibers (Kale et al., 2019). Respectively the detected diffraction angles for the samples L<sub>3</sub>, L<sub>15</sub>, L<sub>30</sub>, L<sub>50</sub>, L<sub>70</sub> and L<sub>100</sub> were 26.02, 26.34, 24.82, 24.3, 24.04 and 24.32°. The peak obtained in all the samples imply that Law enriched CNFs contain graphitic structures and the peak tends to shift a higher value with Law enrichment. As concluded in the chemical and thermal measurement, also the X-ray diffraction proved that the peak tended to its higher degree with a low Law addition.

Based on the Bragg's law equation the D spacing  $d$  (002) of CNF s, L<sub>1</sub>, L<sub>3</sub>, L<sub>15</sub>, L<sub>30</sub>, L<sub>50</sub>, L<sub>70</sub> and L<sub>100</sub> were 3.73, 3.69, 3.65, 3.53, 3.58, 3.38 and 3.42 Å. For the reported  $d$ -spacing of the graphite was about 3.35 Å respectively. The  $d$ -spacing of  $d(002)$  plane for graphite was calculated about 3.35 Å (Huang et al., 2018). from the obtained results that Lawstone enrichment decrease the graphitic interplanar spacing in the CNFs as homogenously obtained result from the Raman spectroscopy analysis.

#### 4.4.3. Raman spectra analysis of Hb enriched CNFs

Raman spectroscopy known as a non-destructive chemical analysis technique giving a wide information about chemical structure, crystallinity and molecular interactions is used in our study for the measurement of carbonized nanofibers for the investigation of the level of graphitic structure in the nanofibers, as presented in the figure below, Two distinct peaks around 1344-1359  $\text{cm}^{-1}$  (D-band) related to disordered carbons and 1582-1594  $\text{cm}^{-1}$  (G-band) related to ordered graphitic phase for the samples were detected. The peak positions and intensities of D and G bands of all the samples are given in appendix 9).

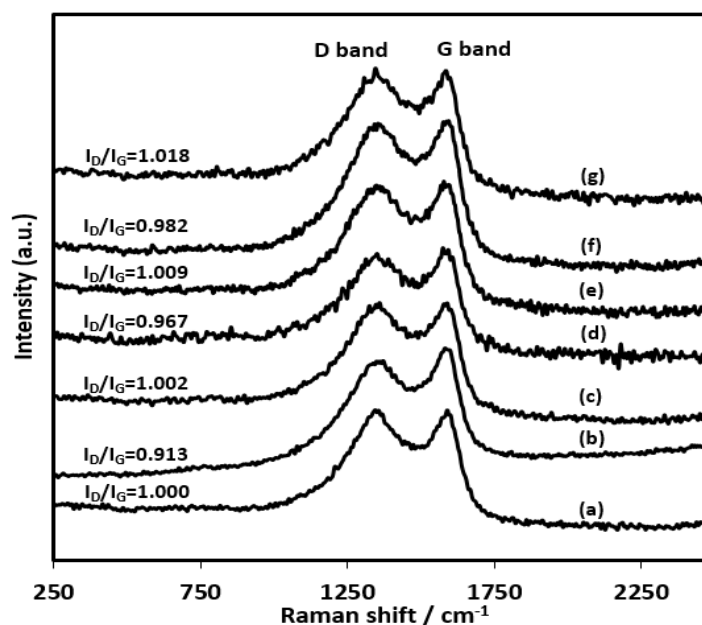


**Figure 4.14.** Raman Spectra of carbonized nanofiber: (a) CNF, (b) CNF/H<sub>0.5</sub>, (c) CNF/H<sub>1</sub>, (d) CNF/H<sub>3</sub>, (e) CNF/H<sub>5</sub>, (f) CNF/H<sub>15</sub>, and (g) CNF/H<sub>30</sub>

In order to determine the level of the structural order property we used to calculate the intensity of these peaks ( $R=I_D/I_G$ ) for each sample and more the ratio decrease more it means an increase of the graphitization level of our structure of nanofibers, The calculated R values were 1, 0.91, 1, 0.96, 1, 0.98 and 1.01 for neat CNFs, CNF/H<sub>0.5</sub>, CNF/H<sub>1</sub>, CNF/H<sub>3</sub>, CNF/H<sub>5</sub>, CNF/H<sub>15</sub> and CNF/H<sub>30</sub> nanofiber samples respectively. The low content of Hb in PAN nanofibers as in the sample H<sub>0.5</sub> showed an enhance of the graphitic level at PAN derived nanofibers. The same results were concluded by the DSC analysis.

The intensity of the exothermic peak increased comparing to pure PAN nanofibers due to more ring formation during stabilization process and led to enhance the graphitic structure after carbonization process.

#### 4.4.4. X-ray diffraction analysis of Hb enriched CNFs

In order to observe the microstructure of the nanofibers, we processed by analysing with the X-Ray diffraction (XRD) analyses of carbonized precursor PAN/Hb nanofibers. As shown in the figure 4.15 , the diffraction peak around  $2\theta = 23.5^\circ$  correspond to (002) layers of graphite parts in the carbon nanofibers (Huang et al., 2018; Kale et al., 2019), The diffraction angles for the samples H<sub>1</sub>, H<sub>3</sub>, H<sub>5</sub>, H<sub>15</sub> and H<sub>30</sub> were  $26.8^\circ$ ,  $24.9^\circ$ ,  $25.68^\circ$ ,  $24.34^\circ$  and  $24.56^\circ$ . this peak present in all the samples means that the Hemoglobin enhanced samples contain graphitic structures in the carbonized nanofibers and this peak tend to shift higher proportionally with the addition of the Hemoglobin amount.

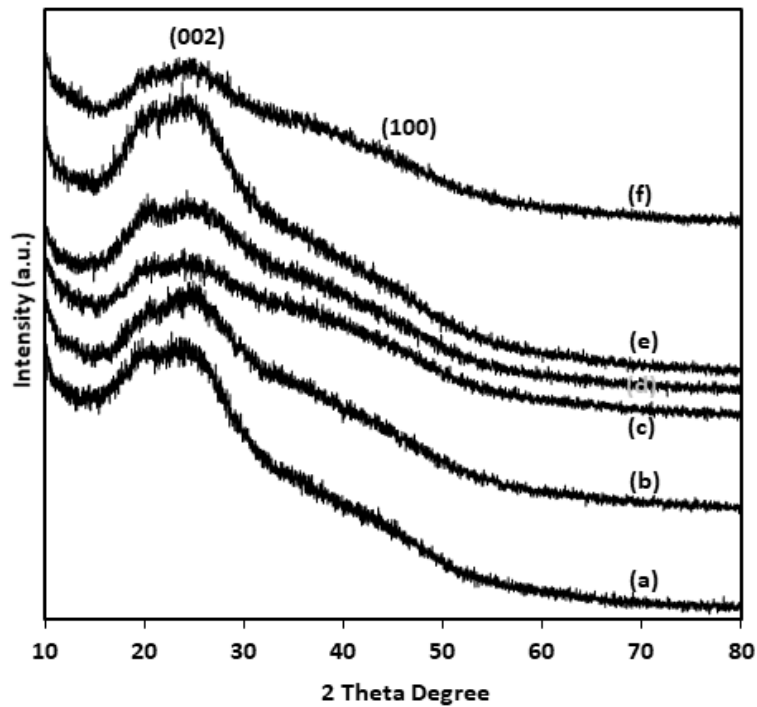


**Figure 4.15.** X-Ray diffraction plots of carbonized nanofibers (a) CNF, (b) CNF/H<sub>1</sub>, (c) CNF/H<sub>3</sub>, (d) CNF/H<sub>5</sub>, (e) CNF/H<sub>15</sub>, and (f) CNF/H<sub>30</sub>

The resulted peaks confirmed that better graphitic structure was seen at H<sub>1</sub> sample as the optimum obtained result comparing to other samples since the closest d-spacing values

was obtained for this sample. As seen Raman, DSC and spectra XRD results confirmed that low Hb addition into the precursor nanofibers led to a better graphitic structure in the carbonized nanofibers.

#### **4.5. Study of the Anti-miRNA immobilization optimization on the screen-printed electrodes without NFs for electrochemical miRNA biosensors**

In this part of the study and in the light of the obtained results from the previous section, an optimization of the anti-miRNA immobilization parameters on the screen-printed electrodes for an efficient electrochemical measurement was investigated.

For this purpose, different concentrations of the miRNA molecules were immobilized on the electrode's surfaces followed by an electrochemical measurement to determine the guanine oxidation signal via differential pulse voltammetry method. The used anti-miRNA in this study is synthetic anti-miRNA451(G) purchased and prepared by dilution in PBS solution. The parameters studied for optimization were the effect of time and temperature by testing the samples at -18, +5 and +25 °C for 1, 3, 14 and 21 days and investigating the obtained result for an optimal future use.

##### **4.5.1. Preparation of samples and chemicals**

As cited in the previous section of this study, the same prepared buffer solutions were used in these measurements. Anti-miRNA stock solutions were prepared as 1000 ppm. The anti-miRNA molecules were firstly dissolved in pure water for a proper stock solution preparation in PBS and kept in -18 °C until usage. For the electrochemical measurement, the stock solutions were diluted as 10 µl in 50 µl of PBS into the PCR tubes.

##### **4.5.2. Immobilization of anti-miRNA molecules on SPEs surfaces**

First, a proper surface cleaning and activation of the electrodes surfaces was made and carried out electrochemically by DPV methods before anti-miRNA molecules immobilization step. As presented in the figure below, this preliminary process was by dropping 100 µl of ABS on the electrode surface and activating the surface by applying 1.4 V deposition potential for 60 sec with 600 number of points, the applied potential was

in the range of 0.7-1.4 V and 10 mV/s as scanning rate. Once the SPEs surfaces were activated, a proper washing was carried out by dropping carefully 300  $\mu$ l PBS and dry for the following measurements.

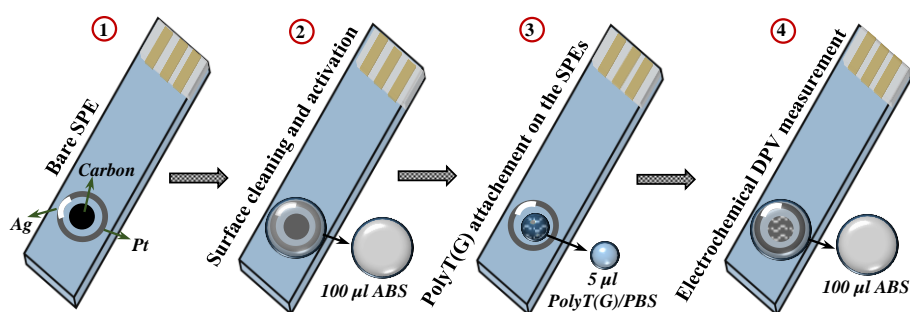


**Figure 4.16.** Surface cleaning and activation, anti-miRNA attachment and measurement process

The immobilization of the anti-miRNA molecules on the electrodes surfaces was carried out by dropping 5  $\mu$ l of the prepared measurement solution on the surface and waited 1h for a proper attachment of the molecules. The electrodes were then washed with 300  $\mu$ l PBS in order to remove the unattached molecules before the electrochemical measurements and kept for a total drying for 1h.

#### 4.5.3. Electrochemical measurements of the biosensory system

As cited previously, the electrochemical measurements were carried out by using Potansiyostat - AUTOLAB AUT204 (Eco Chemie, Nederland) and NOVA 1.11 software. The used SPEs were purchased from Metrohm with DS 150 code (carbon working electrode, platinum auxiliary electrode (PAE) and silver reference electrode), the DS110 coded SPEs (CAE) were tested and tried in the initial measurements. The measurements were carried out between 0.75-1.3 V with 10 mV/s scanning rate by dropping 100  $\mu$ l ABS on the electrode surface.



#### **4.5.4. Results of the DPV measurements by using PBS and ABS buffer solution**

In this part of study, the optimization of the parameters was by testing the efficiency of the results by changing the buffer in the measurements. The used buffers are PBS and ABS and were tested to investigate the appropriate buffer for the DPV measurements.

For this purpose, two methods have been tested. We started by dropping directly the prepared measurement solution (anti-miRNA/PBS) on the SPEs surfaces and the measurements were conducted via DPV method and the resulted plot was illustrated in the figure 4.17 (a and c).

The second method was investigated by dropping the measurement solution on the SPE surfaces and waited for 60 min then washed with PBS in order to remove the unattached molecules from the surface and DPV measurements were carried out as demonstrated in the figure 4.17 (b and d).

For more comparative results, these methods were tested using the purchased SPE, which had platinum auxiliary electrode (PAE) (figure 4.17 (a and b)) and carbon auxiliary electrode (CAE) (figure 4.17 (c and d)).

After the electrochemical measurement, the obtained plots shows both guanine and adenine oxidation peaks as seen in the figure 4.22 below. Based on the literature, the obtained peaks generally are detected around 1 and 1.25 V for the guanine oxidation and apparently shifted to lower voltage in the use of PBS measurement solution and this result was confirmed clearly when ABS cleaning and activation were not applied to the SPEs for this measurement before immobilization of anti-miRNA molecules.

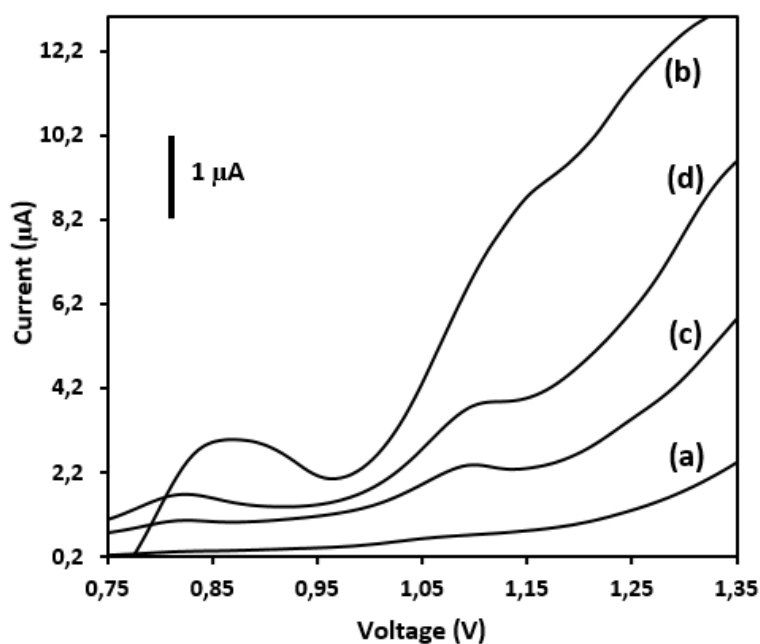


**Figure 4.17.** DPV measurement with PBS: (a) anti-miRNA/PBS (with PAE), (b) anti-miRNA/PBS wait 60 min-wash –measure (with PAE), (c) anti-miRNA/PBS (with CAE) and (d) anti-miRNA/PBS wait 60 min-wash – measure (with CAE)

The use of ABS was also investigated during the DPV measurements. A plethora of research papers have been using the ABS as measurement solution instead of PBS. For this study, the use of ABS solutions was combined with the use of Metrohm with DS 150 product code SPEs at all the measurements.

For this purpose, after a proper cleaning and activation of the SPEs surfaces, 5 µl of anti-miRNA measurement solution was dropped and waited for 1h for a proper immobilization of the molecules, then the process was followed by a proper cleaning with PBS and dried until use for the measurements.

The DPV measurements were carried out by dropping 100 µl of ABS solution during the measurement and the obtained plot is presented in the figure 4.18 below. As expected, both of guanine and adenine oxidation peak appeared as cited in a wide range of literature reviews and matching with the commonly appeared positions.

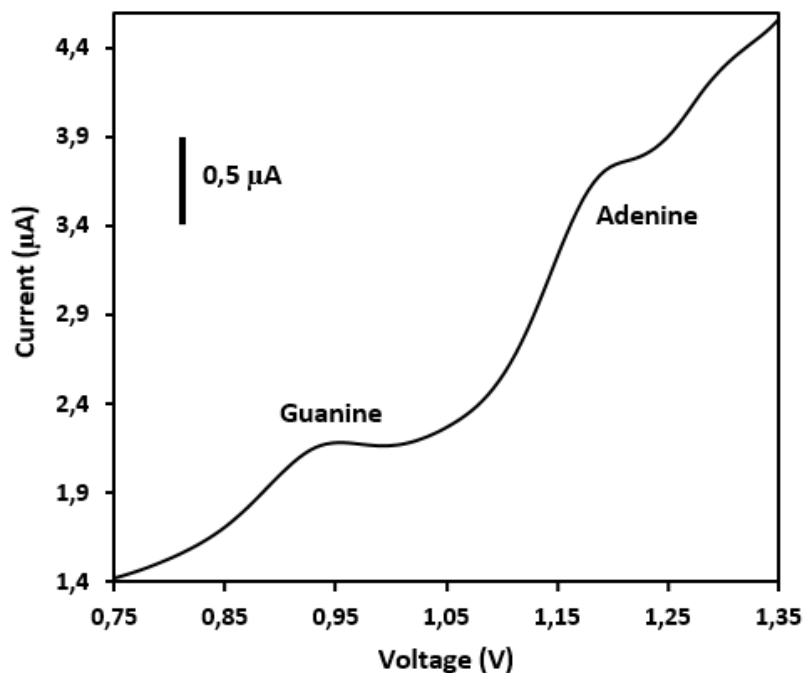


**Figure 4.18.** DPV measurement with ABS buffer solution

In order to decide the efficient measurement buffer and after the analyses of the obtained results of PBS and ABS solutions with the literature, all the results and peaks were compatible with the use of ABS use as a buffer solution for the measurements.

#### **4.5.5. Results of the DPV measurements with different rate of anti-miRNA immobilized SPEs**

In this study of parameter's optimization, we also investigate the effect of changing the rate of immobilized molecules on the SPEs surfaces on the obtained oxidation signal to determine the optimal and efficient concentration for a future analysis.

For the purpose, five different diluting concentrations were prepared, the dilution process was by adjusting the anti-miRNA measurement solution/PBS (v/v) rate as 1/50, 2/50, 5/50, 10/50 and 20/50. The obtained solutions were dropped on the surface of the cleaned and activated SPEs, then waited for 1h and washed with PBS and dried for 1h for the following measurements. The obtained plot was presented in the figure 4.19.

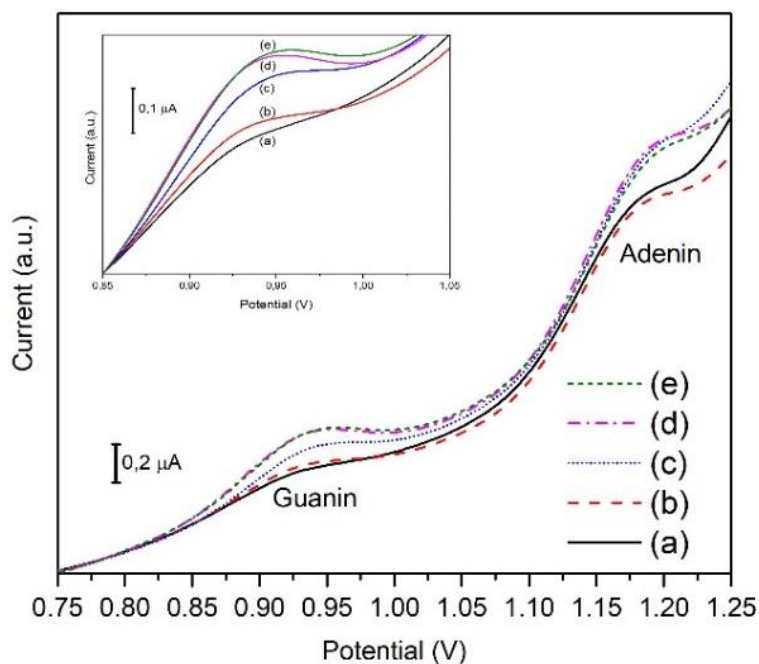


**Figure 4.19.** DPV measurement with different rate of anti-miRNA attached SPEs: anti-miRNA measurement solution/PBS (v/v) rates are (a) 1/50, (b) 2/50, (c) 5/50, (d) 10/50 and (e) 20/50

As expected, the guanine and adenine oxidation peaks appeared clearly around 1 and 1.25 V sequentially. An increase of the intensity of the guanine oxidation peak was observed when the ratio of the anti-miRNA molecules was increased in the measurement solution up to 10/50 anti-miRNA measurement solution/PBS rate, also an important increase of the adenine oxidation signal was noted when the anti-miRNA measurement solution/PBS rate increased from 2/50 to 5/50. This result puts the light on the obtained previous analysis confirming that guanine and adenine oxidation peaks are detectable at all concentrations and the minimum concentrations can be used in the future studies.

#### 4.5.6. Storage time and temperature study of anti-miRNA immobilized SPEs

The last parameter studied is the storage time and temperature due to their importance on the measurement process. To investigate the optimal and efficient conditions (time and temperature storage) of the anti-miRNA immobilized SPEs. Different DPV measurements were carried out with samples stored at -18, +5 and +25 °C for 1, 3, 14 and 21 days. The obtained plots were illustrated in the figure 4.20.

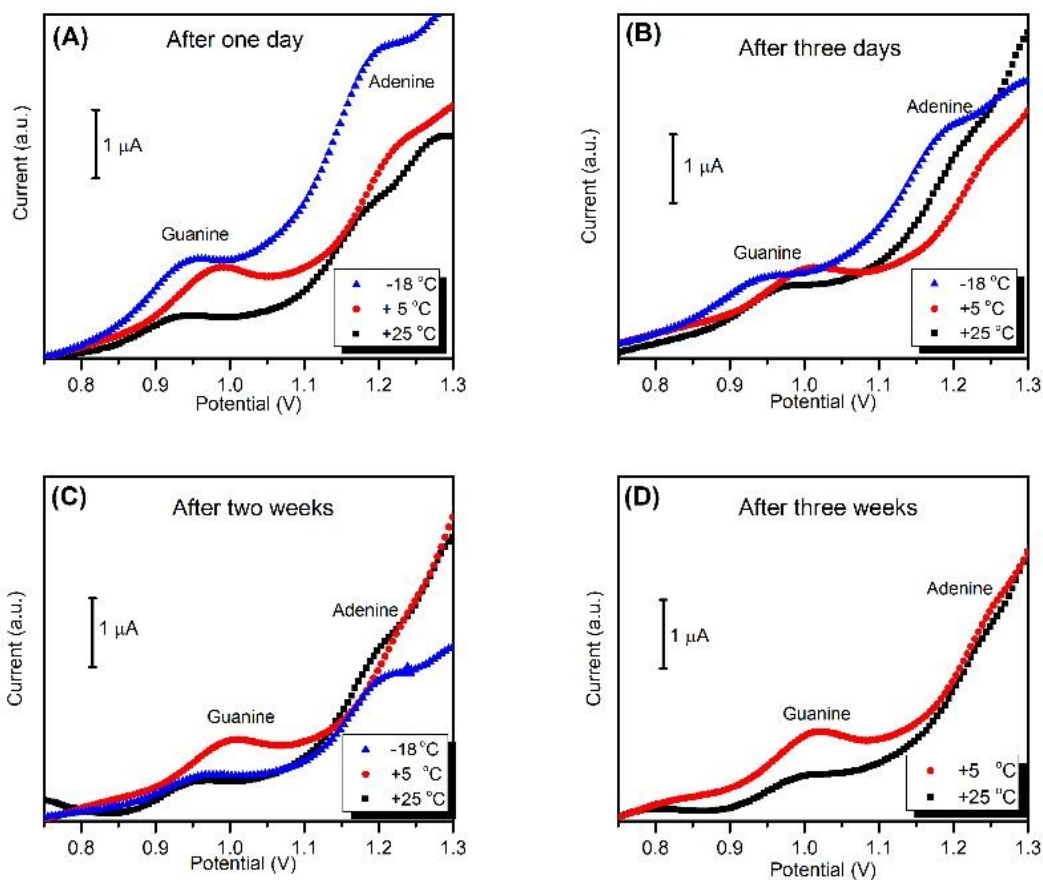


**Figure 4.20.** DPV measurements of anti-miRNA attached SPEs at different storage times at -18, +5 and +25 °C stored samples: (A) 1 day, (B) 3 days, (C) 14 days and (D) 21 days

The obtained results demonstrated that, focusing on the guanine oxidation signal around 0.9-1.0 V, an important decrease at the -18 °C stored sample was observed when the measurement was done after for one day of stored samples.

No significant changes were noted for the +5 ve +25 °C stored samples. The measured oxidation signal was lower at -18 °C and +25 °C than +5 °C stored sample. This leads to conclude that the optimal and efficient storage temperature for the samples after anti-miRNA attachment is +5 °C until measurements.

## **4.6. Electrochemical analysis for miRNA detection by using law enriched CNFs immobilized on screen printed electrodes**

### **4.6.1. Preliminary guanine oxidation measurements**

The guanine and adenine oxidation can be generally detected by DPV and showed a peak around +1.0 V and 1.25 V respectively (Bagni et al., 2005; Lin et al., 2017). For this reason, to properly analyze the corresponding guanine and/or adenine oxidation signal from the prepared oligonucleotides, PolyA, anti-miRNA (PolyT(G) and PolyT(I)), and miRNA molecules were gently attached separately on the surface of the prepared SPEs and preliminary measurements were elaborated with bare and ABS activated SPEs (in this step we didn't CNFs immobilization).

As expected, after DPV measurements, the obtained plot showed a guanine oxidation peak around 0.93 V for miRNA and poly T(G), and adenine peak was seen around 1.15 V for all the molecules including PolyA, PolyT(G), PolyT(I), and miRNA. There is no guanine base in PolyA and PolyT(I) molecules and this result is confirmed in the obtained plots in the figure 4.21.

After a proper preparation of the SPEs surfaces and their activation and a following NHS/EDC surface modification, Law enriched CNFs were immobilized on the SPEs surfaces. For an interpretable measurement, both of pure CNFs and Law enriched CNFs were electrochemically measured.

For the electrochemical measurements, first PolyA molecules were attached on the SPEs surfaces then a following anti-miRNA molecules (including both with guanine (PolyT (G)) and inosine (PolyT(I)) were immobilized and interacted separately with the SPEs surfaces then electrochemically measured, the obtained plots of the attached d PolyT (G) and Poly (I) samples were demonstrated in the figure 4.21. As expected, both guanine and adenine peaks were observed respectively around 0.9–1.0 and 1.15–1.25 V at PolyT (G) attached samples and just the adenine peak was observed at PolyT(I) attached samples.no effect on the signal intensities were detected by using Law enriched CNFs for this part of measurements.

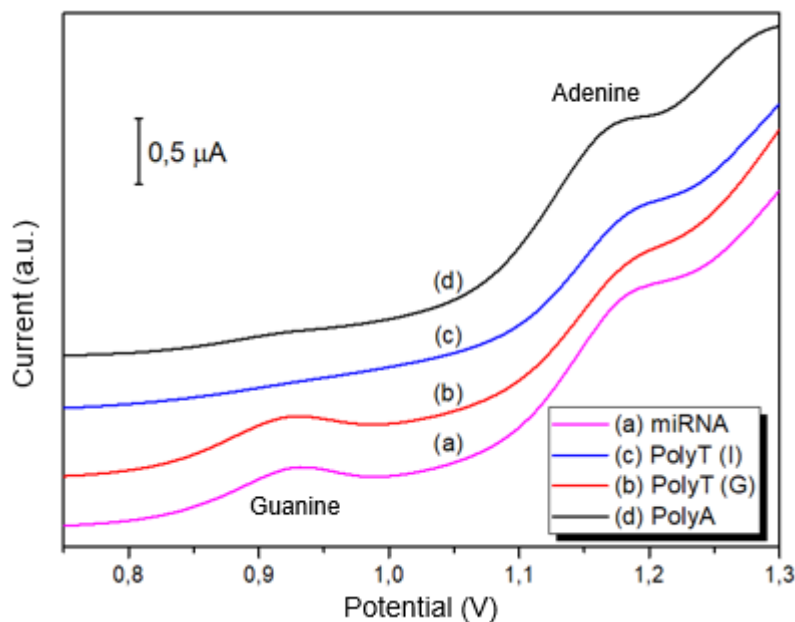


**Figure 4.21.** Guanine and adenine oxidation peaks of (a) miRNA, (b) PolyT(G), (c) PolyT(I), and (d) PolyA, anti-miRNA via DPV measurement by using bare SPEs

#### 4.6.2. Selectivity of the miRNA biosensory system

In order to efficiently assimilate a good selectivity of the prepared biosensory system, the hybridization of miRNA with anti-miRNA molecules on the SPEs surfaces were measured by using bare SPEs as a reference and CNFs immobilized SPEs, plotted and investigated.

First, anti-miRNA molecules including PolyT(G) and PolyT(I) were attached separately on the SPEs surfaces and interacted for hybridization with miRNA, SM. miRNA, and NC. miRNA molecules by dropping the prepared oligonucleotides on the SPEs surfaces.

The hybridization resulted as expected a decrease of the guanine oxidation signal as an interaction between miRNA and PolyT(G) molecules as illustrated in figure 4.22 (A). and (B). in the case of PolyT(I) attached samples, no guanine oxidation signal was detected as demonstrated in figure 4.22 (E), a guanine oxidation signal was becoming clearly detectable after hybridization with miRNA molecules on the PolyT(I) attached SPEs surfaces (figure 4.22 (F)). The same results were obtained after hybridization PolyT(G) and PolyT(I) attached surfaces with the single-base mismatched miRNA (SM. miRNA) molecules as demonstrated in figure 4.22 (C) and (G).

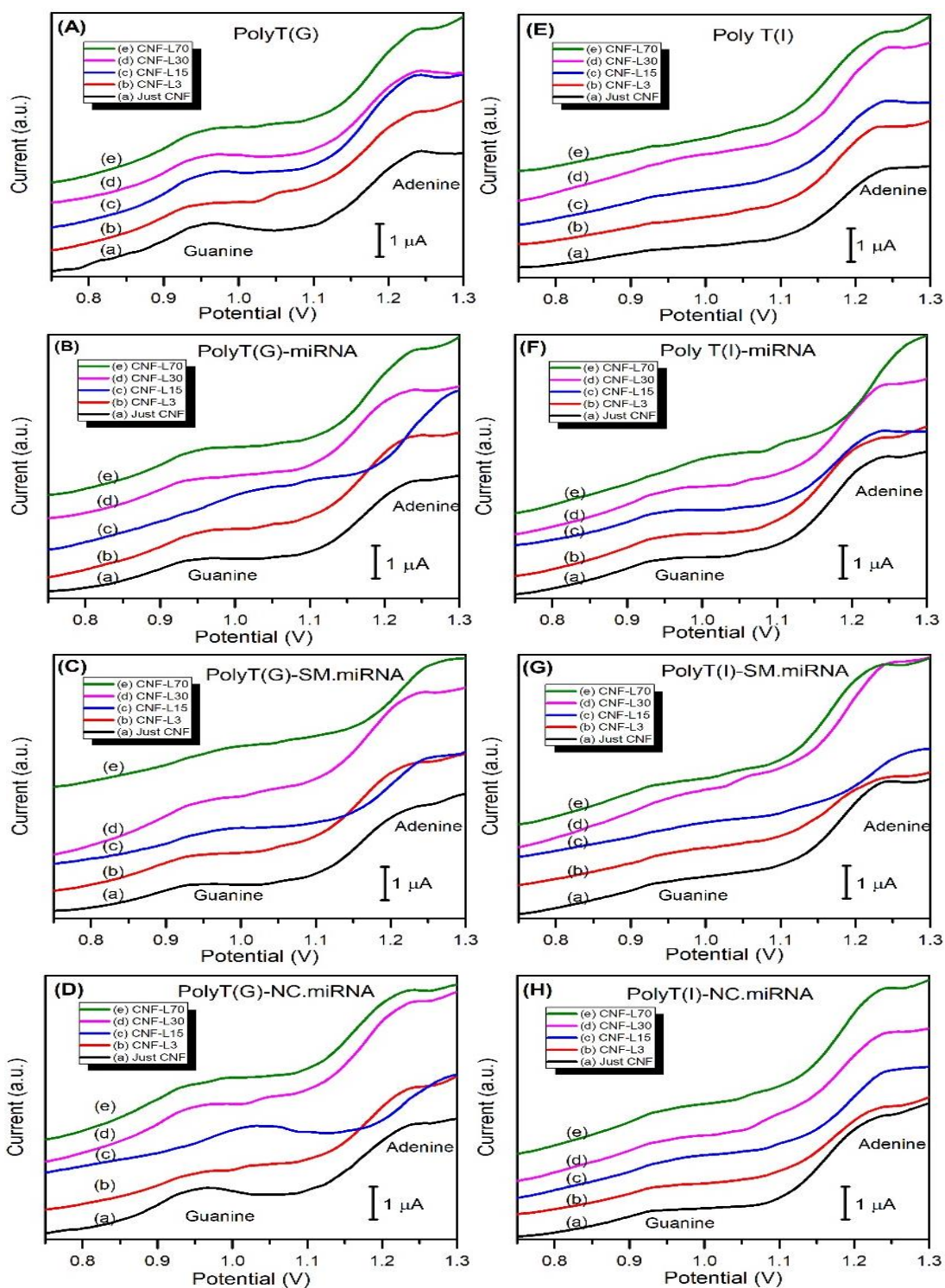


**Figure 4.22.** Electrochemical biosensor measurements plots after attachment of miRNA, anti-miRNA molecules and their hybridized forms by using NHS/EDC modified and CNFs immobilized SPEs: (A) PolyT(G), (B) PolyT(G)-miRNA, (C) PolyT(G)-SM.miRNA, (D) PolyT(G)-NC.miRNA, (E) PolyT(I), (F) PolyT(I)-miRNA, (G) PolyT(I)-SM.miRNA, and (H) PolyT(I)-NC.miRNA



As expected, no hybridization occurs between anti-miRNA molecules and non-complementary miRNA (NC. miRNA) molecules and as seen from the plot A and D.

The guanine oxidation signal was not decreased after the interaction between NC.miRNA and PolyT(G) attached SPE surfaces and the same results were obtained with PolyT(I) molecules with a weak guanine peaks detected at PolyT(I)-NC.miRNA samples explained as a result of the existence of residual NC.miRNA molecules on SPE after washing (figure 4.22 (H)).

The enrichment of CNFs with Law didn't have a significant and prominent change on the electrochemical results but the measurements confirm a good selectivity of the miRNA biosensor systems using CNFs immobilized SPEs and can be a subject of development.

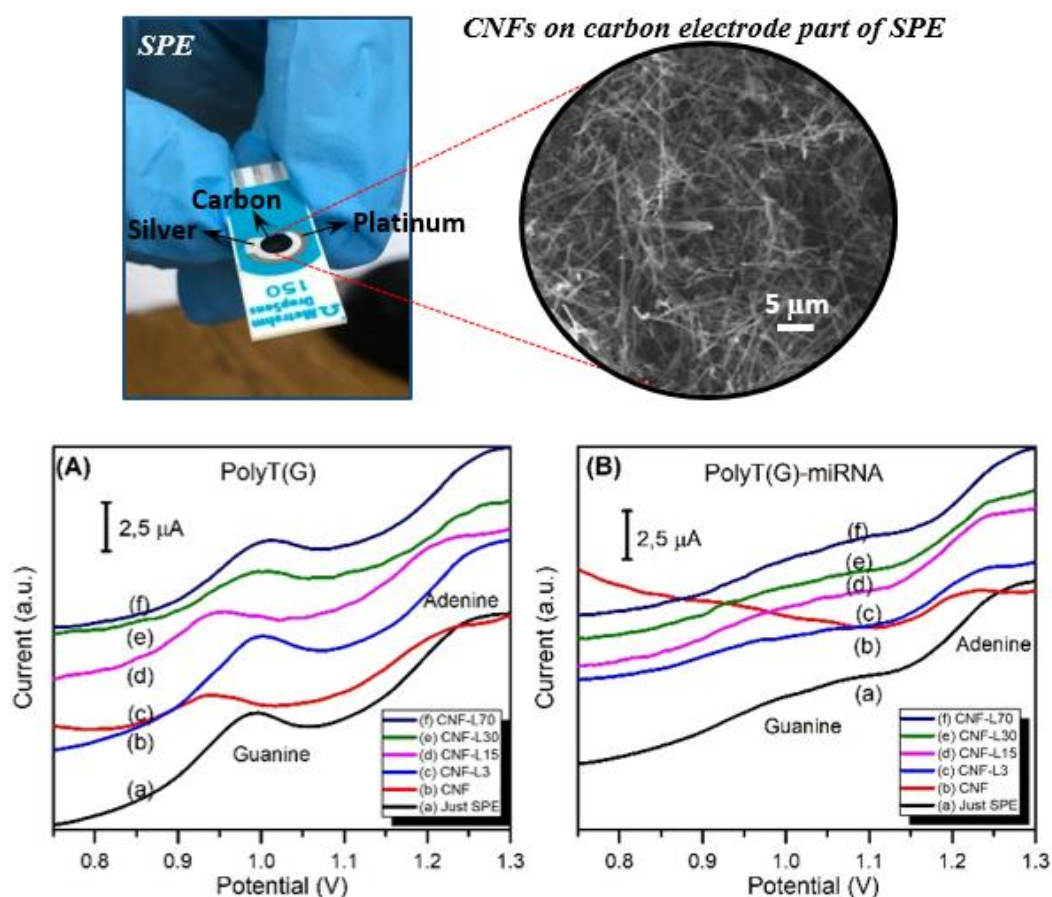


**Figure 4.23.** Electrochemical biosensor measurements plots of guanine containing anti-miRNA and its hybridized form with miRNA by using just CNFs immobilized SPEs without NHS/EDC modification: (A) PolyT(G) and (B) PolyT(G)-miRNA. the image is the illustration of SPE with immobilized CNFs on its carbon electrode part

As we cited in the previous part of materials and methods, CNFs were also directly immobilized on the SPEs surfaces without NHS/EDC modification. In this regard, the previously prepared CNFs were dropped on the working electrode surfaces and dried for the following electrochemical measurements.

The prepared PolyT(G) molecules were immobilized on the CNFs modified SPEs surfaces and DPV measurements were carried before and after hybridization with miRNA molecules as illustrated in figure 4.23.

The obtained signal led to conclude that the guanine oxidation signal was significantly enhanced for PolyT(G) compared to the results obtained with NHS/EDC modified samples. The guanine oxidation signal tends to decrease when PolyT(G) attached surface were hybridized with miRNA molecules which is the expected result.

From the investigated plots, even though the guanine oxidation signal intensity was enhanced with the use of CNF-L<sub>3</sub> sample, no significant enhancements of the CNFs usage and Law enrichment on the electrochemical efficiency and performance results. This can be explained by the weak graphitization degree of the CNFs (carbonized at 800°C) and lead to focus on the studying the enhancement of the e carbonization temperature and/or time for an amelioration of the performance of the graphitized CNFs in order to be used for a qualitative signal intensity level.

## **4.7. Electrochemical investigation for a selective miRNA detection by using Hb enriched CNFs immobilized on screen printed electrodes**

### **4.7.1. Preliminary electrochemical measurements**

In order to investigate the efficiency of the biosensory system using Hb enriched CNFs, a proper electrode surfaces preparation was firstly done. Bare SPEs were cleaned and activated to prevent any contamination as detailly presented in the previous part.

The Hb enriched CNFs prepared solutions were dropped on the working electrode part of the SPEs modified with NHS/EDC solution. The purchased PolyA containing NH groups were firstly attached on the electrode surface before the immobilization of oligonucleotides. Then, separately, the anti-miRNA molecules including both of

PolyT(G) and PolyT(I) were immobilized on the SPEs surfaces and electrochemically measured via DPV in order to investigate the guanine oxidation signal of the attached molecules as shown in the figure 4.24 (A and E).

The guanine and adenine oxidation peaks of the prepared oligonucleotides (miRNA, PolyT(G), PolyT(I), and PolyA, anti-miRNA) via DPV by using bare SPEs were presented in the figure 4.21.

#### **4.7.2. Selectivity and investigation of the biosensory system**

The hybridization of miRNA with anti-miRNA molecules on the SPEs surfaces were measured by using bare SPEs as a reference and CNFs immobilized SPEs, plotted and investigated.

First, the prepared anti-miRNA molecules (PolyT(G) and PolyT(I)) were immobilized on the SPEs surfaces separately for a proper hybridization with miRNA molecules, SM.miRNA, and NC.miRNA molecules by dropping the prepared oligonucleotides on the SPEs surfaces .

As expected, the guanine and adenine oxidation signal were detected around 0.9–1.05 and 1.15–1.25 V respectively when PolyT(G) were measured on the CNFs immobilized SPEs and only adenine's oxidation signal was detected at PolyT(I) immobilized samples as illustrated in figure 4.24 (A and E). and a weak signal enhancement obtained CNF-H<sub>3</sub>. in this stage, no significant signal enhancement was observed with the use of Hb enhanced CNFs in the electrochemical measurements.

The selectivity of the prepared biosensory system was studied by investigating the hybridization signal, the immobilized anti-miRNA molecules were separately interacted with target miRNA, single-base mismatched miRNA (SM.miRNA), and non-complementary miRNA (NC.miRNA) molecules and the guanine oxidation signals were observed.

The hybridization resulted a dramatic decrease of the guanine oxidation signal of PolyT(G) with miRNA and SM.mirRNA as illustrated in the figure 4.24 (B and C). and

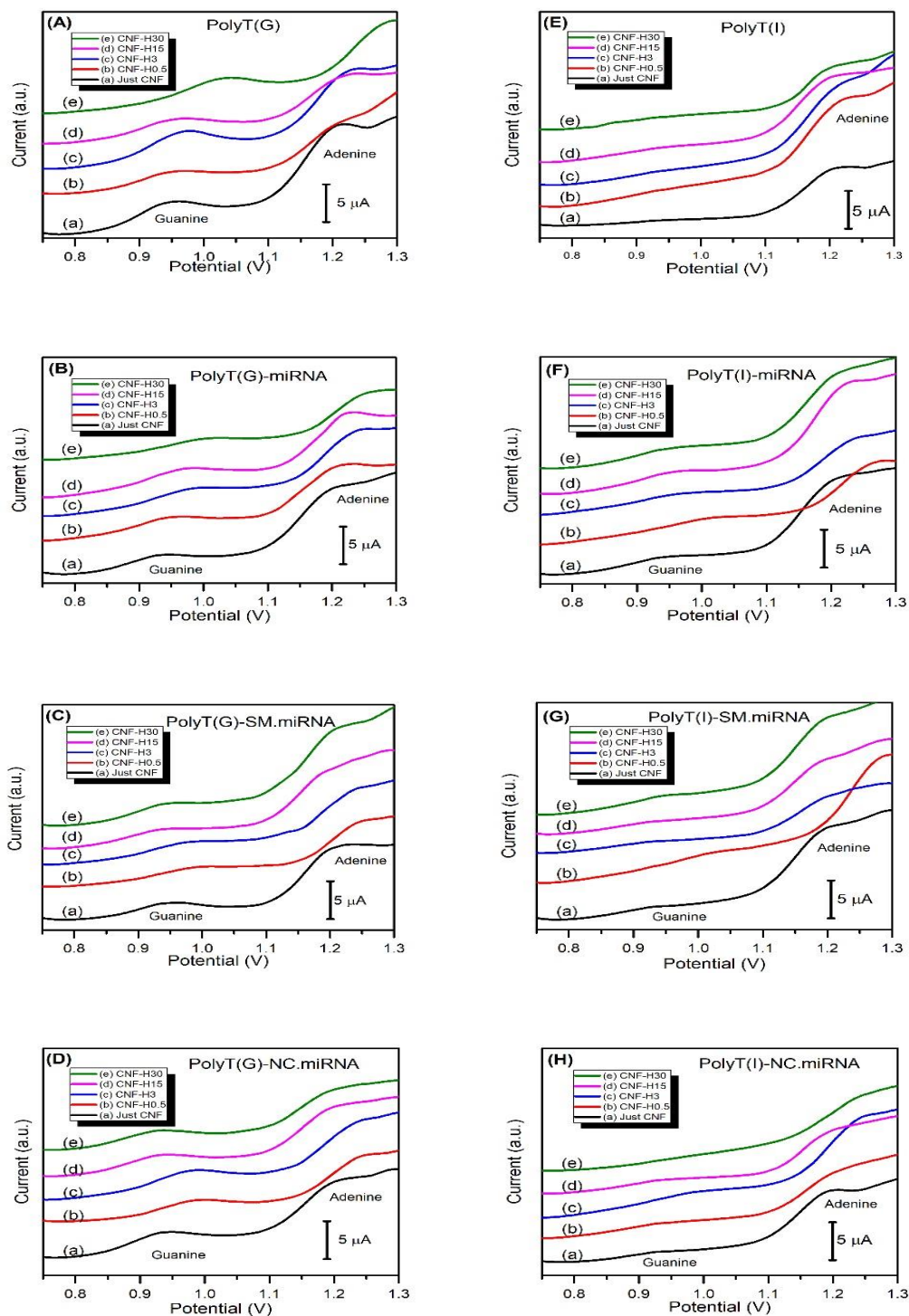


**Figure 4.24.** Electrochemical miRNA biosensor measurements plots by using NHS/EDC modified and Hb-CNFs immobilized SPEs: (A) PolyT(G), (B) PolyT(G)-miRNA, (C) PolyT(G)-SM.miRNA, (D) PolyT(G)-NC.miRNA, (E) PolyT(I), (F) PolyT(I)-miRNA, (G) PolyT(I)-SM.miRNA, and (H) PolyT(I)-NC.miRNA

as expected, no significant change was observed for the interaction between PolyT(G) and NC.miRNA molecules figure 4.24 (D).

The guanine oxidation signal was not detected at PolyT(I) immobilized samples figure E but become clearly apparent after the interaction of PolyT(I) with miRNA, SM.miRNA and become weakest with NC.miRNA molecules due to a non-hybridization occurred and NC.miRNA molecules that were picked from the electrode's surface with a PBS washing process before the measurements as demonstrated in figure 4.24 (F,G and H).

As cited in the materials and methods section, CNFs were also immobilized directly on the SPEs surfaces without NHS/EDC modification

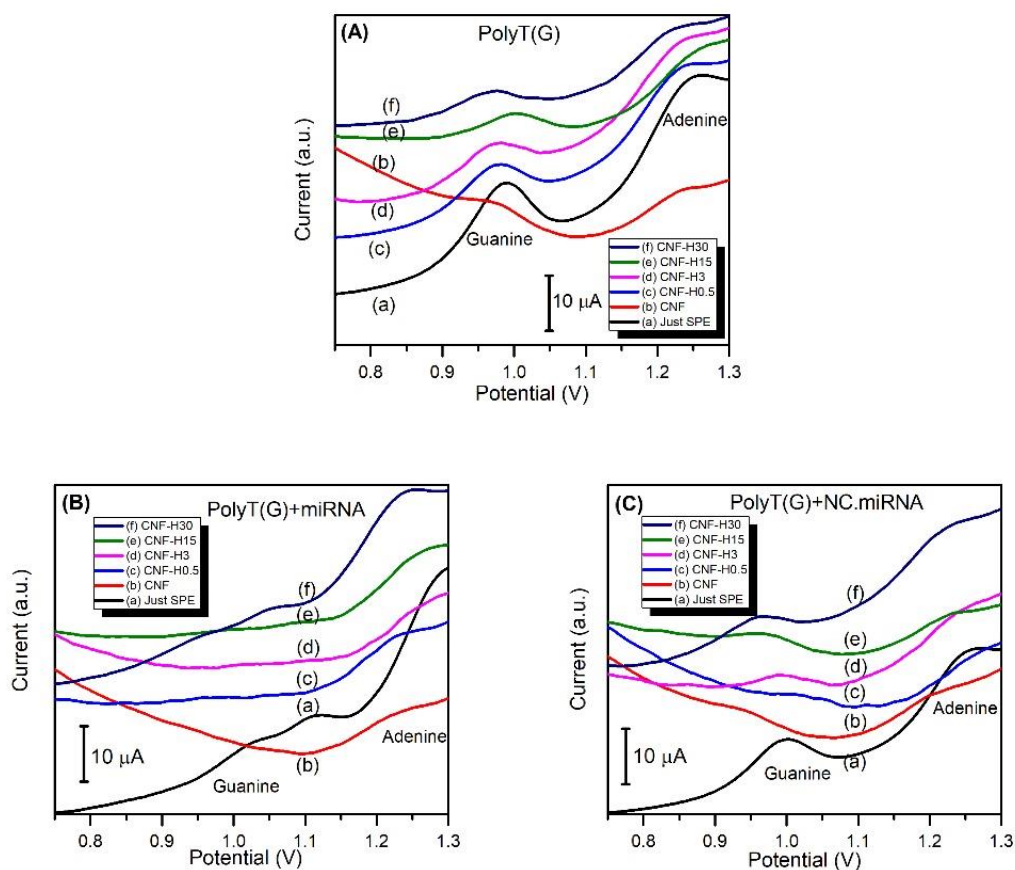


**Figure 4.25.** Electrochemical miRNA biosensor measurements plots by using just Hb-CNFs immobilized SPEs without NHS/EDC modification: A) PolyT (G), (B) PolyT (G)-miRNA, and (C) PolyT(G)-NC.miRNA

Shortened CNFs were directly immersed in ethanol and immobilized on the SPEs surfaces for an electrochemical measurements and analysis. The PolyT(G) as an anti-miRNA molecules were used for this measurement and attached on the Hb enriched CNFs immobilized SPEs surfaces by a physical adsorption and interacted with h target miRNA and non-complementary miRNA (NC.miRNA) separately for hybridization. As seen from the plots below, the guanine oxidation intensity changed and were plotted before and after hybridization for an efficient analyse.

Guanine oxidation signal was detected around 0.9–1.05 (figure 4.25 (a)) as expected at PolyT(G) attached samples and a slight enhancement of the signal was detected when Hb enrichment was applied to the CNFs. The guanine oxidation signal decreased after hybridization of PolyT(G) with miRNA as demonstrated in figure 4.25 (b).

The interaction of PolyT(G) with NC.miRNA didn't result a decrease of the guanine oxidation signal (figure 4.25 (c)) due to a non-hybridization occurred resulting of the mismatch of genetic codes and agreed as expected result.

From the obtained results, the enhancement observed of the guanine oxidation signal after using Hb enriched CNFs compared to neat CNFs is explained by the enhancement of the graphitic properties of the CNFs with the Hb addition to the precursor PAN/Hb previously investigated and lead to an enhancement of the catalytic effect on carbonization process. The more graphitic properties are enhanced the more the detected signal intensity can be qualitatively adequate to a biosensory use.

## 5. CONCLUSION

The conception of an efficient biosensor implies the study of the used transducer and the methodology of measurement. For this purpose, this thesis was focused on the enhancement of the signal obtained from the surface of the biosensor electrochemically.

### 5.1. Effect of Lawson enhancement on the miRNA biosensor performance

A uniform PAN/Law nanofibers were produced via electrospinning process for a selective miRNA detection. The experimental process was firstly by preparing the electrospinning solution with different concentrations rates and the obtained nanofibers were stabilized and carbonized. The samples were carefully kept for the electrochemical measurements that were processed by a preparation of the SPEs surfaces to prevent any contaminations and then the Law enriched CNFs previously prepared were dropped, attached and the guanine oxidation signals were detected and analyzed.

Three different miRNA molecules including the target (miRNA), single-base mismatched (SM.miRNA) and non-complementary (NC. miRNA) were hybridized with the previously attached anti-miRNA molecules (with guanine [PolyT(G)] and without guanine [PolyT(I)]) on the CNFs immobilized SPE surfaces.

Nanofiber's diameters decreased dramatically after carbonisation due to the formation of graphitic structure and the removal of the volatiles during the heat treatment process. The DSC measurements demonstrated that even though initial addition of Law enhance the cyclization to form extended conjugate ring system and a formation of more graphitic structure. The results also revealed that with increasing the Law content inhibits the occurrence of formation of graphitic structures in CNFs that visibly decreased by increasing Law ratio in the precursor nanofibers. The reduction of the graphitic level at high Law ratios was also confirmed after Raman spectroscopy investigations. The electrochemical measurements carried out by DPV methods were investigated and confirms the enhanced selectivity of the miRNA molecules by using CNFs with SPEs and the conceived biosensory system could be used to detect specific RNA molecules.

## **5.2. Effect of Hemoglobin enhancement on the miRNA biosensor performance**

As cited above for the Lawsons enriched CNFs, PAN/Hb hybrid nanofibers were produced with different ratio via electrospinning method. Once the samples were prepared, a proper heat treatment of stabilization followed by a carbonization was applied. The morphological characterization of the obtained nanofibers confirms the formation of beaded defect in the nanofibrous mat, but nanofiber uniformity was not lost and kept their continuous fashion. As expected, a decrease of the nanofiber diameters was calculated after carbonization process.

The low addition of Hb into the precursor PAN nanofibers leads to better graphitic structure after carbonization process and was confirmed by Raman spectra and X-Ray diffraction measurements. A low addition of Hb caused exothermic peak and more cyclization reaction occurred and more ring structures were formed, a better graphitic structure was obtained after carbonization of the nanofibers.

We can conclude that a few amounts of Hb addition can enhance the graphitic properties in the carbonized nanofibers.

Electrochemical measurements were also investigated, the prepared carbon nanofibers were immobilized on the SPEs surfaces previously prepared and activated. selective miRNA detection by focusing on guanine oxidation signal. Firstly, anti-miRNA molecules were immobilized on the SPE surfaces, hybridization with miRNA and DPV measurements were conducted to analyze the guanine oxidation signal intensity change.

We can conclude that, compared to pure CNFs and hemoglobin enriched CNFs, the obtained signal was not dramatically changing and low addition of hemoglobin into the precursor nanofibers caused a catalytic effect and enhanced the graphitic structures of the carbon nanofibers and that led to a little efficient increase of the signal intensity.



## REFERENCES

- Abu-Salah, K. M., Zourob, M. M., Mouffouk, F., Alrokayan, S. A., Alaamery, M. A., & Ansari, A. A. (2015). DNA-based nanobiosensors as an emerging platform for detection of disease. *Sensors*, 15(6), 14539–14568. <https://doi.org/10.3390/s150614539>
- Ahmadi, S., Hivechi, A., Bahrami, S. H., Milan, P. B., & Ashraf, S. S. (2021). Cinnamon extract loaded electrospun chitosan/gelatin membrane with antibacterial activity. *International Journal of Biological Macromolecules*, 173, 580–590. <https://doi.org/10.1016/j.ijbiomac.2021.01.156>
- Aladag Tanik, N., Demirkan, E., & Aykut, Y. (2018). Guanine oxidation signal enhancement in DNA via a polyacrylonitrile nanofiber-coated and cyclic voltammetry-treated pencil graphite electrode. *Journal of Physics and Chemistry of Solids*, 118, 73–79. <https://doi.org/10.1016/j.jpics.2018.03.001>
- Alocilja, E. C., & Radke, S. M. (2003). Market analysis of biosensors for food safety. *Biosensors and Bioelectronics*, 18(5–6), 841–846. [https://doi.org/10.1016/S0956-5663\(03\)00009-5](https://doi.org/10.1016/S0956-5663(03)00009-5)
- Amin, M., Isa, M. M., Sidek, R. M., & Yusof, N. A. (2016). An embedded processing of differential pulse voltammetry (DPV) data using ARM processor (LPC1768). *Proceeding - 2015 IEEE International Circuits and Systems Symposium (ICSyS)*, 80–84. <https://doi.org/10.1109/CircuitsAndSystems.2015.7394069>
- Andreescu, S., & Sadik, O. A. (2004). Trends and challenges in biochemical sensors for clinical and environmental monitoring. *Pure and Applied Chemistry*, 76(4), 861–878. <https://doi.org/10.1351/pac200476040861>
- Avci, H., Monticello, R., & Kotek, R. (2013). Preparation of antibacterial PVA and PEO nanofibers containing Lawsonia Inermis (henna) leaf extracts. *Journal of Biomaterials Science, Polymer Edition*, 24(16), 1815–1830. <https://doi.org/10.1080/09205063.2013.804758>
- Aykut, Y. (2011). Polymer Assisted Functional Ceramic Nanofibrous Structures for Potential Optoelectronic and Photocatalytic Applications.
- Aykut, Y. (2012). Enhanced field electron emission from electrospun Co-loaded activated porous carbon nanofibers. *ACS Applied Materials and Interfaces*, 4(7), 3405–3415. <https://doi.org/10.1021/am3003523>
- Azimzadeh, M., Rahaie, M., Nasirizadeh, N., Daneshpour, M., & Naderi-Manesh, H. (2017). Electrochemical miRNA biosensors: The benefits of nanotechnology. *Nanomedicine Research Journal*, 2(1), 36–48. <https://doi.org/10.22034/NMRJ.2017.23336>
- Babiarz, J. E., Ruby, J. G., Wang, Y., Bartel, D. P., & Belloch, R. (2008). Mouse ES cells express endogenous shRNAs, siRNAs, and other microprocessor-independent,

dicer-dependent small RNAs. *Genes and Development*, 22(20), 2773–2785. <https://doi.org/10.1101/gad.1705308>

Badoni Semwal, R., Semwal, D. K., Combrinck, S., Cartwright-Jones, C., & Viljoen, A. (2014). *Lawsonia inermis* L. (henna): Ethnobotanical, phytochemical and pharmacological aspects. *Journal of Ethnopharmacology*, 155(1), 80–103. <https://doi.org/10.1016/j.jep.2014.05.042>

Baghayeri, M., & Veisi, H. (2015). Fabrication of a facile electrochemical biosensor for hydrogen peroxide using efficient catalysis of hemoglobin on the porous Pd@Fe<sub>3</sub>O<sub>4</sub>-MWCNT nanocomposite. *Biosensors and Bioelectronics*, 74, 190–198. <https://doi.org/10.1016/j.bios.2015.06.016>

Bagni, G., Hernandez, S., Mascini, M., Sturchio, E., Boccia, P., & Marconi, S. (2005). DNA Biosensor for Rapid Detection of Genotoxic Compounds in Soil Samples. *Sensors*, 5(6), 394–410. <https://doi.org/10.3390/S5060394>

Bai, H., & Wu, S. (2019). Mir-451: A novel biomarker and potential therapeutic target for cancer. *Oncotargets and Therapy*, 12, 11069. <https://doi.org/10.2147/OTT.S230963>

Bakirhan, N. K., Kaya, S. I., & Ozkan, S. A. (2021). Basics of electroanalytical methods and their applications with quantum dot sensors. In : *Electroanalytical Applications of Quantum Dot-Based Biosensors*. Elsevier, 37–80. <https://doi.org/10.1016/b978-0-12-821670-5.00011-7>

Bakirhan, N. K., & Ozkan, S. A. (2018). Quantum dots as a new generation nanomaterials and their electrochemical applications in pharmaceutical industry. In *Handbook of Nanomaterials for Industrial Applications*. Elsevier, 520–529. <https://doi.org/10.1016/B978-0-12-813351-4.00029-8>

Bano, E., Fradet, L., Ollivier, M., Choi, J. H., & Stambouli, V. (2016). SiC Nanowire-Based Transistors for Electrical DNA Detection. In *Silicon Carbide Biotechnology*, 261–310. <https://doi.org/10.1016/B978-0-12-802993-0.00009-5>

Barnes, C. P., Smith, M. J., Bowlin, G. L., Sell, S. A., Tang, T., Matthews, J. A., ... Nimtz, J. C. (2006). Feasibility of Electrospinning the Globular Proteins Hemoglobin and Myoglobin, 1(2), 155892500600100. <https://doi.org/10.1177/155892500600100202>

Bartel, D. P. (2009). MicroRNAs: Target Recognition and Regulatory Functions. *Cell*, 136(2), 215–233. <https://doi.org/10.1016/j.cell.2009.01.002>

Beattie, K. L., Beattie, W. G., Meng, L., Turner, S. L., Coral-Vazquez, R., Smith, D. D., ... Dao, D. D. (1995). Advances in genosensor research. *Clinical Chemistry*, 41(5), 700–706. <https://doi.org/10.1093/clinchem/41.5.700>

Bergveld, P., & Thevenot, D. R. (1993). *Sensor operating principles*, 27–90. Retrieved from <https://hal.archives-ouvertes.fr/hal-01179726>

Bertini, I., Gray, H. B., Lippard, S. J., Selverstone Valentine, J., Lippard, S., & Valentine,

- J. (1994). *Bioinorganic Chemistry, Metal/Nucleic-Acid Interactions*, 8.
- Bettazzi, F., Hamid-Asl, E., Esposito, C. L., Quintavalle, C., Formisano, N., Laschi, S., ... Palchetti, I. (2013). Electrochemical detection of miRNA-222 by use of a magnetic bead-based bioassay. *Analytical and Bioanalytical Chemistry*, 405(2), 1025–1034. <https://doi.org/10.1007/s00216-012-6476-7>
- Bhalla, N., Jolly, P., Formisano, N., & Estrela, P. (2016). Introduction to biosensors. *Essays in Biochemistry*, 60(1), 1–8. <https://doi.org/10.1042/EBC20150001>
- Bohnsack, M. T., Czaplinski, K., & Görlich, D. (2004). Exportin 5 is a RanGTP-dependent dsRNA-binding protein that mediates nuclear export of pre-miRNAs. *RNA*, 10(2), 185–191. <https://doi.org/10.1261/rna.5167604>
- Bostanci, A., Tanik, N. A., & Aykut, Y. (2019). Cellulose monoacetate/nafion (CMA/N) hybrid nanofibers as interface for electrochemical DNA biosensors. *Tekstil ve Konfeksiyon*, 29(3), 228–236. <https://doi.org/10.32710/tekstilvekonfeksiyon.501435>
- Boulikas, T., & Vougiouka, M. (2003). Cisplatin and platinum drugs at the molecular level. *Oncology Reports*, 10(6), 1663–1682. <https://doi.org/10.3892/OR.10.6.1663>
- Brázdilová, P., Vrábek, M., Pohl, R., Pivoňková, H., Havran, L., Hocek, M., & Fojta, M. (2007). Ferrocenylethynyl derivatives of nucleoside triphosphates: Synthesis, incorporation, electrochemistry, and bioanalytical applications. *Chemistry - A European Journal*, 13(34), 9527–9533. <https://doi.org/10.1002/chem.200701249>
- Cagnin, S., Caraballo, M., Guiducci, C., Martini, P., Ross, M., Santaana, M., ... & Lanfranchi, G. (2009). Overview of electrochemical DNA biosensors: New approaches to detect the expression of life. *Sensors*, 9(4), 3122–3148. <https://doi.org/10.3390/s90403122>
- Cahová, H., Havran, L., Brázdilová, P., Pivoňková, H., Pohl, R., Fojta, M., & Hocek, M. (2008). Aminophenyl- and Nitrophenyl-Labeled Nucleoside Triphosphates: Synthesis, Enzymatic Incorporation, and Electrochemical Detection. *Angewandte Chemie*, 120(11), 2089–2092. <https://doi.org/10.1002/ange.200705088>
- Cai, X., Hagedorn, C. H., & Cullen, B. R. (2004). Human microRNAs are processed from capped, polyadenylated transcripts that can also function as mRNAs. *RNA*, 10(12), 1957–1966. <https://doi.org/10.1261/rna.7135204>
- Cam, E., Tanik, N. A., Cerkez, I., Demirkan, E., & Aykut, Y. (2018). Guanine oxidation signal enhancement in single strand DNA with polyacrylonitrile/polyaniline (PAN/PAni) hybrid nanofibers. *Journal of Applied Polymer Science*, 135(3), 45567. <https://doi.org/10.1002/app.45567>
- Cammann, K. (1977). Bio-sensors based on ion-selective electrodes. *Fresenius' Zeitschrift Für Analytische Chemie*, 287(1), 1–9. <https://doi.org/10.1007/BF00539519>
- Cass, A. E. G., Davis, G., Francis, G. D., Allen, H., Hill, O., Aston, W. J., ... & Turner,

A. P. F. (1984). Ferrocene-Mediated Enzyme Electrode for Amperometric Determination of Glucose. *Analytical Chemistry*, 56(4), 667–671. <https://doi.org/10.1021/ac00268a018>

Chaki, N. K., & Vijayamohanan, K. (2002). Self-assembled monolayers as a tunable platform for biosensor applications. *Biosensors and Bioelectronics*, 17(1–2), 1–12. [https://doi.org/10.1016/S0956-5663\(01\)00277-9](https://doi.org/10.1016/S0956-5663(01)00277-9)

Chan, J. F. W., Yip, C. C. Y., To, K. K. W., Tang, T. H. C., Wong, S. C. Y., Leung, K. H., ... & Yuen, K. Y. (2020). Improved molecular diagnosis of COVID-19 by the novel, highly sensitive and specific COVID-19-RdRp/Hel real-time reverse transcription-PCR assay validated in vitro and with clinical specimens. *Journal of Clinical Microbiology*, 58(5). <https://doi.org/10.1128/JCM.00310-20>

Chen, C., Fu, K., Lu, Y., Zhu, J., Xue, L., Hu, Y., & Zhang, X. (2015). Use of a tin antimony alloy-filled porous carbon nanofiber composite as an anode in sodium-ion batteries. *RSC Advances*, 5(39), 30793–30800. <https://doi.org/10.1039/c5ra01729g>

Chiang, H. R., Schoenfeld, L. W., Ruby, J. G., Auyeung, V. C., Spies, N., Baek, D., ... & Bartel, D. P. (2010). Mammalian microRNAs: Experimental evaluation of novel and previously annotated genes. *Genes and Development*, 24(10), 992–1009. <https://doi.org/10.1101/gad.1884710>

Chung, D. J., Kim, K. C., & Choi, S. H. (2011). Electrochemical DNA biosensor based on avidin-biotin conjugation for influenza virus (type A) detection. *Applied Surface Science*, 257(22), 9390–9396. <https://doi.org/10.1016/j.apsusc.2011.06.015>

Chung, G. S., Jo, S. M., & Kim, B. C. (2005). Properties of carbon nanofibers prepared from electrospun polyimide. *Journal of Applied Polymer Science*, 97(1), 165–170. <https://doi.org/10.1002/app.21742>

Clark, L. C. (1956). Monitor and control of blood and tissue oxygen tensions. *Transactions - American Society for Artificial Internal Organs*, 2(1), 41–46. [https://journals.lww.com/asaiojournal/Citation/1956/04000/Monitor\\_and\\_Control\\_of\\_Blood\\_and\\_Tissue\\_Oxygen.7.aspx](https://journals.lww.com/asaiojournal/Citation/1956/04000/Monitor_and_Control_of_Blood_and_Tissue_Oxygen.7.aspx)

Clark, Leland C., & Lyons, C. (1962). Electrode systems for continuous monitoring in cardiovascular surgery. *Annals of the New York Academy of Sciences*, 102(1), 29–45. <https://doi.org/10.1111/j.1749-6632.1962.tb13623.x>

Collings, A. F., & Caruso, F. (1997). Biosensors: Recent advances. *Reports on Progress in Physics*, 60(11), 1397–1445. <https://doi.org/10.1088/0034-4885/60/11/005>

Condrat, C. E., Thompson, D. C., Barbu, M. G., Bugnar, O. L., Boboc, A., Cretoiu, D., ... & Voinea, S. C. (2020). miRNAs as Biomarkers in Disease: Latest Findings Regarding Their Role in Diagnosis and Prognosis. *Cells*, 9(2), 276 <https://doi.org/10.3390/cells9020276>

Ozkan-Ariksoysal, D., Kara, P., & Ozsoz, M. (2012). Electrochemical DNA Biosensors for Detection of Compound-DNA Interactions. In *Electrochemical DNA Biosensors*,

397–420. <https://doi.org/10.1201/b11988-13>

Damiati, S., & Schuster, B. (2020). Electrochemical biosensors based on S-layer proteins. *Sensors*, *20*(6), 1721. <https://doi.org/10.3390/s20061721>

Davis-Dusenbery, B. N., & Hata, A. (2010). Mechanisms of control of microRNA biogenesis. *The Journal of Biochemistry*, *148*(4), 381–392. <https://doi.org/10.1093/jb/mvq096>

Dequeker, E., Stuhmann, M., Morris, M. A., Casals, T., Castellani, C., Claustres, M., ... & Girodon, E. (2009). Best practice guidelines for molecular genetic diagnosis of cystic fibrosis and CFTR-related disorders - Updated European recommendations. *European Journal of Human Genetics*, *17*(1), 51–65. <https://doi.org/10.1038/ejhg.2008.136>

Doğru, E., Erhan, E., & Arıkan, O. A. (2017). The Using Capacity of Carbon Fiber Microelectrodes in DNA Biosensors. *Electroanalysis*, *29*(1), 287–293. <https://doi.org/10.1002/elan.201600354>

Dong, R., Shen, Z., Zheng, C., Chen, G., & Zheng, S. (2016). Serum microRNA microarray analysis identifies miR-4429 and miR-4689 are potential diagnostic biomarkers for biliary atresia. *Scientific Reports*, *6*(1), 1–11. <https://doi.org/10.1038/srep21084>

Downard, A. J. (2000). Electrochemically Assisted Covalent Modification of Carbon Electrodes. *Electroanalysis*, *12*(14), 1085–1096. [https://doi.org/10.1002/1521-4109\(200010\)12:14<1085::AID-ELAN1085>3.0.CO;2-A](https://doi.org/10.1002/1521-4109(200010)12:14<1085::AID-ELAN1085>3.0.CO;2-A)

Matthews, D. R., Holman, R. R., Bown, E., Steemson, J., Watson, A., Hughes, S., & Scott, D. (1987). Pen-sized digital 30-second blood glucose meter. *Lancet*, *1*(8536), 778–779. [https://doi.org/10.1016/S0140-6736\(87\)92802-9](https://doi.org/10.1016/S0140-6736(87)92802-9)

Drummond, T. G., & Michael, G. (2003). Hill, and Jacqueline K. Barton. “Electrochemical DNA sensors.”, *Nature biotechnology*, *21*(10), 1192–1199. <https://doi.org/10.1038/nbt873>

Durası, İ. M. (2018). *Identification of miRNA regulatory pathways in complex diseases* (Doctoral dissertation).

Durst, R. A., Bäumner, A. J., Murray, R. W., Buck, R. P., & Andrieux, C. P. (1997). Chemically modified electrodes: Recommended terminology and definitions (IUPAC Recommendations 1997). *Pure and Applied Chemistry*, *69*(6), 1317–1323. <https://doi.org/10.1351/pac199769061317>

Eichhorn, G. L., & Shin, Y. A. (1968). Interaction of metal ions with polynucleotides and related compounds. XII. The relative effect of various metal ions on DNA helicity. *Journal of the American Chemical Society*, *90*(26), 7323–7328. <https://doi.org/10.1021/JA01028A024>

Eksin, E., & Erdem, A. (2016). Chitosan-carbon Nanofiber Modified Single-use Graphite

Electrodes Developed for Electrochemical Detection of DNA Hybridization Related to Hepatitis B Virus. *Electroanalysis*, 28(10), 2514–2521. <https://doi.org/10.1002/elan.201501113>

Eksin, E., Zor, E., Erdem, A., & Bingol, H. (2017). Electrochemical monitoring of biointeraction by graphene-based material modified pencil graphite electrode. *Biosensors and Bioelectronics*, 92, 207–214. <https://doi.org/10.1016/j.bios.2017.02.016>

El Aamri, M., Yammouri, G., Mohammadi, H., Amine, A., & Korri-Youssoufi, H. (2020). Electrochemical Biosensors for Detection of MicroRNA as a Cancer Biomarker: Pros and Cons. *Biosensors*, 10(11), 186. <https://doi.org/10.3390/bios10110186>

Elgrishi, N., Rountree, K. J., McCarthy, B. D., Rountree, E. S., Eisenhart, T. T., & Dempsey, J. L. (2018a). A Practical Beginner's Guide to Cyclic Voltammetry. *Journal of Chemical Education*, 95(2), 197–206. <https://doi.org/10.1021/acs.jchemed.7b00361>

Elgrishi, N., Rountree, K. J., McCarthy, B. D., Rountree, E. S., Eisenhart, T. T., & Dempsey, J. L. (2018b). A Practical Beginner's Guide to Cyclic Voltammetry. *Journal of Chemical Education*, 95(2), 197–206. <https://doi.org/10.1021/acs.jchemed.7b00361>

Endrini, S., Rahmat, A., Ismail, P., & Hin, T.-Y. Y. (2002). Anticarcinogenic Properties and Antioxidant Activity of Henna (*Lawsonia inermis*). *J Med Sci*, 2(4), 194–197. <https://doi.org/10.3923/jms.2002.194.197>

Erdem, A., Eksin, E., & Congur, G. (2015). Indicator-free electrochemical biosensor for microRNA detection based on carbon nanofibers modified screen printed electrodes. *Journal of Electroanalytical Chemistry*, 755, 167–173. <https://doi.org/10.1016/j.jelechem.2015.07.031>

Erdem, A., Kerman, K., Meric, B., Akarca, S., & Ozsoz, M. (1999). DNA Electrochemical Biosensor for the Detection of Short DNA Sequences Related to the Hepatitis B Virus. *Electroanalysis*, 11(8), 586–588. [https://doi.org/10.1002/\(SICI\)1521-4109\(199906\)11:8](https://doi.org/10.1002/(SICI)1521-4109(199906)11:8)

Erdem, A., & Ozsoz, M. (2001). Interaction of the anticancer drug epirubicin with DNA. *Analytica Chimica Acta*, 437(1), 107–114. [https://doi.org/10.1016/S0003-2670\(01\)00942-4](https://doi.org/10.1016/S0003-2670(01)00942-4)

Erdem, A., Pividori, M. I., Del Valle, M., & Alegret, S. (2004). Rigid carbon composites: A new transducing material for label-free electrochemical genosensing. *Journal of Electroanalytical Chemistry*, 567(1), 29–37. <https://doi.org/10.1016/j.jelechem.2003.10.049>

Doğru, E. (2017). Carbon fiber based DNA biosensor design.

Fojta, M. (2002). Electrochemical sensors for DNA interactions and damage. *Electroanalysis*, 14(21), 1449–1463. [https://doi.org/10.1002/1521-4109\(200211\)14:21<1449::AID-ELAN1449>3.0.CO;2-Z](https://doi.org/10.1002/1521-4109(200211)14:21<1449::AID-ELAN1449>3.0.CO;2-Z)

Fuji-Keizai USA Inc. (2004). *Biosensor Market, R&D Applications & Commercial Implication: W.S. & Worldwide*. [https://books.google.com.tr/books/about/Biosensor\\_Market\\_R\\_D\\_Applications\\_Comm.html?id=qo9VYgEACAAJ&redir\\_esc=y](https://books.google.com.tr/books/about/Biosensor_Market_R_D_Applications_Comm.html?id=qo9VYgEACAAJ&redir_esc=y)

Gergin, İ., Ismar, E., & Sarac, A. S. (2017). Oxidative stabilization of polyacrylonitrile nanofibers and carbon nanofibers containing graphene oxide (GO): a spectroscopic and electrochemical study. *Beilstein journal of nanotechnology*, 8(1), 1616–1628. <https://doi.org/10.3762/bjnano.8.161>

Gil, R., Amorim, C. G., Araújo, A. N., & Montenegro, M. C. (2019). Process analysis | electroanalytical techniques. In *Encyclopedia of Analytical Science*, 384–388. <https://doi.org/10.1016/B978-0-12-409547-2.14541-X>

Giuliani, A. L., Sarti, A. C., & Di Virgilio, F. (2019). Extracellular nucleotides and nucleosides as signalling molecules. *Immunology Letters*, 205, 16–24. <https://doi.org/10.1016/j.imlet.2018.11.006>

Gooding, J. J., Mearns, F., Yang, W., & Liu, J. (2003). Self-assembled monolayers into the 21st century: Recent advances and applications. *Electroanalysis* 15(2), 81-96. <https://doi.org/10.1002/elan.200390017>

Goodsell, D., & Dickerson, R. E. (1986). Isohelical analysis of DNA groove-binding drugs. *Journal of Medicinal Chemistry*, 29(5), 727–733. <https://doi.org/10.1021/JM00155A023>

Goumi, Y. El. (2017). Electrochemical Genosensors: Definition and Fields of Application. *International Journal of Biosensors & Bioelectronics*, 3(5), 353–355. <https://doi.org/10.15406/ijbsbe.2017.03.00080>

Graves, P., & Zeng, Y. (2012). Biogenesis of Mammalian MicroRNAs: A Global View. *Genomics, Proteomics and Bioinformatics*, 10, 239–245. <https://doi.org/10.1016/j.gpb.2012.06.004>

Grieshaber, D., MacKenzie, R., Vörös, J., & Reimhult, E. (2008). Electrochemical Biosensors - Sensor Principles and Architectures. *Sensors*, 8(3), 1400–1458. <https://doi.org/10.3390/s80314000>

Guilbault, G. G., & Montalvo, J. G. (1969). A Urea-Specific Enzyme Electrode. *Journal of the American Chemical Society*, 91(8), 2164–2165. <https://doi.org/10.1021/ja01036a083>

Gokce, Z.G., Akalin, P., Kok, F. N., & Sarac, A. S. (2018). Impedimetric DNA biosensor based on polyurethane/poly(m-anthranilic acid) nanofibers. *Sensors and Actuators, B: Chemical*, 254, 719–726. <https://doi.org/10.1016/j.snb.2017.07.136>

Gulyaeva, L. F., & Kushlinskiy, N. E. (2016). Regulatory mechanisms of microRNA expression. *Journal of Translational Medicine*, 14(1), 1–10. <https://doi.org/10.1186/s12967-016-0893-x>

Gupta, A., & Dhakate, S. R. (2017). Development of structurally stable electrospun carbon nanofibers from polyvinyl alcohol. *Materials Research Express*, 4(4), 045021. <https://doi.org/10.1088/2053-1591/aa6a89>

Gutiérrez, A., Gutierrez, F. A., Eguílaz, M., González-Domínguez, J. M., Hernández-Ferrer, J., Ansón-Casaos, A., ... & Rivas, G. A. (2016). Electrochemical sensing of guanine, adenine and 8-hydroxy-2'-deoxyguanosine at glassy carbon modified with single-walled carbon nanotubes covalently functionalized with lysine. *RSC Advances*, 6(16), 13469–13477. <https://doi.org/10.1039/c5ra22556f>

Ha, M., & Kim, V. N. (2014). Regulation of microRNA biogenesis. *Nature Reviews Molecular Cell Biology*, 15(8), 509–524. <https://doi.org/10.1038/nrm3838>

Ha, M., Pang, M., Agarwal, V., & Chen, Z. J. (2008). Interspecies regulation of microRNAs and their targets. *Biochimica et Biophysica Acta (BBA)- Gene Regulatory Mechanisms*, 1779(11), 735–742. <https://doi.org/10.1016/j.bbagr.2008.03.004>

Hadisi, Z., Nourmohammadi, J., & Nassiri, S. M. (2018). The antibacterial and anti-inflammatory investigation of Lawsonia Inermis-gelatin-starch nano-fibrous dressing in burn wound. *International Journal of Biological Macromolecules*, 107, 2008–2019. <https://doi.org/10.1016/j.ijbiomac.2017.10.061>

Hall, E. A. (1990). *Biosensors* (Prentice Hall, Ed.). Open university press.

Han, S., Liu, W., Zheng, M., & Wang, R. (2020). Label-Free and Ultrasensitive Electrochemical DNA Biosensor Based on Urchinlike Carbon Nanotube-Gold Nanoparticle Nanoclusters. *Analytical Chemistry*, 92(7), 4780–4787. <https://doi.org/10.1021/acs.analchem.9b03520>

Huang, H. H., De Silva, K. K. H., Kumara, G. R. A., & Yoshimura, M. (2018). Structural Evolution of Hydrothermally Derived Reduced Graphene Oxide. *Scientific Reports*, 8(1), 1–9. <https://doi.org/10.1038/s41598-018-25194-1>

Huang, J., Liu, Y., & You, T. (2010). Carbon nanofiber based electrochemical biosensors: A review. *Analytical Methods*, 2(3), 202–211. <https://doi.org/10.1039/b9ay00312f>

Teh, H. F., Gong, H., Dong, X. D., Zeng, X., Tan, A. L. K., Yang, X., & Tan, S. N. (2005). Electrochemical biosensing of DNA with capture probe covalently immobilized onto glassy carbon surface. *Analytica Chimica Acta*, 551(1–2), 23–29. <https://doi.org/10.1016/j.aca.2005.07.008>

Hung, K. F., Sun, Y. C., Chen, B. H., Lo, J. F., Cheng, C. M., Chen, C. Y., ... Kao, S. Y. (2020). New COVID-19 saliva-based test: How good is it compared with the current nasopharyngeal or throat swab test? *Journal of the Chinese Medical Association*, 83(10), 891–894. <https://doi.org/10.1097/JCMA.0000000000000396>

Huntzinger, E., & Izaurralde, E. (2011). Gene silencing by microRNAs: Contributions of translational repression and mRNA decay. *Nature Reviews Genetics*, 12(2), 99–110. <https://doi.org/10.1038/nrg2936>



- Im, H. I., & Kenny, P. J. (2012). MicroRNAs in neuronal function and dysfunction. *Trends in Neurosciences*, 35(5), 325–334. <https://doi.org/10.1016/j.tins.2012.01.004>
- Inagaki, M., Yang, Y., & Kang, F. (2012). Carbon nanofibers prepared via electrospinning. *Advanced Materials*, 24(19), 2547–2566. <https://doi.org/10.1002/adma.201104940>
- Joshi, P.N., & Waghmode, S. (2016). Graphene quantum dot-based on-chip electrochemical DNA hybridization sensor for pancreatic cancer. *Reports in Electrochemistry*, 6, 31–40. <https://doi.org/10.2147/rie.s83253>
- Kale, S. B., Mahadalkar, M. A., Kim, C. H., Kim, Y. A., Jayswal, M. S., Yang, K. S., & Kale, B. B. (2019). N-Enriched carbon nanofibers for high energy density supercapacitors and Li-ion batteries. *RSC Advances*, 9(62), 36075–36081. <https://doi.org/10.1039/c9ra05780c>
- Kelley, S. O., Boon, E. M., Barton, J. K., Jackson, N. M., & Hill, M. G. (1999). Single-base mismatch detection based on charge transduction through DNA. *Nucleic Acids Research*, 27(24), 4830–4837. <https://doi.org/10.1093/nar/27.24.4830>
- Kerman, K., Meric, B., Ozkan, D., Kara, P., Erdem, A., & Ozsoz, M. (2001). Electrochemical DNA biosensor for the determination of benzo[a]pyrene–DNA adducts. *Analytica Chimica Acta*, 450(1–2), 45–52. [https://doi.org/10.1016/S0003-2670\(01\)01346-0](https://doi.org/10.1016/S0003-2670(01)01346-0)
- Keshavarz, M., Behpour, M., & Rafiee-Pour, H. A. (2015). Recent trends in electrochemical microRNA biosensors for early detection of cancer. *RSC Advances*, 5(45), 35651–35660. <https://doi.org/10.1039/c5ra01726b>
- Keshavarzi, M., Sorayayi, S., Jafar Rezaei, M., Mohammadi, M., Ghaderi, A., Rostamzadeh, A., ... Mirzaei, H. (2017). MicroRNAs-Based Imaging Techniques in Cancer Diagnosis and Therapy. *Journal of Cellular Biochemistry*, 118(12), 4121–4128. <https://doi.org/10.1002/jcb.26012>
- Khayyam, H., Jazar, R. N., Nunna, S., Golkarnarenji, G., Badii, K., Fakhrhoseini, S. M., ... & Naebe, M. (2020). PAN precursor fabrication, applications and thermal stabilization process in carbon fiber production: Experimental and mathematical modelling. *Progress in Materials Science*, 107, 100575. <https://doi.org/10.1016/j.pmatsci.2019.100575>
- Kim, V. N., Han, J., & Siomi, M. C. (2009). Biogenesis of small RNAs in animals. *Nature Reviews Molecular Cell Biology*, 10(2), 126–139. <https://doi.org/10.1038/nrm2632>
- Kirkland, D., & Marzin, D. (2003). An assessment of the genotoxicity of 2-hydroxy-1,4-naphthoquinone, the natural dye ingredient of Henna. *Mutation Research - Genetic Toxicology and Environmental Mutagenesis*, 537(2), 183–199. [https://doi.org/10.1016/S1383-5718\(03\)00077-9](https://doi.org/10.1016/S1383-5718(03)00077-9)
- Kozomara, A., & Griffiths-Jones, S. (2014). MiRBase: Annotating high confidence microRNAs using deep sequencing data. *Nucleic Acids Research*, 42(D1), D68–D73.

<https://doi.org/10.1093/nar/gkt1181>

Krol, J., Loedige, I., & Filipowicz, W. (2010, July 27). The widespread regulation of microRNA biogenesis, function and decay. *Nature Reviews Genetics*, 11(9), 597–610. <https://doi.org/10.1038/nrg2843>

Bankoti, A. K. S. (2009). *Synergistic study on electrochemically deposited thin film with a spectrum from micro to nano range structures* (Doctoral dissertation).

Kurtyka, R., Pokora, W., Tukaj, Z., & Karcz, W. (2016). Effects of juglone and lawsone on oxidative stress in maize coleoptile cells treated with IAA. *AoB PLANTS*, 8. <https://doi.org/10.1093/aobpla/plw073>

Kutner, W., Wang, J., L'her, M., & Buck, R. P. (1998). Analytical aspects of chemically modified electrodes: Classification, critical evaluation and recommendations (IUPAC Recommendations 1998). *Pure and Applied Chemistry*, 70(6), 1301–1318. <https://doi.org/10.1351/pac199870061301>

Labuda, J., Bučková, M., Heilerová, L., Šilhár, S., & Štěpánek, I. (2003). Evaluation of the redox properties and anti/pro-oxidant effects of selected flavonoids by means of a DNA-based electrochemical biosensor. *Analytical and Bioanalytical Chemistry*, 376(2), 168–173. <https://doi.org/10.1007/s00216-003-1884-3>

Lee, K. J., Shiratori, N., Lee, G. H., Miyawaki, J., Mochida, I., Yoon, S. H., & Jang, J. (2010). Activated carbon nanofiber produced from electrospun polyacrylonitrile nanofiber as a highly efficient formaldehyde adsorbent. *Carbon*, 48(15), 4248–4255. <https://doi.org/10.1016/j.carbon.2010.07.034>

Lee, Y., Kim, M., Han, J., Yeom, K. H., Lee, S., Baek, S. H., & Kim, V. N. (2004). MicroRNA genes are transcribed by RNA polymerase II. *EMBO Journal*, 23(20), 4051–4060. <https://doi.org/10.1038/sj.emboj.7600385>

Levicky, R., Herne, T. M., Tarlov, M. J., & Satija, S. K. (1998). Using self-assembly to control the structure of DNA monolayers on gold: A neutron reflectivity study. *Journal of the American Chemical Society*, 120(38), 9787–9792. <https://doi.org/10.1021/ja981897r>

Li, F., Han, X., & Liu, S. (2011). Development of an electrochemical DNA biosensor with a high sensitivity of fM by dendritic gold nanostructure modified electrode. *Biosensors and Bioelectronics*, 26(5), 2619–2625. <https://doi.org/10.1016/j.bios.2010.11.020>

Li, J., Liu, E. H., Li, W., Meng, X. Y., & Tan, S. T. (2009). Nickel/carbon nanofibers composite electrodes as supercapacitors prepared by electrospinning. *Journal of Alloys and Compounds*, 478(1–2), 371–374. <https://doi.org/10.1016/j.jallcom.2008.11.024>

Li, J., Ng, H. T., Cassell, A., Fan, W., Chen, H., Ye, Q., ... & Meyyappan, M. (2003). Carbon nanotube nanoelectrode array for ultrasensitive DNA detection. *Nano Letters*, 3(5), 597–602. <https://doi.org/10.1021/nl0340677>

- Liedberg, B., Nylander, C., & Lunström, I. (1983). Surface plasmon resonance for gas detection and biosensing. *Sensors and Actuators*, 4, 299–304. [https://doi.org/10.1016/0250-6874\(83\)85036-7](https://doi.org/10.1016/0250-6874(83)85036-7)
- Ligaj, M., Jasnowska, J., Musiał, W. G., & Filipiak, M. (2006). Covalent attachment of single-stranded DNA to carbon paste electrode modified by activated carboxyl groups. *Electrochimica Acta*, 51(24), 5193–5198. <https://doi.org/10.1016/j.electacta.2006.03.053>
- Lin, X., Ni, Y., Pei, X., & Kokot, S. (2017). Electrochemical detection of DNA damage induced by clenbuterol at a reduced graphene oxide-Nafion modified glassy carbon electrode. *Analytical Methods*, 9(7), 1105–1111. <https://doi.org/10.1039/C6AY03022J>
- Liu, A., Wang, K., Weng, S., Lei, Y., Lin, L., Chen, W., ... & Chen, Y. (2012a). Development of electrochemical DNA biosensors. *TrAC - Trends in Analytical Chemistry*, 37, 101–111. <https://doi.org/10.1016/j.trac.2012.03.008>
- Liu, A., Wang, K., Weng, S., Lei, Y., Lin, L., Chen, W., ... Chen, Y. (2012b). Development of electrochemical DNA biosensors. *TrAC - Trends in Analytical Chemistry*, 37, 101–111. <https://doi.org/10.1016/j.trac.2012.03.008>
- Liu, H., Ge, J., Ma, E., & Yang, L. (2019). Advanced biomaterials for biosensor and theranostics. In *Biomaterials in Translational Medicine: A Biomaterials Approach*, 213–255. <https://doi.org/10.1016/B978-0-12-813477-1.00010-4>
- Liu, J., Wang, S., Yang, J., Liao, J., Lu, M., Pan, H., & An, L. (2014). ZnCl<sub>2</sub> activated electrospun carbon nanofiber for capacitive desalination. *Desalination*, 344, 446–453. <https://doi.org/10.1016/j.desal.2014.04.015>
- Llenado, R. A., & Rechnitz, G. A. (1971). Improved Enzyme Electrode for Amygdalin. *Analytical Chemistry*, 43(11), 1457–1461. <https://doi.org/10.1021/ac60305a009>
- Luong, J. H., Male, K. B., & Glennon, J. D. (2008). Biosensor technology: Technology push versus market pull. *Biotechnology Advances*, 26(5), 492–500. <https://doi.org/10.1016/j.biotechadv.2008.05.007>
- Magri, F., Vanoli, F., & Corti, S. (2018). miRNA in spinal muscular atrophy pathogenesis and therapy. *Journal of Cellular and Molecular Medicine*, 22(2), 755–767. <https://doi.org/10.1111/jcmm.13450>
- Mahmoudi-Moghaddam, H., Tajik, S., & Beitollahi, H. (2019). A new electrochemical DNA biosensor based on modified carbon paste electrode using graphene quantum dots and ionic liquid for determination of topotecan. *Microchemical Journal*, 150, 104085. <https://doi.org/10.1016/j.microc.2019.104085>
- Mandoj, F., Nardis, S., Di Natale, C., & Paolesse, R. (2018). Porphyrinoid thin films for chemical sensing. In *Encyclopedia of Interfacial Chemistry: Surface Science and Electrochemistry*, 422–443. <https://doi.org/10.1016/B978-0-12-409547-2.11677-4>
- Marrazza, G., Chianella, I., & Mascini, M. (1999). Disposable DNA electrochemical

sensor for hybridization detection. *Biosensors and Bioelectronics*, 14(1), 43–51. [https://doi.org/10.1016/S0956-5663\(98\)00102-X](https://doi.org/10.1016/S0956-5663(98)00102-X)

Marrington, R., Dafforn, T. R., Halsall, D. J., & Rodger, A. (2004). Micro-Volume Couette Flow Sample Orientation for Absorbance and Fluorescence Linear Dichroism. *Biophysical Journal*, 87(3), 2002–2012. <https://doi.org/10.1529/BIOPHYSJ.103.035022>

Mashreghi, M., Azarpara, H., Bazaz, M. R., Jafari, A., Masoudifar, A., Mirzaei, H., & Jaafari, M. R. (2018). Angiogenesis biomarkers and their targeting ligands as potential targets for tumor angiogenesis. *Journal of Cellular Physiology*, 233(4), 2949–2965. <https://doi.org/10.1002/jcp.26049>

Mendoza, S., Bustos, E., Manriquez, J., & Godinez, L. (2015). Voltammetric techniques. *Agricultural and Food Electroanalysis*, 23–48.

Meric, B., Kerman, K., Ozkan, D., Kara, P., Erdem, A., Kucukoglu, O., ... & Ozsoz, M. (2002). Electrochemical biosensor for the interaction of DNA with the alkylating agent 4,4'-dihydroxy chalcone based on guanine and adenine signals. *Journal of Pharmaceutical and Biomedical Analysis*, 30(4), 1339–1346. [https://doi.org/10.1016/S0731-7085\(02\)00477-6](https://doi.org/10.1016/S0731-7085(02)00477-6)

Millan, K. M., & Mikkelsen, S. R. (1993). Sequence-Selective Biosensor for DNA Based on Electroactive Hybridization Indicators. *Analytical Chemistry*, 65(17), 2317–2323. <https://doi.org/10.1021/ac00065a025>

Millan, K. M., Spurmanis, A. J., & Mikkelsen, S. R. (1992). Covalent immobilization of DNA onto glassy carbon electrodes. *Electroanalysis*, 4(10), 929–932. <https://doi.org/10.1002/elan.1140041003>

Miller, J. A. (1994). Recent Studies on the Metabolic Activation of Chemical Carcinogens1. *CANCER RESEARCH (SUPPL.)*, 54(7), 1879–1881. [http://aacrjournals.org/cancerres/articlepdf/54/7\\_Supplement/1879s/2456805/cr054007s1879s.pdf](http://aacrjournals.org/cancerres/articlepdf/54/7_Supplement/1879s/2456805/cr054007s1879s.pdf)

Mirmoghtadaie, L., Ensafi, A. A., Kadivar, M., & Norouzi, P. (2013). Highly selective electrochemical biosensor for the determination of folic acid based on DNA modified-pencil graphite electrode using response surface methodology. *Materials science & engineering. C, Materials for biological applications*, 33(3), 1753–1758.5 <https://doi.org/10.1016/j.msec.2012.12.090>

Mirzaei, H., Ferns, G. A., Avan, A., & Mobarhan, M. G. (2017). Cytokines and MicroRNA in Coronary Artery Disease. *Advances in Clinical Chemistry*, 82, 47–70. <https://doi.org/10.1016/bs.acc.2017.06.004>

Muhammad, H. S., & Muhammad, S. (2005). The use of *Lawsonia inermis linn.* (henna) in the management of burn wound infections. *African Journal of Biotechnology*, 4(9), 934–937. <https://doi.org/10.4314/ajb.v4i9.71132>

Naboka, O., Rodriguez, K., Toomadj, A. F., Sanz-Velasco, A., Toriz, G., Lundgren, P.,

...& Gatenholm, P. (2013). Carbon nanofibers synthesized from electrospun cellulose for advanced material applications. *Materials Science Forum*, 730–732, 903–908. <https://doi.org/10.4028/www.scientific.net/MSF.730-732.903>

Najeeb, M. A., Ahmad, Z., Shakoor, R. A., Mohamed, A. M. A., & Kahraman, R. (2017). A novel classification of prostate specific antigen (PSA) biosensors based on transducing elements. *Talanta*, 168, 52–61. <https://doi.org/10.1016/j.talanta.2017.03.022>

Naveen, M. H., Gurudatt, N. G., & Shim, Y. B. (2017). Applications of conducting polymer composites to electrochemical sensors: A review. *Applied Materials Today*, 9, 419–433. <https://doi.org/10.1016/j.apmt.2017.09.001>

Neidle, S. (1994). DNA structure and recognition / Stephen Neidle. In D. Rickwood (Ed.), *DNA Structure and Recognition* (1st ed.). Oxford: Oxford University Press.

Newman, J. D., Tigwell, L. J., Turner, A. P. F., & Warner, P. J. (2004). Biosensors: a clearer view. *Biosensors*.

Mohd Said, N. A. (2014). Electrochemical biosensor based on microfabricated electrode arrays for life sciences applications (Doctoral dissertation, University College Cork).

Odenthal, K. J., & Gooding, J. J. (2007). An introduction to electrochemical DNA biosensors. *Analyt*, 132(7), 603–610. <https://doi.org/10.1039/b701816a>

Ohashi, T., & Dai, L. (2006). C60 and carbon nanotube sensors. In *Carbon Nanotechnology*, 525–575. <https://doi.org/10.1016/B978-044451855-2/50018-8>

Ossila. Reference Electrode | Ag/AgCl and Ag/Ag<sup>+</sup> Electrodes | Ossila. from <https://www.ossila.com/products/reference-electrode>

Ozkan-Ariksoysal, D., Kayran, Y. U., Yilmaz, F. F., Ciucu, A. A., David, I. G., David, V., ... & Ozsoz, M. (2017). DNA-wrapped multi-walled carbon nanotube modified electrochemical biosensor for the detection of Escherichia coli from real samples. *Talanta*, 166, 27–35. <https://doi.org/10.1016/j.talanta.2017.01.005>

Ozkan-Ariksoysal, D., Kara, P., & Ozsoz, M. (2012). Electrochemical DNA Biosensors for Detection of Compound-DNA Interactions. In *Electrochemical DNA Biosensors*, 12, 397–420. <https://doi.org/10.1201/b11988-14>

Ozkan, D., Erdem, A., Kara, P., Kerman, K., Justin Gooding, J., Nielsen, P. E., & Ozsoz, M. (2002a). Electrochemical detection of hybridization using peptide nucleic acids and methylene blue on self-assembled alkanethiol monolayer modified gold electrodes. In *Electrochemistry Communications*, 4(10), 796–802. [https://doi.org/10.1016/S1388-2481\(02\)00448-4](https://doi.org/10.1016/S1388-2481(02)00448-4)

Ozkan, D., Erdem, A., Kara, P., Kerman, K., Justin Gooding, J., Nielsen, P. E., & Ozsoz, M. (2002b). Electrochemical detection of hybridization using peptide nucleic acids and methylene blue on self-assembled alkanethiol monolayer modified gold electrodes. *Electrochemistry Communications*, 4(10), 796–802. <https://doi.org/10.1016/S1388->

2481(02)00448-4

Ozkan, D., Erdem, A., Kara, P., Kerman, K., Meric, B., Hassmann, J., & Ozsoz, M. (2002). Allele-specific genotype detection of factor V Leiden mutation from polymerase chain reaction amplicons based on label-free electrochemical genosensor. *Analytical Chemistry*, 74(23), 5931–5936. <https://doi.org/10.1021/ac0257905>

Palchetti, I., & Mascini, M. (2010). Biosensor Technology: A Brief History. *In Sensors and Microsystems*, 15–23. [https://doi.org/10.1007/978-90-481-3606-3\\_2](https://doi.org/10.1007/978-90-481-3606-3_2)

Paleček, E. (1960). Oscillographic polarography of highly polymerized Deoxyribonucleic acid. *Nature*, 188(4751), 656–657. <https://doi.org/10.1038/188656a0>

Palecek, E., & Fojta, M. (2005). Electrochemical DNA Sensors. *In Bioelectronics: From Theory to Applications*, 127–192. <https://doi.org/10.1002/352760376X.CH5>

Paleček, E., & Jelen, F. (2002). Electrochemistry of nucleic acids and development of DNA sensors. *Critical Reviews in Analytical Chemistry*, 32(3), 261–270. <https://doi.org/10.1080/10408340290765560>

Park, M., Won, J., Choi, B. Y., & Lee, C. J. (2020). Optimization of primer sets and detection protocols for SARS-CoV-2 of coronavirus disease 2019 (COVID-19) using PCR and real-time PCR. *Experimental and Molecular Medicine*, 52(6), 963–977. <https://doi.org/10.1038/s12276-020-0452-7>

Park, S. H., Jo, S. M., Kim, D. Y., Lee, W. S., & Kim, B. C. (2005). Effects of iron catalyst on the formation of crystalline domain during carbonization of electrospun acrylic nanofiber. *Synthetic Metals*, 150(3), 265–270. <https://doi.org/10.1016/j.synthmet.2005.02.010>

Patel, B. A. (2020). Introduction to electrochemistry for bioanalysis. *In Electrochemistry for Bioanalysis*, 1–8. <https://doi.org/10.1016/b978-0-12-821203-5.00006-3>

Peng, Y., & Croce, C. M. (2016). The role of microRNAs in human cancer. *Signal Transduction and Targeted Therapy*, 1(1), 1–9. <https://doi.org/10.1038/sigtrans.2015.4>

Pfeffer, S., Sewer, A., Lagos-Quintana, M., Sheridan, R., Sander, C., Grässer, F. A., ... & Tuschl, T. (2005). Identification of microRNAs of the herpesvirus family. *Nature Methods*, 2(4), 269–276. <https://doi.org/10.1038/nmeth746>

Pividori, M. I., Merkoçi, A., & Alegret, S. (2000). Electrochemical genosensor design: Immobilisation of oligonucleotides onto transducer surfaces and detection methods. *Biosensors and Bioelectronics*, 15(5–6), 291–303. [https://doi.org/10.1016/S0956-5663\(00\)00071-3](https://doi.org/10.1016/S0956-5663(00)00071-3)

Ramos-Pérez, C., Lorenzo-Castrillejo, I., Quevedo, O., García-Luis, J., Matos-Perdomo, E., Medina-Coello, C., ... & MacHín, F. (2014). Yeast cytotoxic sensitivity to the antitumour agent  $\beta$ -lapachone depends mainly on oxidative stress and is largely independent of microtubule- or topoisomerase-mediated DNA damage. *Biochemical*

*Pharmacology*, 92(2), 206–219. <https://doi.org/10.1016/j.bcp.2014.09.006>

Rasheed, P. A., & Sandhyarani, N. (2017). Electrochemical DNA sensors based on the use of gold nanoparticles: a review on recent developments. *Microchimica Acta*, 184(4), 981–1000. <https://doi.org/10.1007/s00604-017-2143-1>

Rashid, J. I. A., & Yusof, N. A. (2017). The strategies of DNA immobilization and hybridization detection mechanism in the construction of electrochemical DNA sensor: A review. *Sensing and Bio-Sensing Research*, 16, 19–31. <https://doi.org/10.1016/j.sbsr.2017.09.001>

Rosenberg, B., Van Camp, L., & Krigas, T. (1965). Inhibition of cell division in *Escherichia coli* by electrolysis products from a platinum electrode. *Nature*, 205, 698–699. <https://doi.org/10.1038/205698a0>

Roy, S., & Pandit, S. (2019). Microbial electrochemical system: Principles and application. In *Biomass, Biofuels, Biochemicals: Microbial Electrochemical Technology: Sustainable Platform for Fuels, Chemicals and Remediation*, 19–48. Elsevier. <https://doi.org/10.1016/B978-0-444-64052-9.00002-9>

Saeedi Borujeni, M. J., Esfandiary, E., Taheripak, G., Codoñer-Franch, P., Alonso-Iglesias, E., & Mirzaei, H. (2018). Molecular aspects of diabetes mellitus: Resistin, microRNA, and exosome. *Journal of Cellular Biochemistry*, 119(2), 1257–1272. <https://doi.org/10.1002/jcb.26271>

Salarinia, R., Sahebkar, A., Peyvandi, M., Reza Mirzaei, H., Reza Jaafari, M., Matbou Riahi, M., ... & Mirzaei, H. (2016). Epi-Drugs and Epi-miRs: Moving Beyond Current Cancer Therapies. *Current Cancer Drug Targets*, 16(9), 773–788. <https://doi.org/10.2174/1568009616666151207110143>

Shabaninejad, Z., Yousefi, F., Movahedpour, A., Ghasemi, Y., Dokanehiifard, S., Rezaei, S., ... & Mirzaei, H. (2019). Electrochemical-based biosensors for microRNA detection: Nanotechnology comes into view. *Analytical Biochemistry*, 581, 113349. <https://doi.org/10.1016/j.ab.2019.113349>

Shah, P. K., Sriprya, S., Narendran, V., & Pandian, A. J. (2016). Prenatal genetic diagnosis of retinoblastoma and report of RB1 gene mutation from India Prenatal genetic diagnosis of retinoblastoma and report of RB1 gene mutation from India. *Ophthalmic Genetics*, 37(4), 430-433. <https://doi.org/10.3109/13816810.2015.1107595>

Sharma, S., Mehtab, S., & Zaidi, M. G. H. (2020). Chapter-7 Voltammetry: An Electrochemical Analytical Method. *Chemical Sciences*, 1, 127.

Silva, T. A., Moraes, F. C., Campos Janegitz, B., & Fatibello-Filho, O. (2017). Electrochemical Biosensors Based on Nanostructured Carbon Black: A Review. *Journal of Nanomaterials*, 2017, 1-14. <https://doi.org/10.1155/2017/4571614>

Singh, V., Zharnikov, M., Gulino, A., & Gupta, T. (2011). DNA immobilization, delivery and cleavage on solid supports. *Journal of Materials Chemistry*, 21(29), 10602–10618.

<https://doi.org/10.1039/c0jm04359a>

Singhal, K., Mehtab, S., Zaidi, M., & Sharma, S. (2021). Carbon Based Nanocomposites for Electrochemical Sensing of Adenine and Guanine Purine Bases: A Review. *Nano Progress*, 3(5), 1–9. <https://doi.org/10.36686/ariviyal.np.2021.03.05.021>

Sobiepanek, A., & Kobiela, T. (2018). Application of biosensors in cancer research. *Review and Research on Cancer*, 4(1), 4-12.

Kounaves, S. P. (1997). Voltammetric techniques. *Handbook of instrumental techniques for analytical chemistry*, 709-726.

Spichiger-Keller, U. E. (1998). Chemical sensors and biosensors for medical and biological applications. *Optical Sensors, Optodes*, 1, 259–319.

Steel, A. B., Herne, T. M., & Tarlov, M. J. (1998). Electrochemical quantitation of DNA immobilized on gold. *Analytical Chemistry*, 70(22), 4670–4677. <https://doi.org/10.1021/ac980037q>

Suganya, S., Senthil Ram, T., Lakshmi, B. S., & Giridev, V. R. (2011). Herbal drug incorporated antibacterial nanofibrous mat fabricated by electrospinning: An excellent matrix for wound dressings. *Journal of Applied Polymer Science*, 121(5), 2893–2899. <https://doi.org/10.1002/app.33915>

Suzuki, S., Takahashi, F., Satoh, I., & Sonobe, N. (1975). Ethanol and Lactic Acid Sensors Using Electrodes Coated with Dehydrogenase—Collagen Membranes. *Bulletin of the Chemical Society of Japan*, 48(11), 3246–3249. <https://doi.org/10.1246/bcsj.48.3246>

Takenaka, S., Yamashita, K., Takagi, M., Uto, Y., & Kondo, H. (2000). DNA sensing on a DNA probe-modified electrode using ferrocenylnaphthalene diimide as the electrochemically active ligand. *Analytical Chemistry*, 72(6), 1334–1341. <https://doi.org/10.1021/ac991031j>

Tavakolizadeh, J., Roshanaei, K., Salmaninejad, A., Yari, R., Nahand, J. S., Sarkarizi, H. K., ... & Mirzaei, H. (2018). MicroRNAs and exosomes in depression: Potential diagnostic biomarkers. *Journal of Cellular Biochemistry*, 119(5), 3783–3797. <https://doi.org/10.1002/jcb.26599>

Thévenot, D. R., Toth, K., Durst, R. A., & Wilson, G. S. (2001). Electrochemical biosensors: Recommended definitions and classification. *Biosensors and Bioelectronics*, 16(1–2), 121–131. [https://doi.org/10.1016/S0956-5663\(01\)00115-4](https://doi.org/10.1016/S0956-5663(01)00115-4)

Tran, H., Piro, B., Reisberg, S., Tran, L., Duc, H., & Pham, M. (2013). Label-free and reagentless electrochemical detection of microRNAs using a conducting polymer nanostructured by carbon nanotubes: Application to prostate cancer biomarker miR-141. *Biosensors and Bioelectronics*, 49, 164–169. <https://doi.org/10.1016/j.bios.2013.05.007>

Tripathy, S., Vanjari, S. R. K., Singh, V., Swaminathan, S., & Singh, S. G. (2017).



Electrospun manganese (III) oxide nanofiber based electrochemical DNA-nanobiosensor for zeptomolar detection of dengue consensus primer. *Biosensors and Bioelectronics*, *90*, 378-387.

Tripathy, S., Naithani, A., Vanjari, S. R. K., & Singh, S. G. (2017). Electrospun polyaniline nanofiber based chemiresistive nanobiosensor platform for DNA Hybridization detection. *Proceedings of IEEE Sensors, 2017*, 1–3. <https://doi.org/10.1109/ICSENS.2017.8234342>

Turner, A. P. F., Karube, I., Wilson, G. S., & Worsfold, P. J. (1987). Biosensors: fundamentals and applications. *Analytica Chimica Acta*, *201*, 363–364. [https://doi.org/10.1016/s0003-2670\(00\)85361-1](https://doi.org/10.1016/s0003-2670(00)85361-1)

Urdike, S. J., & Hicks, G. P. (1967). The enzyme electrode. *Nature*, *214*(5092), 986–988. <https://doi.org/10.1038/214986a0>

Vamvakaki, V., Fouskaki, M., & Chaniotakis, N. (2007). Electrochemical biosensing systems based on carbon nanotubes and carbon nanofibers. *Analytical Letters*, *4*(12), 2271–2287. <https://doi.org/10.1080/00032710701575520>

Vamvakaki, V., Tsagaraki, K., & Chaniotakis, N. (2006). Carbon nanofiber-based glucose biosensor. *Analytical Chemistry*, *78*(15), 5538–5542. <https://doi.org/10.1021/ac060551t>

Van, T. T., Miller, J., Warshauer, D. M., Reisdorf, E., Jernigan, D., Humes, R., & Shulta, P. A. (2012). Pooling nasopharyngeal/throat swab specimens to increase testing capacity for influenza viruses by PCR. *Journal of Clinical Microbiology*, *50*(3), 891–896. <https://doi.org/10.1128/JCM.05631-11>

Velusamy, V., Arshak, K., Korostynska, O., Oliwa, K., & Adley, C. (2009). Conducting polymer based DNA biosensor for the detection of the *Bacillus cereus* group species. *Sensing for Agriculture and Food Quality and Safety*, *7315*, 19-26. <https://doi.org/10.1117/12.818631>

Wang, D., & Farhana, A. (2021). Biochemistry, RNA Structure. In *StatPearls*. 32644425.

Wang, J. (2002). Electrochemical nucleic acid biosensors. *Analytica Chimica Acta*, *469*(1), 63–71. [https://doi.org/10.1016/S0003-2670\(01\)01399-X](https://doi.org/10.1016/S0003-2670(01)01399-X)

Wang, J., Cai, X., Rivas, G., Shiraishi, H., Farias, P. A. M., & Dontha, N. (1996). DNA electrochemical biosensor for the detection of short DNA sequences related to the human immunodeficiency virus. *Analytical Chemistry*, *68*(15), 2629–2634. <https://doi.org/10.1021/ac9602433>

Wang, J., Palecek, E., Nielsen, P. E., Rivas, G., Cai, X., Shiraishi, H., ...& Farias, P. A. M. (1996). Peptide nucleic acid probes for sequence-specific DNA biosensors. *Journal of the American Chemical Society*, *118*(33), 7667–7670. <https://doi.org/10.1021/ja9608050>

Wang, Y., Stricker, H. M., Gou, D., & Liu, L. (2007). MicroRNA: past and present. *Frontiers in Bioscience*, *12*(2316), 2316–2329.

Weetall, H. H. (1999). Chemical sensors and biosensors, update, what, where, when and how. *Biosensors & Bioelectronics*, *14*(2), 237–224.

Wooster, R., & Weber, B. L. (2003). Breast and Ovarian Cancer. *The New England Journal of Medicine*, *348*(23), 2339–2347. <https://doi.org/10.1056/NEJMra012284>

Xavier, M. R., Santos, M. M. S., Queiroz, M. G., de Lima Silva, M. S., Goes, A. J. S., & De Morais, M. A. (2020). Lawsone, a 2-hydroxy-1,4-naphthoquinone from *Lawsonia inermis* (henna), produces mitochondrial dysfunctions and triggers mitophagy in *Saccharomyces cerevisiae*. *Molecular Biology Reports*, *47*(2), 1173–1185. <https://doi.org/10.1007/s11033-019-05218-3>

Yang, M., McGovern, M. E., & Thompson, M. (1997). Genosensor technology and the detection of interfacial nucleic acid chemistry. *Analytica Chimica Acta*, *346*(3), 259–275. [https://doi.org/10.1016/s0003-2670\(97\)90055-6](https://doi.org/10.1016/s0003-2670(97)90055-6)

Yarin, A. L., Koombhongse, S., & Reneker, D. H. (2001). Taylor cone and jetting from liquid droplets in electrospinning of nanofibers. *Journal of Applied Physics*, *90*(9), 4836–4846. <https://doi.org/10.1063/1.1408260>

Yoo, E. H., & Lee, S. Y. (2010). Glucose Biosensors: An Overview of Use in Clinical Practice. *Sensors*, *10*(5), 4558–4576. <https://doi.org/10.3390/S100504558>

Yu, N., Wang, Z., Wang, C., Han, J., & Bu, H. (2017). Combining padlock exponential rolling circle amplification with CoFe<sub>2</sub>O<sub>4</sub> magnetic nanoparticles for microRNA detection by nanoelectrocatalysis without a substrate. *Analytica chimica acta*, *962*, 24–31. <https://doi.org/10.1016/j.aca.2017.01.069>

Zhang, C. (2008). MicroRNomics: A newly emerging approach for disease biology. *Physiological Genomics*, *33*(2), 139–147. <https://doi.org/10.1152/physiolgenomics.00034.2008>

Zhang, L., Aboagye, A., Kelkar, A., Lai, C., & Fong, H. (2014a). A review: Carbon nanofibers from electrospun polyacrylonitrile and their applications. *Journal of Materials Science*, *49*(2), 463–480. <https://doi.org/10.1007/s10853-013-7705-y>

Zhang, L., Aboagye, A., Kelkar, A., Lai, C., & Fong, H. (2014b). A review: Carbon nanofibers from electrospun polyacrylonitrile and their applications. *Journal of Materials Science*, *49*(2), 463–480. <https://doi.org/10.1007/s10853-013-7705-y>

Zhang, T., Chai, H., Meng, F., Guo, Z., Jiang, Y., & Miao, P. (2018). DNA-Functionalized Porous Fe<sub>3</sub>O<sub>4</sub> Nanoparticles for the Construction of Self-Powered miRNA Biosensor with Target Recycling Amplification. *ACS Applied Materials and Interfaces*, *10*(43), 36796–36804. <https://doi.org/10.1021/acsami.8b15419>

Zhou, D., Lin, X., Gao, W., Piao, J., Li, S., He, N., ... Gong, X. (2019). A novel template

repairing-PCR (TR-PCR) reaction platform for microRNA detection using translesional synthesis on DNA templates containing abasic sites. *Chemical Communications*, 55(20), 2932–2935. <https://doi.org/10.1039/c8cc10226k>

Zhou, Y., Fang, Y., & Ramasamy, R. P. (2019). Non-covalent functionalization of carbon nanotubes for electrochemical biosensor development. *Sensors*, 19(2), 392 <https://doi.org/10.3390/s19020392>

Zhu, W., Liu, M., Fan, Y., Ma, F., Xu, N., & Xu, B. (2018). Dynamics of circulating microRNAs as a novel indicator of clinical response to neoadjuvant chemotherapy in breast cancer. *Cancer Medicine*, 7(9), 4420–4433. <https://doi.org/10.1002/cam4.1723>

## APPENDIX

### APPX 1 Differential calorimetry analysis results for PAN and Law/PAN samples.

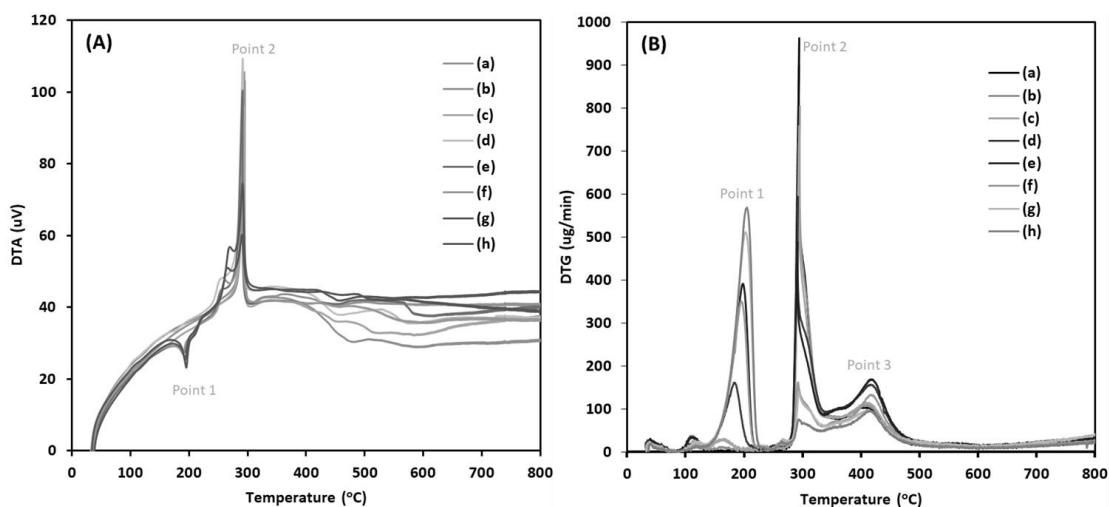
Maximum peak points were considered for T<sub>m</sub> determination

Samples	Peaks related to PAN part						Peaks related to Law part		
	Tg Max (°C)	Tg Onset (°C)	Entalpy ΔH <sub>g</sub> (J/g)	Tm Max (°C)	Tm Onset (°C)	Entalpy ΔH <sub>m</sub> (J/g)	Tm Max (°C)	Onset (°C)	Entalpy ΔH <sub>m</sub> (J/g)
PAN				296.59	292.12	454.41			
L1				295.70	292.64	445.69			
L3				295.35	292.55	464.31			
L15				296.73	292.60	575.30			
L30	101.18	87.89	13.919	299.23	293.19	536.60	183.93	171.30	29.853
L50	104.76	91.02	8.068	298.21	287.54	491.40	180.60	163.06	19.230
L70	105.60	79.55	25.921	298.91	260.94	583.85	182.85	166.49	25.187
L100	108.53	94.11	6.765	284.21	272.43	556.34	192.55	184.32	76.915

### APPX 2 Thermogravimetric (TGA) analysis of PAN and PAN/Law nanofibers

Sample	Point 1		Point 2		Point 3		Point 4		Point 5	
	Position (°C)	Residual (%)	Position (°C)	Residual (%)	Position (°C)	Residual (%)	Position (°C)	Residual (%)	Position (°C)	Residual (%)
PAN	-	-	-	-	284.8	96	456.5	43.1	800	32.1
L1	149,1	97.2	178.6	96.5	284.1	95.1	456.6	44.7	800	32.6
L3	149,4	96.2	179.5	94.8	284.3	92.8	456.5	43.9	800	30.8
L15	149,5	97.2	199.2	89.2	284.7	86.9	456.6	44.1	800	31.3
L30	149,1	96.7	211.8	78.4	284.9	76.6	456.6	38.3	800	26.7
L50	149,2	97.1	206.8	74.6	284.8	72.4	456.5	40.5	800	28.3
L70	149,9	97.2	216.6	69.6	284.7	67.3	456.6	45.3	800	32.8
L100	149,3	97.6	219.6	60.2	284.6	58.2	456.5	35.8	800	25.4

### APPX 3 Representation of A: DTA and B: DTG plots of PAN/Law nanofibers



### APPX 4 Data point obtained from DTA and DTG plots

	DTA				DTG					
	Peak 1		Peak 2		Peak 1		Peak 2		Peak 3	
<u>Samples</u>	Position (°C)	Intensity (uV)	Position (°C)	Intensity (uV)	Position (°C)	Intensity (ug/min)	Position (°C)	Intensity (ug/min)	Position (°C)	Intensity (ug/min)
PAN	-	-	294.4	102.3	-	-	294.4	959.7	407.4	106.6
L1	-	-	295.1	103.1	163.3	10.6	295.3	799.9	410.5	108.8
L3	-	-	293.9	95.8	163.5	28.9	294.1	756.6	411.9	113.4
L15	-	-	291.9	109.3	184.1	160.6	292.1	589.9	417.3	155.9
L30	190.6	27.6	291.6	99.8	198.3	391.1	291.6	483.5	418.8	168.5
L50	189.1	27.0	290.4	70.5	195.6	349.6	292.4	161.3	417.7	132.1
L70	193.9	25.4	291.9	74.3	203.2	510.6	293.8	138.2	413.6	97.5
L100	194.9	23.3	290.2	60.2	204.8	567.3	294.2	73.5	415.9	95.1

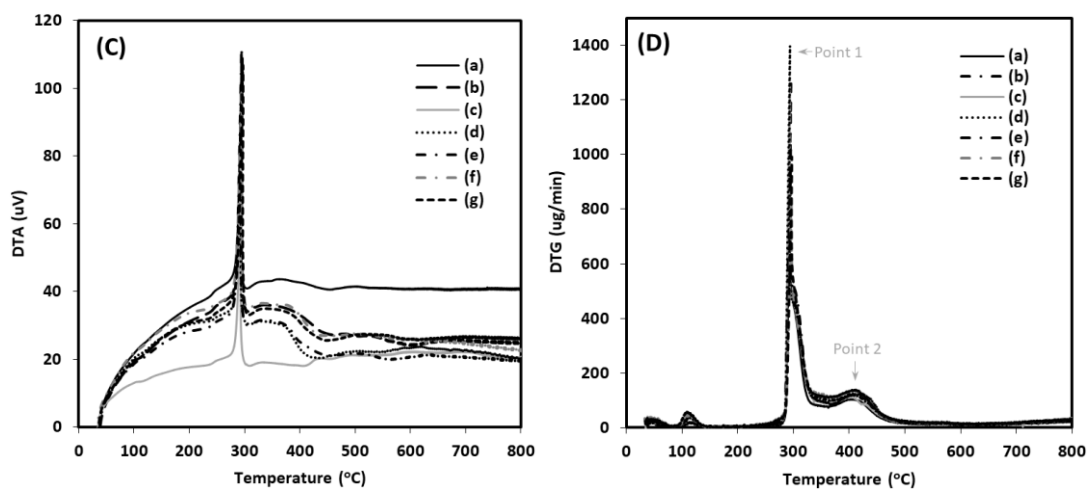
**APPX 5 Maximum peak positions of D and G bands at Raman spectra for PAN and Law/PAN samples**

<u>Samples</u>	<b>D(X)-Raman Shift (cm-1)</b>	<b>D(Y)-Raman Intensity</b>	<b>G(X)- Raman Shift (cm-1)</b>	<b>G(Y)- Raman Intensity</b>	<b>D/G</b>
<b>C</b>	1344	3962	1589	3960	1,0005
<b>L1</b>	1348	4500	1592	4431	1,0155
<b>L3</b>	1365	4380	1582	4781	0,9161
<b>L15</b>	1345	4773	1585	5000	0,9546
<b>L30</b>	1340	5500	1580	5493	1,0012
<b>L50</b>	1339	3800	1592	3282	1,1578
<b>L70</b>	1338	4100	1584	3934	1,0421
<b>L100</b>	1339	4150	1585	4070	1,0196

**APPX 6 Thermogravimetric (TGA) analysis results of PAN and PAN/Hb nanofibers**

	<b>Point 1</b>		<b>Point 2</b>		<b>Point 3</b>		<b>Point 4</b>	
<b>Samples.</b>	<b>Position (°C)</b>	<b>Residual (%)</b>	<b>Position (°C)</b>	<b>Residual (%)</b>	<b>Position (°C)</b>	<b>Residual (%)</b>	<b>Position (°C))</b>	<b>Residual (%)</b>
PAN	284.8	96	321.9	65.5	455.1	44.3	800	32.1
H0.5	285.7	95.2	320.8	64.9	450	42.6	800	31.4
H1	285.1	93	318.1	63.4	447.8	39.6	800	27.1
H3	287.4	94.4	319.2	64.1	452.9	39	800	26.7
H5	285.7	94.7	323.7	66	453.8	43.8	800	32.5
H15	287.6	97.7	325.5	66.6	453.9	43.7	800	32.3
H30	287.6	93.5	325.3	66.5	453.5	43.3	800	33.5

**APPX 7 Representation of C: DTA and D: DTG plots of PAN/Hb nanofibers (a) pure PAN, (b) H<sub>0.5</sub>, (c) H<sub>1</sub>, (d) H<sub>3</sub>, (e) H<sub>5</sub>, (f) H<sub>15</sub> and (g) H<sub>30</sub>.**



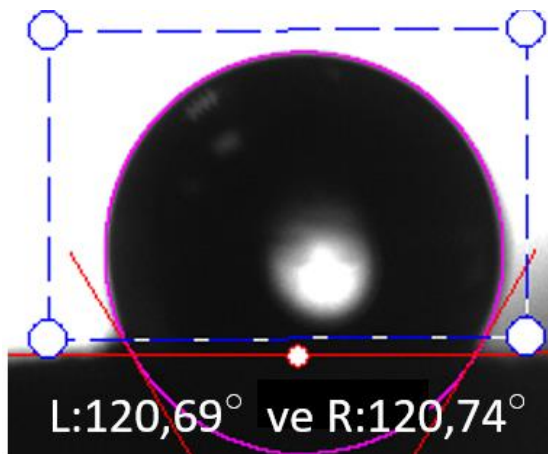
**APPX 8 Data point obtained from DTA and DTG plots**

	DTA		DTG			
	Peak 1		Peak 1		Peak 2	
<u>Samples</u>	Position (°C)	Intensity (uV)	Position (°C)	Intensity (ug/min)	Position (°C)	Intensity (ug/min)
PAN	294.4	102.3	294.4	959.7	407.4	106.6
H <sub>0.5</sub>	295.9	108.6	295.9	1265.3	409.6	119.9
H <sub>1</sub>	293.2	79.0	293.5	1232.6	403.1	112.1
H <sub>3</sub>	293.7	99.2	293.6	1394.5	414.4	124.2
H <sub>5</sub>	294.6	111.8	294.7	1024.9	409.1	125.3
H <sub>15</sub>	295.2	98.5	295.4	876.5	412.3	137.5
H <sub>30</sub>	297.3	105.7	297.3	990	411.5	137.4

**APPX 9 Maximum peak positions of D and G bands at Raman spectra for PAN and PAN/Hb samples**

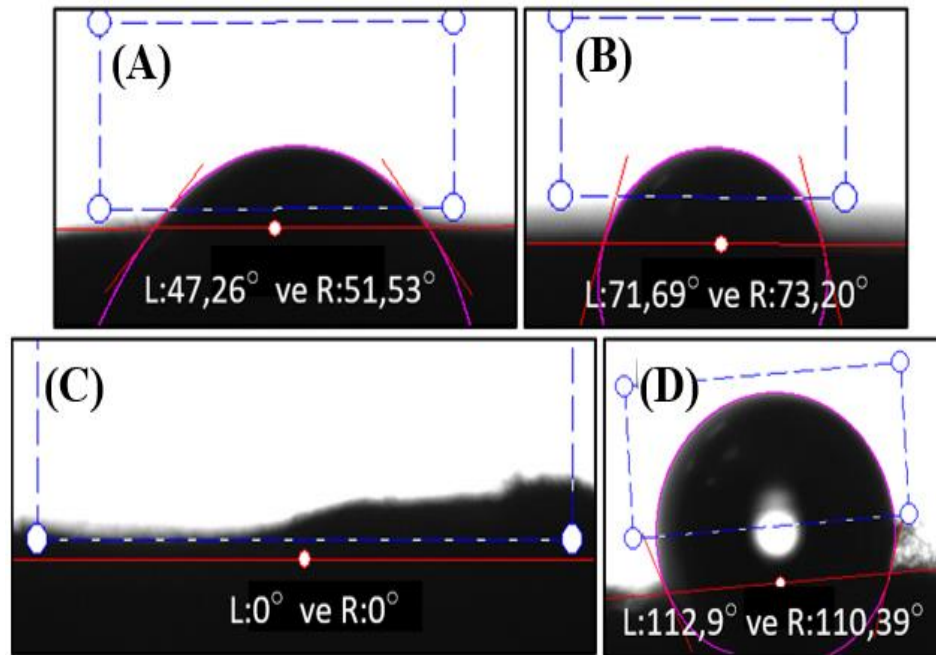
Samples	D(X)-Raman Shift (cm-1)	D(Y)-Raman Intensity	G(X)- Raman Shift (cm-1)	G(Y)- Raman Intensity	D/G
C	1344	3962	1589	3960	1,000505
H <sub>0,5</sub>	1359	4567	1582	5000	0,9134
H <sub>1</sub>	1359	3989	1589	3978	1,002765
H <sub>3</sub>	1351	3789	1593	3917	0,967322
H <sub>5</sub>	1348	4369	1584	4330	1,009007
H <sub>15</sub>	1354	4910	1594	5000	0,982
H <sub>30</sub>	1345	4500	1585	4419	1,01833

**APPX 10 The contact angle for pure carbon nanofibers using PBS buffer**

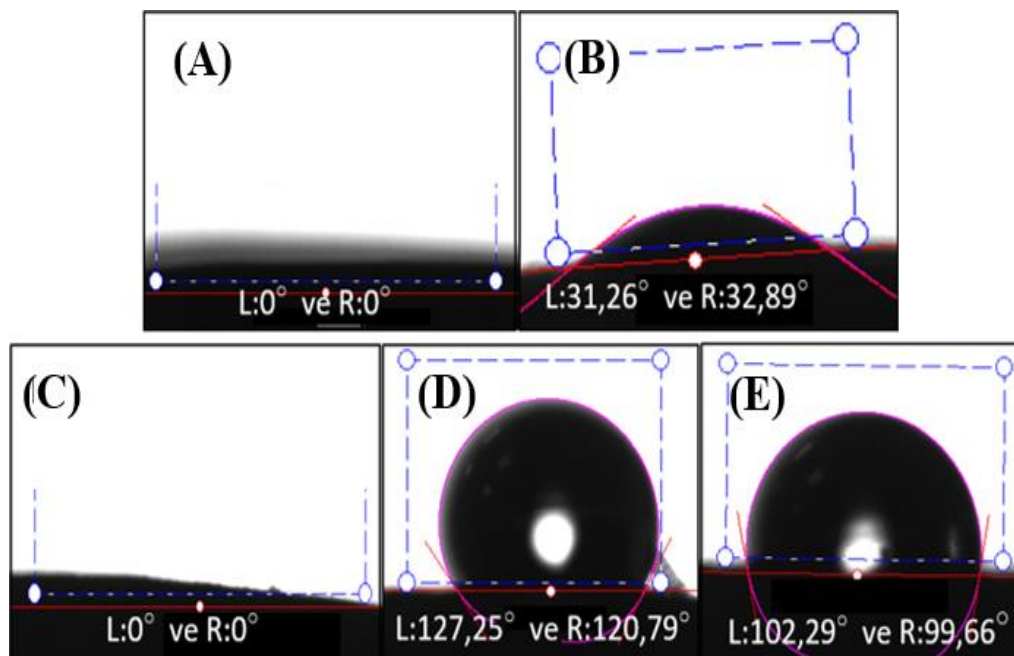




**APPX 11 The contact angle of Lawsone enriched carbon nanofibers with PBS buffer**



**APPX 12 the contact angle of Hemoglobin enriched carbon nanofibers with PBS buffer**



## RESUME

Name Surname : Karima SAHTANI  
Place and Date of Birth : 26/05/1992 MOROCCO  
Foreign Languages : English/ French/Turkish/Arabic/Spanish

Education Status  
High School : Lycee Al-charif al Idrissi Safi Morocco  
Bachelor's : Ecole superieure de technology EST Safi Morocco  
Master's : Ecole Polytechnique Agadir Morocco

### Work Experience

- Consultant for industrial projects in Centaure Innovation consulting Agadir Morocco
- Industrial engineer for CMPE/KNAUF for optimization of the main manufacturing chain and amelioration of the ergonomic and efficiency.

Contact (e-mail) : karimasahtani@gmail.com

### Publications

- Sahtani, K., Aykut, Y., & Aladag Tanik, N. (2022). Lawsone assisted preparation of carbon nanofibers for the selective detection of miRNA molecules. *Journal of Chemical Technology & Biotechnology*, 97(1), 254-269. <https://doi.org/10.1002/jctb.6937>
- Sahtani, K., Aykut, Y., & Aladag Tanik, N. (2021). Hemoglobin assisted carbon nanofiber preparation for selective detection of miRNA molecules. *Journal of Industrial Textiles*, 15280837211049566.
- Sahtani, K., Aykut, Y., & Aladag Tanik, N. (2022). Anti-miRNA immobilization optimization on the screen-printed electrodes for electrochemical miRNA biosensors. *Eskişehir Teknik Üniversitesi Bilim ve Teknoloji Dergisi-C Yaşam Bilimleri Ve Biyoteknoloji*, 11(1), 1-10. <https://doi.org/10.18036/estubtdc.866279>
- Conference: 6. ULPAS: Interaction of Phosphate-Buffered Saline on the Surface of Carbon Nanofiber Electrodes
- Gold and Silver Treatment of Cellulose Monoacetate Micro/Nano Fibers Coated Pencil Graphite Electrodes: Electrochemical Investigations after DNA Immobilization.
- Conference: Comparison of the effect of metal salts with lawsone and hemoglobin on carbon nanofibers preparation and their use as electrochemical miRNA analysis.
- Conference ICTT 2020: Electrospun carbon nanofibers for potential genetic biosensor applications
- Conference: Polyacrylonitrile derived carbon nanofibers in electrochemical genosensors technologies